

https://dspace.org/

Molecular expression patterns during hTGF-3 induced bone formation

Tagliatti, Nicolas

2019

https://hdl.handle.net/10539/29880

Downloaded from a DSpace repository. https://dspace.org/

MSc Dissertation



Molecular Expression Patterns During hTGF-β_3 Induced Bone Formation

Supervisors:

Prof. U. Ripamonti

Prof. R. Duarte

Dr. C. Dickens

Dr. K. Moodley

Nicolas Tagliatti (608407)

29 July 2019

University of the Witwatersrand, Johannesburg

School of Clinical Medicine

I. Declaration by Students

I, Nicolas Tagliatti (Student number: 608407) am a student registered for

MSc in Medicine in the year 2016-18. I hereby declare the following:

- I am aware that plagiarism (the use of someone else's work without their permission and/or without acknowledging the original source) is wrong.
- I confirm that ALL the work submitted for assessment for the above course is my own unaided work except where I have explicitly indicated otherwise.
- It is being submitted for the Degree of Master of Science in medicine at the University of the Witwatersrand, Johannesburg. It has not been submitted before for any degree or examination at any other University.
- I have followed the required conventions in referencing the thoughts and ideas of others.
- I understand that the University of the Witwatersrand may take disciplinary action against me if there is a belief that this is not my own unaided work or that I have failed to acknowledge the source of the ideas or words in my writing.

Signature: _____ Date: _____

II. Abstract

Bone induction involves the enhanced differentiation of osteoblasts and osteoclasts from specific stem cells in response to specific morphogens and occurs within a defined differentiation programme. Contrary to that of rodents, lagomorphs and canines, the recombinant human transforming growth factor-β_3 (hTGF- β_3) induces endochondral bone formation in the non-human primate Chacma baboon *Papio ursinus.* Coral-derived 7% hydroxyapatite/calcium carbonate (CC/HA) preloaded with 125 µg hTGF-β_3 were implanted in the *rectus abdominis* muscle of 4 adult *Papio ursinus.* These constructs along with surrounding muscle tissue were harvested on days 17, 19, 25, 27 and 30 after heterotopic implantation. Tissues were homogenised, and RNA extracted from both the coral-derived devices and the surrounding muscle tissue. Following a reverse transcription step, the extracts were analysed by quantitative reverse-transcriptase polymerase chain reaction to study the temporal changes in gene expression for members of the Transforming Growth Factor-β (TGF-β), Bone Morphogenic Protein (BMP) and Fibroblast Growth Factor (FGF) families and their receptors, WNT signalling, Sma and mad (SMAD) families along with collagen type I (Col1), Noggin, POU Class 5 Homeobox 1 (POU5F1) and SRY (Sex Determining Region Y)-Box 2 (SOX-2). The rapid induction of bone formation was sustained and highlighted by *β-catenin* and *Col1* overexpression at days 19 and 23, with down-regulation of *CD-10, CryαB, Noggin, POU5F1* and *FGF-1, -2* and their receptors. The SMAD signalling cascade is prominent with the up-regulation of *SMAD-2* and *-4* and the down-regulation of *SMAD-5*. Stemness genes, such as *SOX-2*, were over-expressed while *CD-10* and *CD-92* were down-regulated. *BMP-6* was down-regulated with up-regulation of *BMP-2* and *-9*. The study shows that implantation of 125 µg hTGF-β_3 preloaded coral-derived calcium phosphate macroporous bioreactors induces bone formation in heterotopic sites of the *rectus abdominus* muscle by day 19 by the temporal expression of a range of genes implicated in the bone induction cascade.

III. Key words

Transforming Growth Factor-β_3

Bone induction

Bone formation

Papio ursinus

University of the Witwatersrand, Johannesburg

School of Clinical Medicine

IV. Ethics Waiver

ANIMAL RESEARCH ETHICS COMMITTEE

Registration number: AREC-101210-002

August 20, 2018

To whom it may concern,
Reference : Waiver Ripamonti Tagliatti 20180820O
Re: Waiver from the Animal Research Ethics Committee of the University of the Witwatersrand

Applicant : Nicolas Tagliatti
Staff number : 608407
Degree : MSc
Study Title : " Molecular expression patterns during hTGF-β_3 induced bone formation**"**.

Department: Bone Research Laboratory, Oral Medicine and Periodontology

School of Oral Health Sciences

Supervisor: Prof U. Ripamonti

Tel: + 011-7176438 ; Email: Ugo.Ripamonti@wits.ac.za
Ugo Ripamonti, Raquel Duarte, Caroline Dickens and Kiashanee Moodley

Full clearance certificate from the AREC of the University of the Witwatersrand is NOT required.

Reason: There is no "*interventional work on animals*" and the work is strictly related to study & peruse histological sections and perform molecular biology analyses on the expression of several genes from the already harvested and frozen tissue samples.

Comment/Notes : -

This waiver covers the work carried out according to the M&E recommendations signed and approved by Professor Graham Alexander on November 12, 2013 (M&E for study 2008/53/05).

Please contact me should you require further information.

Yours sincerely

Geoff Candy

Geoffrey Candy
Chair : Animal Ethics Research Committee, University of the Witwatersrand

Geoffrey P Candy PhD
Professor, Department of Surgery, Faculty of Health Sciences, University of the Witwatersrand, *7 York Road Parktown 2193, Johannesburg; Tel: 27-11-717-2574; Email: geoffrey.candy@wits.ac.za*

V. Acknowledgements

I would like to acknowledge my deepest and sincerest gratitude to the following individuals for their invaluable support and contribution to this work.

To my supervisor, Professor Ugo Ripamonti, for his guidance and his and scientific stimulation though out the project and friendship. Thank you for allowing me to complete my MSc in collaboration with Professor Duarte in the Bone Research and Internal Medicine Laboratories. Thank you for guidance on bone induction principles and involvement in current research in the Bone Research unit.

I would like to express my sincere gratitude to my co-supervisor Professor Raquel Duarte whose expertise, understanding and guidance were invaluable. Especially her friendship which helped me to believe in myself. I am indebted to Professor Raquel Duarte for her constant encouragement and support on every level helped develop theories, concepts on the current work.

Dr Caroline Dickens and Miss Thérèse Dix-Peek for having been helpful in teaching and expanding my knowledge and protocol basis on quantitative gene procedures and advice and assistance in editing of documents.

Dr Kiashanee Moodley for her friendship and guidance in techniques and protocol advice throughout the project. Thank you for your continuous support and motivation which helped me to reassured in my ability throughout the project.

On a personal note, to my family; for all their love and support throughout this project.

Finally, I appreciate the financial support the AD-HOC grant of the Bone Research Laboratory, the National Research Foundation's (NRF) Innovation Master's Scholarship and the University of Witwatersrand, Post-graduate Merit award.

VI. Table of Contents

I. Declaration by Students ii

II. Abstract iii

III. Key words iii

IV. Ethics Waiver iv

V. Acknowledgements vi

VI. Table of Contents vii

VII. Abbreviation List x

VIII. List of Figures xiii

IX. List of Tables xv

1.Introduction 1

1.1 Bone remodelling 1

1.2 Mesenchymal stem cells involvement in osteogenesis 4

1.3 Bone morphogenetic proteins 5

1.4 Transforming growth factor-beta (TGF-β) involvement in osteogenesis 6

1.5 The SMAD-dependent pathway in TGF- β signalling 8

1.6 The non-SMAD dependent pathway 8

1.7 Interplay between bone morphogenetic proteins and TGF-β signalling in osteoblasts and bone formation 9

1.8 WNT signalling pathway & involvement in bone remodelling 9

1.9 Role of fibroblast growth factors in bone regeneration 10

1.10 Coral-derived macroporous bioreactors as a delivery system for biological activity of the recombinant hTGF-β_3 isoform 11

1.11 The induction of bone by mammalian TGF-β isoforms (hTGF- β_1, hTGF-β_2, hTGF-β_3) 13

2. Research Scope, Aims & Objectives 14

2.1 Problem Statement 14

2.2 Study Rationale 14

2.3 Significance of Research 15
2.4 Primary Aim 15
2.5 Objectives 15
3.Methodology 16
3.1 Primate model for tissue induction and morphogenesis 16
3.2 To investigate the temporal expression pattern of TGF-β isoforms, BMP isoforms, SMADs and stem cell markers using qRT-PCR. 18
3.2.1 RNA extraction 18
3.2.2 Assessment of RNA concentration, quality, and integrity 18
3.3 cDNA synthesis by RT-PCR 19
3.4 Primer design for quantitative reverse transcription polymerase chain reaction (qRT-PCR) 20
3.5 Optimization of PCR annealing temperatures by gradient PCR 20
3.6 Quantitative reverse transcription polymerase chain reaction (qRT-PCR) 21
3.7 Data analysis: Quantitative real-time PCR experiments 22
4. Results 23
4.1 Optimisation of PCR annealing temperatures 23
4.2 qRT-PCR 25
4.2.1 *β-Catenin* 26
4.2.2 *Bone morphogenic protein-2, -3, -4, -6* & *-7* 27
4.2.3 *CD-10* 30
4.2.4 *CD-92* 31
4.2.5 *Collagen type I* 32
4.2.6 *CRYαB-14* 33
4.2.7 *Fibroblast growth factors* 34

4.2.8 *Noggin* 36

4.2.9 *POU5F1* 37

4.2.10 *SMADs* 38

4.2.11 *TGF-β* 41

4.2.12 *SOX-2* 43

5. Discussion 44

6. Limitations and Future Work 59

7. Conclusions 59

8. References 61

9. Appendices 74

VII. Abbreviation List

Alk5	-	TGF-β type I receptor kinase
ALP	-	Alkaline phosphatase
APC	-	Adenomatous polyposis coli
BMP	-	Bone morphogenetic protein
BMU	-	Basic multicellular unit
cAMP	-	Cyclic adenosine monophosphate
cDNA	-	Complimentary deoxyribonucleic acid
CD-10	-	Cluster differentiation
cKO	-	Conditional knockout
ColI	-	Collagen type I
ColIV	-	Collagen type IV
Col2a1	-	Collagen type II alpha 1 chain
CREB	-	cAMP response element binding protein
CRY-αB	-	Crystallin Alpha B
CUX-1	-	CCAAT displacement protein
DNA	-	Deoxyribonucleic acid
EDTA	-	Ethylenediaminetetraacetic acid
ECM	-	Extracellular matrix
EGF	-	Epidermal growth factor
ESC	-	Embryonic stem cell
FFPE	-	Formalin-fixed paraffin-embedded
FGF	-	Fibroblast growth factor
FGFR	-	Fibroblast growth factor receptor
GDF	-	Growth and differentiation factor

GVHD	-	Graft-versus-host disease
HDAC	-	Histone deacetylases
hTGF-β_3	-	Human transforming growth factor-β
hBMSC	-	Human bone marrow stromal cells
IHH	-	Indian hedgehog
I-SMAD	-	Inhibitory SMADs
JNK	-	Jun N-terminal kinase
MAPK	-	Mitogen-activated protein kinase
MAK/ERK	-	Ras-Raf-MEK-ERK pathway
MIQE	-	Minimum information for publication of quantitative real time PCR experiments
MKK	-	Mitogen-activated protein kinase kinase
MME	-	Neprilysin
MMP	-	Matrix metalloproteinase
mPDC	-	Murine periosteum-derived cells
mRNA	-	Messenger RNA
MSC	-	Mesenchymal stem cells
NRQ	-	Normalised relative quantities
OP	-	Osteogenic protein
OSX	-	Osterix
PCR	-	Polymerase chain reaction
POU5F1	-	POU Class 5 Homeobox 1
pRb	-	Retinoblastoma protein
PTH	-	Parathyroid hormone

PTH1R	-	Parathyroid hormone 1 receptor
qPCR	-	Quantitative polymerase chain reaction
SOX-2	-	SRY (Sex Determining Region Y)-Box 2
RNA	-	Ribonucleic acid
R-SMADs	-	Receptor-regulated SMAD
RUNX-2	-	Runt-related transcription factor 2
SMAD	-	Sma and mad (mothers against decapentaplegic)
TAE	-	Tris-acetate-EDTA
TAB-1	-	Transforming growth factor-beta activated kinase 1 (MAP3K7) binding protein 1
TAK-1	-	Transforming growth factor beta-activated kinase 1
TGF	-	Transforming growth factor
VSMC	-	Vascular smooth muscle cell
WNT	-	Wingless/Integrated

VIII. List of Figures

Figure 1: Bone remodelling……...3

Figure 2: Illustration of the MSCs lineage-specific differentiation……4

Figure 3: TGF-β & BMP signalling and negative regulation in bone formation…….7

Figure 4: Heterotopic *rectus abdominis* implantation design and surgical model for 4 adult baboons, *Papio ursinus*……17

Figure 5: Composite 1% Agarose gel of optimized qRT-PCR primer amplicons …..….23

Figure 6: 1% Agarose gel of optimized qRT-PCR primer amplicons ...……...24

Figure 7: 1% Agarose gel of optimized qRT-PCR primer amplicons ……..25

Figure 8: Relative changes in the expression of *β-catenin* at 17, 19, 23, 25, 27 and 30 days after implantation of the 125 µg hTGF-β_3 preloaded coral derived constructs into the *rectus abdominis* muscle of four adult *Papio ursinus*…...26

Figure 9: Relative changes in the expression of *BMP-2* (A), *BMP-4* (B), *BMP-6* (C), *BMP-7* (D) and *BMP-9* (E) at 17, 19, 23, 25, 27 and 30 days after implantation of the 125 µg hTGF-β_3 preloaded coral derived constructs into the *rectus abdominis* muscle of four adult *Papio ursinus*……..29

Figure 10: Relative changes in the expression of *CD-10* at 17, 19, 23, 25, 27 and 30 days after implantation of the 125 µg hTGF-β_3 preloaded coral derived constructs into the *rectus abdominis* muscle of four adult *Papio ursinus*……...30

Figure 11: Relative changes in the expression of *CD-92* at 17, 19, 23, 25, 27 and 30 days after implantation of the 125 µg hTGF-β_3 preloaded coral derived constructs into the *rectus abdominis* muscle of four adult *Papio ursinus* ……..31

Figure 12: Relative changes in the expression of *Collagen type I* at 17, 19, 23, 25, 27 and 30 days after implantation of the 125 µg hTGF-β_3 preloaded coral derived constructs into the *rectus abdominis* muscle of four adult *Papio ursinus*……..32

Figure 13: Relative changes in the expression of *CRYαB-14* at 17, 19, 23, 25, 27 and 30 days after implantation of the 125 µg hTGF-β_3 preloaded coral derived constructs into the *rectus abdominis* muscle of four adult *Papio ursinus*……..33

Figure 14: Relative changes in the expression of *FGF-1* (A), *FGF-2* (B), *FGF-R1* (C), *FGF-R2* (D) at 17, 19, 23, 25, 27 and 30 days after implantation of the 125 µg hTGF-β_3 preloaded coral derived constructs into the *rectus abdominis* muscle of four adult *Papio ursinus*……35

Figure 15: Relative changes in the expression of *Noggin* at 17, 19, 23, 25, 27 and 30 days after implantation of the 125 µg hTGF-β_3 preloaded coral derived constructs into the *rectus abdominis* muscle of four adult *Papio ursinus*……...36

Figure 16: Relative changes in the expression of *POU5F1* at 17, 19, 23, 25, 27 and 30 days after implantation of the 125 µg hTGF-β_3 preloaded coral derived constructs into the *rectus abdominis* muscle of four adult *Papio ursinus*……...37

Figure 17: Relative changes in the expression of *SMAD-1* (A), *SMAD-2* (B), *SMAD-3* (C), *SMAD-4* (D) and *SMAD-5* (E) at 17, 19, 23, 25, 27 and 30 days after implantation of the 125 µg hTGF-β_3 preloaded coral derived constructs into the *rectus abdominis* muscle of four adult *Papio ursinus*……40

Figure 18: Relative changes in the expression of *TGF-β_1* (A), *TGF-β_2* (B) and *TGF-β_3* (C) at 17, 19, 23, 25, 27 and 30 days after implantation of the 125 µg hTGF-β_3 preloaded coral derived constructs into the *rectus abdominis* muscle of four adult *Papio ursinus*……...42

Figure 19: Relative changes in the expression of *SOX-2* at 17, 19, 23, 25, 27 and 30 days after implantation of the 125 µg hTGF-β_3 preloaded coral derived constructs into the *rectus abdominis* muscle of four adult *Papio ursinus*……...43

Figure 20: Overview of proposed heterotrophic transforming growth factor-β (hTGF-β_3) mechanism with *Fibroblast Growth Factor* (FGF), *Indian Hedgehog* (IHH) and *RUNX-2* pathways in bone induction……..…..……52

Appendix 4: Tissue morphogenesis by 125 µg hTGF-β_3 treated coral-derived macroporous bioreactors……77

Appendix 5: Open Access of figure 2…….……...78

IX. List of Tables

Table 1: Master mix component of cDNA synthesis 20µl reactions……...…19

Table 2: Thermocycler conditions……...…20

Table 3: PCR thermocycler conditions……..……21

Table 4: 10x Tris-acetate-EDTA Buffer components…….21

Appendix 1: Real-time PCR reaction volumes……..……74

Appendix 2: Primer sequence of BMP isoforms, FGFs and receptors, SMADs, TGF-β isoforms and stem cell markers…….……74

Appendix 3: Thermocycling parameters for Real-time PCR…….……76

Appendix 6: Appendix6: Gene expression summary of genes of interest at 17 to 30 days after implantation of the 125 µg hTGF-β_3…….……79

1.Introduction

Bone is a specialised connective tissue and forms the key element of the skeletal system. The formation and subsequent transduction of bone is orchestrated by the members of the transforming growth factor (TGF) superfamily. One member of this superfamily, the bone morphogenetic proteins (BMPs), are osteogenic molecules which play a vital role in osteoblast differentiation and the induction of bone as well as the formation of bone itself (Ripamonti, 2006, Rahman *et al.*, 2015). Bone is developed either from distinct osteoinductive intramembranous vessels or via endochondral bone formation. Endochondral ossification involves the progressive remodelling of cartilage into bone while intramembranous ossification shapes bone directly from mesenchymal stem cell (MSCs) condensates lacking a cartilage intermediate (Chen *et al.*, 2012). Osteoclasts, mineralized bone matrix, MSC derived osteoblasts and osteocytes form major components of the bone's microenvironment (Chen *et al.*, 2012). Within the skeleton, bones are continuously remodelled throughout life and any alteration or imbalance in their development can result in bone disease such as osteoporosis. Bone loss through trauma or cancerous metastatic growth is a significant public health issue with $ 2.5 billion being spent in the USA on bone defect repairs and bone trauma was found to be a major cause of mortality in people younger than 40 years (Livingston *et al.*, 2003, Baroli, 2009). Therefore, understanding how TGF superfamily members function *in vivo* to initiate bone induction will allow for novel therapeutics to be developed to combat local bone loss.

1.1 Bone remodelling

Bone remodelling is characterized by a series of critical molecular and cellular events (Parfitt, 1994). Two key cellular lineages play a vital role in mesenchymal osteoblastic cell lines and hematopoietic osteoclastic cell lineages (Chen *et al.*, 2012). The bone remodelling process is a continuous process which arises at specific periods of time within the development of vertebrates (Raisz, 1999). It is not limited to foetal development but is a continuous process in adult vertebrates as it establishes bone homeostasis (Rodan, 1998). Bone homeostasis consists of two fundamental processes: resorption and formation allowing for an equilibrium to be established (Frost, 1990). A balanced number of osteoblasts and osteoclasts facilitates bone remodelling equilibrium to form a basic multicellular unit (BMU) (Chen *et al.*, 2012).

The bone remodelling model has key five phases, namely, activation, absorption, reversal, formation and quiescence (Huang *et al.*, 2007). These phases arise through several signalling

cascades and have been investigated extensively in the bone formation process (Chen *et al.*, 2012).

In the first phase of bone remodelling (activation\resting), the release of cytokines and calcium ions induces oestrogen release and angiogenesis. Mononuclear pre-osteoclasts are recruited from the cellular niche which attach to the bone surface and fuse to form multiple multinucleated osteoclasts (Kular *et al.*, 2012, Klar *et al.*, 2013)(Fig. 1A).

In the reabsorption phase (Fig. 1B), multinucleated osteoclasts aggregate forming a ruffled border allowing them to adhere to the surface of the bone (Kular *et al.*, 2012). This establishes an isolated microenvironment between the underlying bone and the osteoclasts. Osteoclasts establish the release of protons by secreting carbonic anhydrase II that dissolves bone material. This specifically releases hydrogen ions by a membrane bound pump into the localized microenvironment under the ruffled bone and is coupled with the transport of chloride ions via an osteoclast membrane bound chloride channel to maintain electroneutrality in the microenviroment (Tolar *et. al.*, 2004). Subsequently, this leads to osteoclasts' secretion of proteases such as matrix metalloproteinases or cathepsin K, which degrade collagen-rich bone matrix and release calcium ions (Silver et. *al*., 1988; Delaissé *et. al*., 2003). This results in an acidic micro environment that dissolves the collagenous matrix via mononuclear cells; producing an irregular geometry of concavities with various curvatures, radii and dimensions on the bone surface termed cylindrical haversian canals or howship lacunae (Hadjidakis and Androulakis, 2006, Kapinas and Delany, 2011). The dissolving of the collagenous matrix primes the bone surface which, at the same time, deposits proteoglycans and other growth factors onto the surface of the bone matrix to help promote osteoblastogenesis (Kular *et al.*, 2012).

During the reversal phase (Fig. 1C), remodelling starts with mononuclear cells preparing the bone surface for new osteoblasts. The recruitment of mononuclear cells on the bone surface further allows old bone collagenous matrix to degrade and assists in the deposit of rich proteoglycans on the cement lining below the recruited osteoblasts (Kapinas and Delany, 2011, Kular *et al.*, 2012).

Newly differentiated osteoblasts are attracted to the site of resorption and lay down osteoid that is then replaced with calcium and phosphate ions to form new bone (Kapinas and Delany, 2011, Kular *et al.*, 2012) (Fig. 1D). The deposition of new bone matrix continues until the concavity is entirely replaced with new osteogenic material (Kapinas and Delany, 2011, Kular *et al.*,

2012). This is due to osteoblast proliferation and secretion of collagen type I (ColI) into the extracellular matrix (ECM).

The osteoblasts become resting cells on the newly formed bone surface due to maturation of the osteoblast, and apoptosis or terminal differentiation into bone surface lining cells rooted in the calcified matrix and covered with flattened lining cells (Kapinas and Delany, 2011). This forms the quiescence phase (Fig. 1E) in which resting lining cells are integrated and remain dormant until the next cycle.

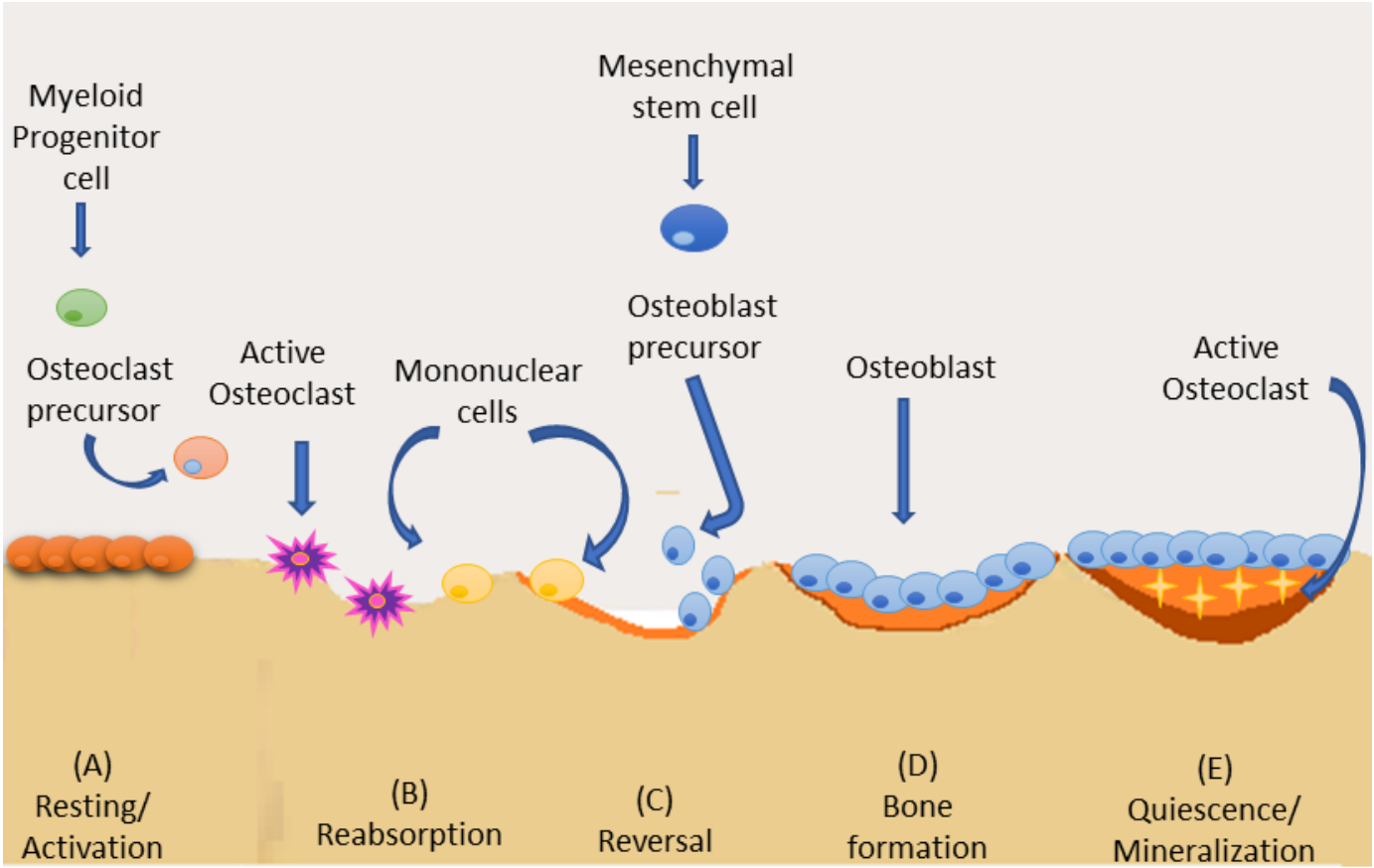


Figure 1: Bone remodelling. Mononuclear pre-osteoclasts are recruited which attach to the bone surface and fuse to form multiple multinucleated osteoclasts (A). Multinucleated osteoclasts aggregate forming a ruffled border to establishes an isolated microenvironment between the underlying bone and the osteoclasts. The osteoclasts establish an acidic microenvironment that dissolves the collagenous matrix producing an irregular geometry of concavities with various curvatures (B). Remodelling of the bone begins with mononuclear cells preparing the bone surface for new osteoblasts as well as the deposition of rich proteoglycans on the cement lining below the recruited osteoblasts (C). Newly differentiated osteoblasts are attracted to the site of resorption and lay down osteoid and form new bone (D). The deposition of concavity is entirely replaced with new osteogenic material leads to the maturation of osteoblast to resting cells, osteocytes and apoptosis or terminal differentiation into bone surface lining cells rooted in the calcified matrix (E). The matrix mineralization and generation of new bone thus completes the remodelling cycle.

This extraordinary potential to regenerate bone has captivated scientists to have a continuous desire to mechanistically understand the induction of bone formation and utilise the capacity of bone formation induction and bone repair in tissue engineering, known as the "*bone induction principle*" (Urist *et al.*, 1967). One area of interest researchers began investigating is the use of mesenchymal stem cells due to their ability to self-renew into multiple cell lineages.

1.2 Mesenchymal stem cells involvement in osteogenesis

Adult mesenchymal stem cells are derived from bone marrow, adipose tissue and peripheral blood, neonatal birth-associated tissues (including placenta, umbilical cord and cord blood) (Beltrami et. al., 2003; Cao and Dong et. al., 2005), hematopoietic stem cells as well as endothelial populations including endothelial progenitor cells and endothelial colony forming cells (Hass et. al., 2011). They differentiate and self-renew into various mesodermal cell lineages such as chondrocytes, adipocytes, osteoblasts and myocytes (Fig. 2). Multipotent stem cells differentiation towards an osteoblastic fate relies on multiple signalling pathways including the BMP pathway (Beederman *et al.*, 2013). Aging reduces the number of available MSCs that are able to differentiate into osteoblasts in the bone marrow, however, if MSCs could be directed toward osteogenic differentiation, they could be a feasible therapeutic option for bone regeneration (Guan *et al.*, 2012).

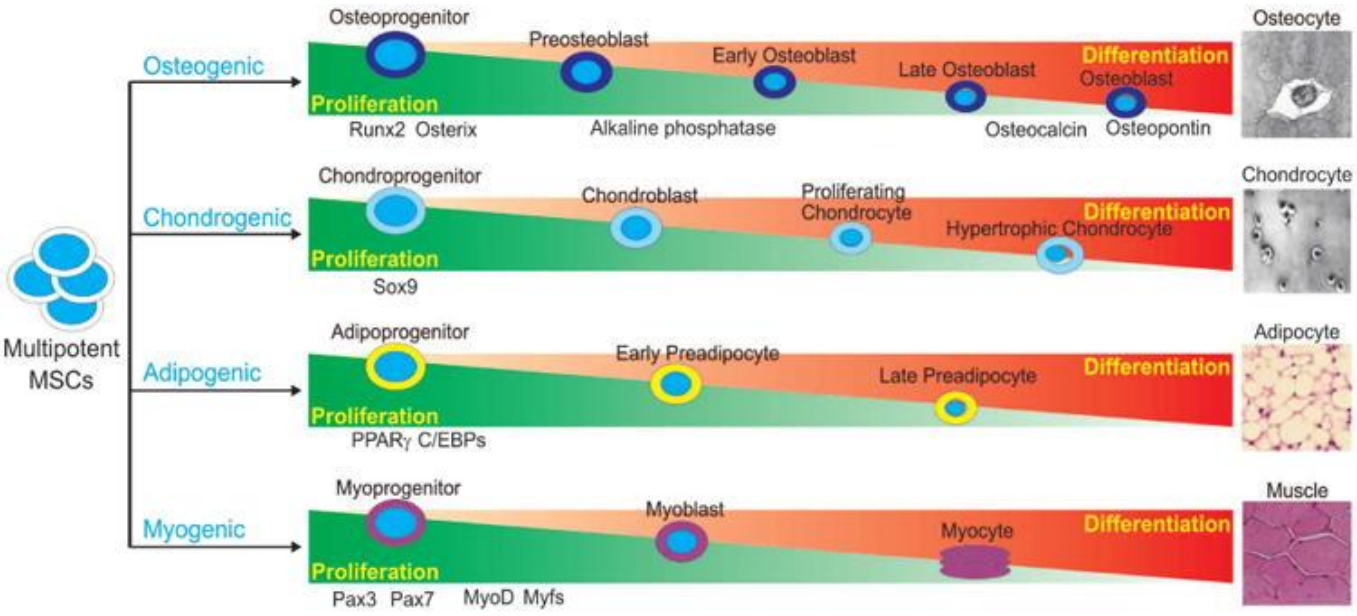


Figure 2: Illustration of the MSCs lineage-specific differentiation. Mesenchymal stem cells form part of pluripotent predecessor cells with the unique ability to differentiate into several lineages, such as adipogenic, osteogenic, myogenic and chondrogenic, giving rise to osteocytes, adipocytes, chondrocytes and muscle respectively. Indicators and regulators of lineage-specific differentiation are shown (Beederman *et al.*, 2013).

Bone stem cell markers have been used to monitor osteogenic differentiation capacity and to monitor the expression profiles of MSCs during bone expansion. Microarray analysis of MSCs in osteogenic differentiation discovered markers such as CRYαB which is involved in the reconstruction of the developmental phases during osteoblast proliferation, differentiation, mineralization and matrix maturation, and further illustrated the essential activation of the Sma and mad (mothers against decapentaplegic) (SMAD) signalling in BMP signalling. Crystallin αB is a novel osteogenic marker specifically expressed during the osteogenic differentiation of MSCs *in vitro* (Kulterer *et al.*, 2007). *CD-10/MME* and *CD-92/SLC* where identified as additional bone stem cell markers, as they represent key genes in osteogenic and adipogenic differentiation of MSCs *in vitro*. The surface markers, CD-10 and CD-92, demonstrated significantly increased expression in MSCs differentiated towards the osteogenic, adipogenic and muscle lineages (Graneli *et al.*, 2014). NANOG is an essential transcription factor involved in maintaining pluripotency within embryonic stem cells (ESC). NANOG together with Sex Determining Region Y-Box 2 (SOX-2) and POU Class 5 Homeobox 1 (POU5F1), are used to characterise ESC. Embryonic stem cells can differentiate into the three germ layers (ectoderm, mesoderm and endoderm). Understanding the underlying mechanisms that maintain a cell's pluripotency is critical for understanding how MSCs lead to bone formation (Gamblin *et al.*, 2014).

1.3 Bone morphogenetic proteins

Bone morphogenetic proteins (BMPs) also termed osteogenic proteins (OPs) are a homologous group of signalling proteins that function as growth factors and form part of the transforming growth factor β (TGF) superfamily. Bone morphogenetic proteins have been broadly studied and found to play vital roles in cell proliferation, organogenesis, embryogenesis, and stem cell differentiation (Hogan, 1996, Zou *et al.*, 1997, Reddi, 1998, Kang *et al.*, 2004). To date, at least 20 different BMPs have been identified and characterized in humans (Beederman *et al.*, 2013). BMPs play an critical role in skeletal bone development and MSC differentiation (Beederman *et al.*, 2013). Tissue-specific knockout studies and signal transduction studies have shown that SMAD-1, -5 and -8 play a fundamental role in BMP signal transduction forming part of the initial signalling cascade downstream of the BMP receptors (Chen *et al.*, 2004).

BMPs are found to bind to both type I and II serine/threonine kinase receptors with both receptors crucial in signal transduction (Fig. 3). After ligand binding, the type I and II receptors form a heterotetrametric-activated complex (Chen *et al.*, 2004). Type I BMP receptors form a complex with the receptor-SMAD (R-SMAD) proteins, and these proteins play a central role

in transmitting signals from the receptor to target genes (Chen *et al.*, 2004). BMP receptors phosphorylate R-SMADs (SMAD-1, -5 and -8) in a ligand-dependent manner (Nishimura *et al.*, 1998). After the phosphorylated SMADs are released from the receptor, they associate with SMAD-4, which is involved in both BMP and TGF-β signalling (Nishimura *et al.*, 1998). This complex then translocates to the nucleus and partakes in gene transcription of osteogenic genes with other transcription factors such as RUNX-2 (Chen *et al.*, 2004).

Bone morphogenetic protein signalling is regulated at multiple molecular levels: firstly, BMP antagonists such as Noggin bind to BMP-2, -4 and -7 to block BMP signalling (Devlin *et al.*, 2003, Wu *et al.*, 2003). Secondly, the binding of SMAD-6 or -7 (inhibitory SMADS (I-SMAD)) to type I BMP receptors prevents SMAD-1, -5 and -8 from being activated downstream (Imamura *et al.*, 1997). This negatively regulates transcription of target genes involved in bone formation and osteoblastic differentiation (Kapinas and Delany, 2011)

1.4 Transforming growth factor-beta (TGF-β) involvement in osteogenesis

Transforming growth factor-α (TGF-α) and transforming growth factor-β (TGF-β) are another two sub-protein groups of the TGF superfamily. The TGF-α sub-group form part of the epidermal growth factor (EGF) receptor family (Roberts *et al.*, 1981, Groenen *et al.*, 1994, Salomon *et al.*, 1995). The TGF-β family of proteins comprises multiple members including TGF-β_1, β_2 and β_3. The three isoforms share approximately 60-80% amino acid homology and their functions range from extracellular matrix (ECM) production and control of cell adhesion, proliferation and differentiation to cell death and survival (Massague, 1990). *Transforming growth factor-β* expression mediates chondrocyte and osteoblast differentiation.

Transforming growth factor-β signalling transmits signals across the plasma membrane by the formation of heteromeric complexes of specific type I and type II serine/threonine kinase receptors (Fig. 3). Within this complex, phosphorylation and activation of the type II receptor leads to phosphorylation of the type I receptor initiating intracellular signalling cascades through the phosphorylation of the R-SMAD proteins SMAD-2 and -3. Activated R-SMADs form a complex with the co-SMAD SMAD-4 which becomes translocated into the nucleus to direct transcriptional responses (Chen *et al.*, 2012). Within a cell, TGF-β signalling can occur via either a SMAD-dependent pathway or non-SMAD dependant pathway.

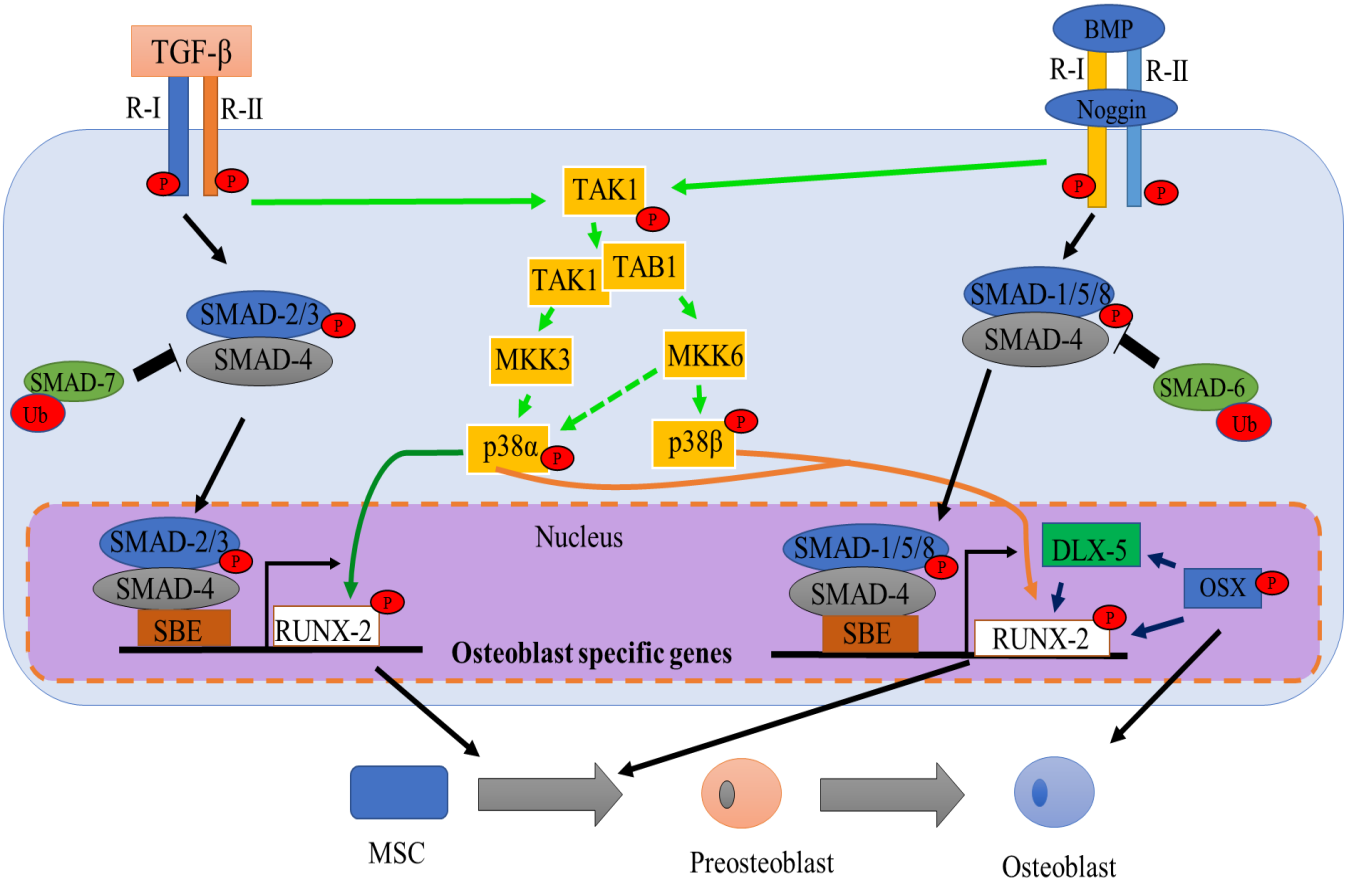


Figure 3: TGF-β & BMP signalling and negative regulation in bone formation. Canonical SMAD-dependent TGF-β signalling starts with TGF-β binding to a type I (R-I) and II (R-II) serine/threonine kinase receptors, causing their phosphorylation. This activates the R-SMADs which form a complex with SMAD-4. This complex translocates into the nucleus where it interacts with transcription factors to trigger target gene expression. SMAD-7, an inhibitor SMAD, interrupts the activated SMAD-2/3 complex formation with SMAD-4. SMAD-7 is targeted to interact with specific histone deacetylases (HDACs), resulting in the deacetylation of SMAD-7. Deacetylation of SMAD-7 promotes its ubiquitination and, allows for the formation of SMAD-2/-3 complexes. SMAD-dependent-BMP signalling, BMP bind to receptor type I (R-I) and receptor type II (R-II). This leads to a signalling transduction of their respective SMADs. Activated SMADs form a complex with SMAD-4 and translocate into the nucleus where it interacts with transcription factors to activate targeted gene expression. Activated SMADs regulate expression of *Dlx5*, *RUNX-2* and Osterix *(OSX)*, which are transcription factors and coactivators important in osteoblastic genesis. The inhibitor SMAD, SMAD-6, binds type I BMP receptors and prevents the activation of SMAD-1/-5/-8. Negative regulation of the induction of bone is present with the expression of *Noggin*. Noggin secretion in MSCs is stimulated by BMPs but decreases once cells undergo differentiation. Noggin regulates BMP activity in undifferentiated cells, through a negative feedback loop to control the rate of cell differentiation. Noggin regulation of BMPs prevents the binding of BMPs with their interaction with their cell surface receptors. Noggin binds with various degrees of affinity to BMP-2/-4/-5/-6 and -7. This decreases signal transduction of BMPs on target cells preventing the activation of downstream SMAD-1/-5/-8 signalling. Inhibitor SMAD-6 interferes with BMP signalling. As SMAD-6 competes with co-SMADs complex formation with R-SMADs preventing its association. Deacetylation of SMAD-6 promotes for its ubiquitination and degradation, allowing for the formation of SMAD-1/-5/-8 complexes. Ub (ubiquitination); P (phosphorylation).

1.5 The SMAD-dependent pathway in TGF- β signalling

TGF-β signalling via SMADs is the canonical signalling pathway. The association of SMAD-2 or -3 with the class II histone deacetylase (HDAC) -4 and -5 complex results in antagonization of RUNX-2 activity (Wu *et al.*, 2016). In the presence of SMAD-3, the SMAD-3-TGF-β complex negatively regulates osteoblastogenesis, due to inhibition of osteoblast differentiation and apoptosis (Wu *et al.*, 2016). SMAD-3-null mice were found to be osteopenic, and had an increased number of osteocytes (Borton *et al.*, 2001). This was due to accelerated chondrocyte hypertrophy and reduced levels of *Noggin* was observed (Borton *et al.*, 2001). Thus, TGF-β-induced inhibition of chondrocyte maturation is reliant on SMAD-3 signalling, and eliminated by the interruption of SMAD-2 or -3 activation (Wu *et al.*, 2016).

Furthermore, SMAD-3-TGF-β signalling has been found to play an essential role in the postnatal maintenance of articular cartilage homeostasis (Kang *et al.*, 2004). SMAD-3-null mice and chondrocyte-specific SMAD-3 conditional knockout mice develop osteoarthritis and articular cartilage degeneration (van de Laar *et al.*, 2011).

1.6 The non-SMAD dependent pathway

In the absence of SMAD-dependant signalling, TGF-β and BMP can signal via a non-SMAD dependant pathway. In the non-SMAD-dependent pathway, there is rapid phosphorylation of the transforming growth factor beta-activated kinase 1 (TAK-1) resulting in the recruitment of TAB1 (Transforming growth factor-beta activated kinase 1 (MAP3K7) binding protein 1) (Fig. 3). Recruitment of TAB1 leads to the activation of the mitogen-activated protein kinase kinase (MKK) three or six (Wu *et al.*, 2016). This leads to the activation of the p38 mitogen-activated protein kinase (MAPK) signalling pathway that has been found to be involved in various regulatory aspects of bone initiation and maintenance (Zarubin and Han, 2005, Thouverey and Caverzasio, 2015). The MAPK p38 group of proteins is comprised of multiple subtypes, namely p38α, p38β, p38γ and p38δ (Zarubin and Han, 2005). Two subtypes are involved in bone formation: p38α, activated by MKK-3/6, and p38β, activated by MKK-6 only (Zarubin and Han, 2005). Both p38α and p38β are closely related proteins that are expressed in most cell types and have overlapping functions (Zarubin and Han, 2005). p38β plays a role in the regulation of late osteoblast differentiation (Zarubin and Han, 2005). The activation of p38α positively regulates the transcriptional and activity of Distal-less homeobox 5, RUNX-2 and OSX, genes involved in bone induction. Distal-less homeobox 5 is a BMP-responsive transcriptional activator required for osteoblast differentiation by stimulating the up-regulation of a variety of promoters such as the SP7/OSX promoter (Xu and Testa, 2009). Mesenchymal

precursor cells require the expression of *RUNX-2* and *OSX* expression to induce differentiation of MSC into osteoblasts (Xu and Testa, 2009).

TGF-β type I receptor kinase (Alk5) is a protein that forms a heteromeric complex with TGF-β receptors and transduces the TGF-beta signalling pathway once activated. Studies performed on an MSC-specific Alk5 conditional knock out mouse model demonstrated that MAPK signalling promoted early osteoblast proliferation (Matsunobu *et al.*, 2009, Lee *et al.*, 2002). The MAPK pathway was found to positively regulate *RUNX-2* expression and function to promote MSC differentiation into osteoblasts (Lee *et al.*, 2002). In another study, TGF-β_2 stimulated cranial healing was promoted by osteoprogenitor proliferation via the MKK–ERK signalling pathway (Lai and Cheng, 2002). These studies demonstrated that TGF-β operates either through either SMAD dependant or non-dependant signalling pathways. Osteoblast progenitor enrichment occurs with early differentiation, but is negatively regulated by osteoblast differentiation and mineralization at latter stages (van de Laar *et al.*, 2011).

1.7 Interplay between bone morphogenetic proteins and TGF-β signalling in osteoblasts and bone formation

Transforming growth factor-β/Bone morphogenetic proteins have been widely researched and are recognized for their role in bone formation during mammalian tissue induction. Disruptions of TGF-β/BMP signalling have been implicated in several bone diseases such as osteoarthritis, brachydactyly type A2 and tumour metastasis in cancer (Siegel and Massague, 2003, Papachroni *et al*., 2009, Chen *et al.*, 2012).

Recent studies have demonstrated that TGF-β and BMPs interplay is essential for bone formation (Chen *et al.*, 2012, Rahman *et al.*, 2015). Transforming growth factor-β_1 infused coral implants used in mice increase bone formation five-fold compared to bone induction by direct injection BMP-2 of alone (Tachi *et al*., 2011). The interaction of TGF-β_1, FGF-2 and platelet-derived growth factor-AB with BMPs is believed to allow for increased osteogenic function of BMP *in vitro* (Singhatanadgit *et al.*, 2006). This indicates a strong relationship between TGF-β and BMP signalling in osteoblast differentiation.

1.8 WNT signalling pathway & involvement in bone remodelling

Wingless-type MMTV integration site family (WNT) genes play a central role in the early organs and tissues development such as bone, neural structures and musculoskeletal (Gordon and Nusse, 2006, Issack *et al.*, 2008). Activation of WNT mediated signals have been found to play a role in bone remodelling under physiological and pathological conditions (Kobayashi,

2012). Although WNT has been identified in bone remodelling, the molecular mechanism of WNT action in human bone development is not fully understood (Nusse, 2005, Kobayashi, 2012).

WNT proteins bind to cell-surface receptors and activate signalling pathways which control gene expression in cell growth and differentiation (Issack *et al.,* 2008). WNT signalling has two distinct pathways, the independent non-canonical pathways and β-catenin independent canonical. Within the β-catenin independent canonical pathway WNTs act on precursor osteoblasts and assist in the promotion of precursor osteoblasts differentiation into mature osteoblasts and osteogenesis (Kobayashi, 2012). However, activation of the β-catenin-independent non-canonical pathway has been found to enhance osteoclast formation (Gordon and Nusse, 2006).

WNT signalling gain-of-function mutations or specific loss-of-function in humans and mice that has resulted in increased bone formation or loss in bone development, respectively (Issack *et al.,* 2008). These results demonstrate that WNT-mediated signals are involved in several aspects of bone formation and bone resorption.

1.9 Role of fibroblast growth factors in bone regeneration

Fibroblast growth factors (FGFs) are pleiotropic growth factors that regulate cell proliferation, differentiation, and the migration of cells within multiple organs including bone (Boilly *et al.*, 2000). Fibroblast growth factor 1 (FGF-1) protects osteoblast cell lineages from cell death during bone fracture healing. Fibroblast growth factor 1 was found to enhance cellular growth by increasing endogenous levels of tyrosine phosphorylation and inducing expression of both *osteocalcin* and *osteopontin* mRNA. Fibroblast growth factor 1 also renders osteoblast precursors and osteoblasts resistant to cytotoxic signals which consequently promotes the initiation of bone repair mechanisms after fracture trauma (Kelpke *et al.*, 2001) .

Fibroblast growth factor 2 (FGF-2) is expressed in osteoblast lineage cells and is a critical component of maintenance in stem cell cultures (Kuro-o, 2008). Stabilization of *FGF-2* levels in culture medium improved stem cell marker expression, resulting in decreased spontaneous differentiation and increased number of stem cells (Lotz *et al.*, 2013). The addition of FGF-2 to murine periosteum-derived cells (mPDC) during culture expansion enhanced bone formation by promoting mPDC proliferation and inhibiting culture-induced senescence (Charoenlarp *et al.*, 2017).

Structural interaction studies have revealed that FGF-1 binds to fibroblast growth factor receptor 2 (FGF-R2) and FGF-2 to fibroblast growth factor receptor 1(FGF-R1) (Stauber *et al.*, 2000). Furthermore, both FGF-R1 and FGF-R2 are expressed in condensing mesenchyme cells during early bud development. In developing bone, FGF-R2 is mainly localized to periosteal and perichondrial tissue and also is expressed in differentiating osteoblasts and osteocytes playing a vital role in human skeletal development (Chen *et al.*, 2012). Fibroblast growth factor receptor 1 is involved in endochondral ossification. Activating mutations in FGF-R1 cause osteoglophonic dysplasia, which is a rare syndrome characterized by rhizomelic dwarfism (Orr-Urtreger *et al.*, 1993). Activating FGF-R2 mutations have a variety of effects on differentiation of MSC and cranial cell replication in mice and humans (Chen *et al.*, 2012). More than 10 gain-of-function mutations in FGF-R2 are known to cause multiple types of craniosynostoses, for example Apert syndrome (Orr-Urtreger *et al.*, 1993).

Thus, FGF-1/-2 and their receptors play on essential role in the regulation of cell proliferation, differentiation, and the migration of cells within bone. Fibroblast growth factor signalling protects osteoblast cell lineages from cell death and consequently promotes the progression of bone repair mechanisms after fracture trauma (Kelpke *et al.*, 2001).

1.10 Coral-derived macroporous bioreactors as a delivery system for biological activity of the recombinant hTGF-β_3 isoform

Nature has a conserved molecular mechanism tailored to allow for the emergence of tissues. Accepted theories on the induction of bone formation require the use of an insoluble substratum, combined with soluble proteins to set in motion a rapid, ripple-like cascade inducing bone formation (Reddi, 1994, Reddi, 2000, Ripamonti, 2004, Ripamonti, 2006). Studies have shown that ECM macroenvironments can be tailored to duplicate the formation of bone by the combination of stem cells and inductive soluble signals, allowing for the assembly of new biomimetic matrices that initiate the induction of bone (Reddi, 2000, Ripamonti *et al.*, 2007, Ripamonti, 2009).

Systematic studies have shown that calcium phosphate-based bioreactors, implanted in intramuscular heterotopic sites in a non-human primate *Papio ursinus*, also known as the Chacma baboon, could reproducibly induce new bone formation (Ripamonti, 1991, Ripamonti *et al*., 1993, Ripamonti *et al.*, 1996, Ripamonti, 2009). *Papio ursinus* species have been found to share similar and comparable osteonic bone remodelling and bone physiology with humans (Schnitzler *et al.*, 1993). *In vivo,* time studies suggest that myoblast stem cells adhere to the

peripheral surface of the bioreactors and lead to the proliferation and differentiation into osteoblastic-like cells (Ripamonti *et al.* 1993; Ripamonti *et al.* 2009). Morphological and immunohistochemical studies have demonstrated that activation of angiogenesis allows for a continuous migration of stem cells and osteoblasts to attach to the implanted bioreactors (Ripamonti *et al.* 1993). Immunohistochemical staining demonstrated high levels of sprouting and invading capillaries within the macroporous spaces of the implanted bioreactors during the developmental processes culminating in bone differentiation, and were associated with alkaline phosphatase and laminin expression (Ripamonti *et al.* 1993).

Alkaline phosphatase activity of the invading capillaries was additionally associated with increased expression of *collagen type IV* (ColIV) (Ripamonti *et al.* 1993). The temporal induction of ColIV and its association of angiogenesis was proposed to assist in the initiation of bone formation. Mesenchymal collagenous condensations at the hydroxyapatite surface suggest a prominent differentiating event precedes the induction of bone within the coral-derived bioreactors (Ripamonti, 1991, Ripamonti *et al*., 1993, Ripamonti *et al.*, 1996, Ripamonti, 2009).

In *Papio ursinus* substantial bone induction was induced by the implantation of super-activated coral-derived bioreactors implanted with hTGF-β_3 into heterotopic sites. Studies have demonstrated that bone induction is proportional to the amount of hTGF-β_3 protein used within the implanted bioreactors (Ripamonti *et al*., 2012). High doses of the hTGF-β_3 demonstrated pronounced induction of bone formation compared to low doses of hTGF-β_3 (Ripamonti *et al.*, 2012). Bone formation was seen to form significantly at the periphery of the devices, suggesting that a rapid cascade of bone differentiation is set into motion at the site of ligand binding at the peripheral regions of the super activated construct (Ripamonti *et al.*, 2012). This is demonstrated by a rich capillary network with paravascular myoendothelial stem cells present at the periphery which later differentiate towards osteoblastic cell lineages under the influence of hTGF-β_3 protein (Ripamonti *et al.*, 2012).

To summarise, induction of bone formation requires the combination of soluble osteogenic molecular signals in combination with an insoluble substratum that resembles the geometry of *in vivo* bone to induce its formation (Sampath and Reddi, 1981, Khouri et al., 1991, Reddi, 1994, Reddi, 2000, Ripamonti et al., 1993, Ripamonti, 2006).

1.11 The induction of bone by mammalian TGF-β isoforms (hTGF- β_1, hTGF-β_2, hTGF-β_3)

The induction of bone initiated by hTGF- β_3 in the *rectus abdominis* muscle of *Papio ursinus* is accomplished via the BMP pathway (Ripamonti *et al*., 2016a). Human- transforming growth factor-β_3 controls the induction of bone formation by the regulating of the expression of *BMP*s through *Noggin*, *Noggin* being an antagonist of the BMP pathway (Ripamonti *et al.*, 2016a). All three TGF-β isoforms have been found to be involved in osteogenesis and bone remodelling as well as the induction of bone formation (Ripamonti *et al.*, 2016a). Initially, TGF-β isoforms were not believed to be osteoinductive due to their inability to stimulate bone formation in rodent models (Roberts *et al.*, 1981). This was refuted in studies showing that TGF-β_1 loaded into a collagenous-matrix carrier and implanted in heterotopic extra skeletal muscle sites of the *rectus abdominis* muscle of *Papio ursinus* could induce new bone formation (Ripamonti *et al*., 1997)

Osteoinduction is not restricted solely to naturally derived or recombinant BMPs/OPs, but includes mammalian TGF-β_1, TGF-β_2 and TGF-β_3 (Ripamonti *et al.*, 1997, Ripamonti *et al.*, 2000, Ripamonti *et al.*, 2008). When insoluble collagenous bone matrix was combined with hTGF-β_3 it induced rapid endochondral bone formation within the *rectus abdominis* muscle of *Papio ursinus* (Ripamonti *et al.*, 2008). Further studies have shown that hTGF-β_2 and hTGF-β_3 in particular loaded into either macroporous calcium phosphate-based or coral-derived biomimetic devices can induce bone formation when implanted into heterotopic intra-muscular *rectus abdominis* sites of the baboon (Ripamonti *et al.*, 2000, Ripamonti *et al.*, 2008).

Early molecular expression experiments suggested that the TGF-β_3 isoforms regulated certain BMPs (Ripamonti and Klar, 2010) and further demonstrated that the osteoinductive capability of TGF-β_3 was due to its capacity to indirectly initiate bone induction by modulating *Noggin* expression (Klar *et al.*, 2014). As a result, TGF-β_3 regulated the extent of BMP expression and increased the rate of new bone formation within coral-derived macroporous devices (Klar *et al.*, 2014). Altered genetic expression patterns were observed between day 15 and day 30 in *in vivo* implanted heterotopic coral-derived macroporous devices treated with 125µg hTGF-β_3 (Klar *et al.*, 2014). This correlated with the time period during which new bone formation was first detected histologically (Klar *et al.*, 2014). Coral derived bioreactors pre-treated with hTGF-β_3 induce structural organization of fibrin/fibronectin rings within the macroporous spaces as early as day 15 (Klar *et al.*, 2014). Bone has been found to form rapidly by day 30 with substantial induction and invasion of the macroporous spaces. This has indicated that the induction of bone formation must initiate between 15 and 30 days exploiting early tissue

morphogenesis and ECM patterning with fibrin/fibronectin rings. Though the model of molecular gene transcription during *in vivo* bone induction was made clearer by Klar *et al.* (2013; 2014) studies, a fuller understanding of the cellular activation and transition of the signal over time remains a challenge and needs to be evaluated.

2. Research Scope, Aims & Objectives

2.1 Problem Statement

Bone induction involves the enhanced differentiation of osteoblasts from specific stem cells in response to specific morphogens and occurs within a set period of time. Osteoclasts derived from blood monocytes, stem from haemopeoitic cells in the bone marrow. Monocytes are released into the blood stream and collect at bone resorption sites. Monocytes fuse to allow the formation of multinucleated osteoclasts, which attach to the bone surface, and reabsorb bone matrix. It is still unknown when genes related to the osteogenic and TGF-β/BMP pathways are initiated or change their expression patterns temporally during the 17- 30 day time period of heterotopic bone formation. Therefore, this study focuses on elucidating the temporal gene expression using real-time PCR. This study will also elucidate how cells of the microenvironment respond to hTGF-β_3 by the use of Real Time gene expression data. This will further facilitate the understanding of key signalling pathways that drive bone formation during the 30 day implantation period allowing for a greater clarity in understanding the complex pathways involved in the regulation and enhancement of bone formation *in vivo*.

2.2 Study Rationale

The rapid induction of bone formation by the hTGF-β_3 isoform in *Papio ursinus* has forced re-evaluation of the mechanistic insights of this process. Bone induction occurs 17-30 days after implantation of hTGF-β_3 treated coral-derived bioreactors into the muscle tissue of the Chacma baboon, but it is still unclear how the hTGF-β_3 isoform initiates bone induction at a molecular level. In order to understand how hTGF-β_3 affects the expression of key genes and alters signal transduction pathways, coral-derived macroporous devices, treated with 125 µg hTGF-β_3, were implanted into the *rectus abdominis* muscle of *Papio ursinus* for 17, 19, 23, 25, 27 and 30 days. Samples harvested from the various time points were subjected to molecular analysis. qRT-PCR was used to analyse the temporal changes in gene expression for members of the *TGF-β, BMP, FGF* and *SMAD* families along with *ColI, Noggin, POU5F1* and *SOX-2*. This will enable the investigation of the influence of hTGF-β_3 on the cellular microenvironment and on gene expression changes linked to bone induction.

2.3 Significance of Research

This research sought to elucidate and map the molecular signals and cellular mechanisms allowing for a rapid initiation of the induction of bone cascade by super-activated coral-derived calcium carbonate/hydroxyapatite-based bioreactors and expand the current developed paradigm of bone formation in the primate *Papio ursinus*.

2.4 Primary Aim

The aim of this study is to evaluate the molecular mechanisms underlying the rapid induction of bone formation by hTGF-β_3 in *Papio ursinus* using qRT-PCR.

2.5 Objectives

To investigate the temporal gene expression pattern of *TGF-β*s, *BMP*s, *FGF*s and their receptors, *SMAD*s, WNT signalling and stem cell markers in tissues heterotopically implanted with hTGF-β_3 treated devices and the surrounding tissue using qRT-PCR.

This was achieved by:

i. Extraction of RNA from four cylinders of coral-derived calcium carbonate macroporous constructs implanted heterotopically, in duplicate, within the *rectus abdominis* muscle of four adult baboons, along with newly formed bone tissue surrounding the coral- derived macroporous devices, at varying time periods from 17 to 30 days.
ii. Reverse transcription of mRNA to cDNA from extracted RNA samples for time periods 17 to 30 days.
iii. Quantitative Real-time PCR to track the relative expression levels of TGF isoforms, BMP isoforms, FGFs and receptors, SMADs, stem cell markers, WNT signalling and reference genes involved in bone formation over the time course.

3.Methodology

3.1 Primate model for tissue induction and morphogenesis

The preparation of the macroporous hydroxyapatite replicas of the calcium carbonate exoskeletal macrostructure of the coral genus *Goniopora* was as previously described (Ripamonti *et al.,* 2012). Briefly, 7% hydroxyapatite/calcium carbonate macroporous constructs (7% HA/CC) were loaded with 125 µg hTGF-β_3 by pipetting vertically on top of the constructs to ensure an even distribution of hTGF-β_3 throughout the macroporous spaces. The coral-derived macroporous constructs pre-loaded with 125µg hTGF-β_3 (experimental group), were implanted in the *rectus abdominis* muscle of four clinically healthy non-human primate *Papio ursinus.* Baboons with a mean (±SD) weight of 21.2 (±1.48) Kg were selected from the primate colony of the University of the Witwatersrand, Johannesburg. Criteria for selection, housing conditions and diets were as previously described (Ripamonti, 1991, Ripamonti, 1992, Ripamonti *et al*., 1997, Ripamonti *et al.*, 2000, Ripamonti *et al*., 2008, Klar *et al.*, 2014, Ripamonti *et al.*, 2015). Research protocols were approved by the Animal Ethics Screening Committee of the University (AESC#: M&E ex 2008/53/05). Animals were housed by the University and in compliance with the National Code for Animal Use in Research, Education and Diagnosis in South Africa (Public Service Department, 1990). Premedication, before induction of general anaesthesia, was by midazolam hydrochloride (Dormicum 3 mg/kg IM, Roche, Illovo, South Africa). Animals were anaesthetized with ketamine hydrochloride (5–15 mg/kg; Eutaphent Kyron Laboratories, Johannesburg, South Africa) and general anaesthesia maintained by Isofor (1.5–2%; Safe Line Pharmaceutical, Johannesburg, South Africa), after oro-tracheal intubation (Ripamonti, 2009, Ripamonti and Klar, 2010). Sixteen 7% HA/CC treated macroporous constructs were implanted bilaterally in intramuscular pouches surgically created by sharp and blunt dissection within the *rectus abdomini*s muscle in four animals for harvesting after 17, 19, 23, 25, 27 and 30 days *in vivo*. Implants were aligned longitudinally ~2 cm apart (Ripamonti, 2010). Post-operative pain and inflammation were controlled by buprenorphine hydrochloride (Temgesic 0.3 mg/kg IM), and carpofan (Rimadyl 3 mg/kg subcutis) (Fig. 4).

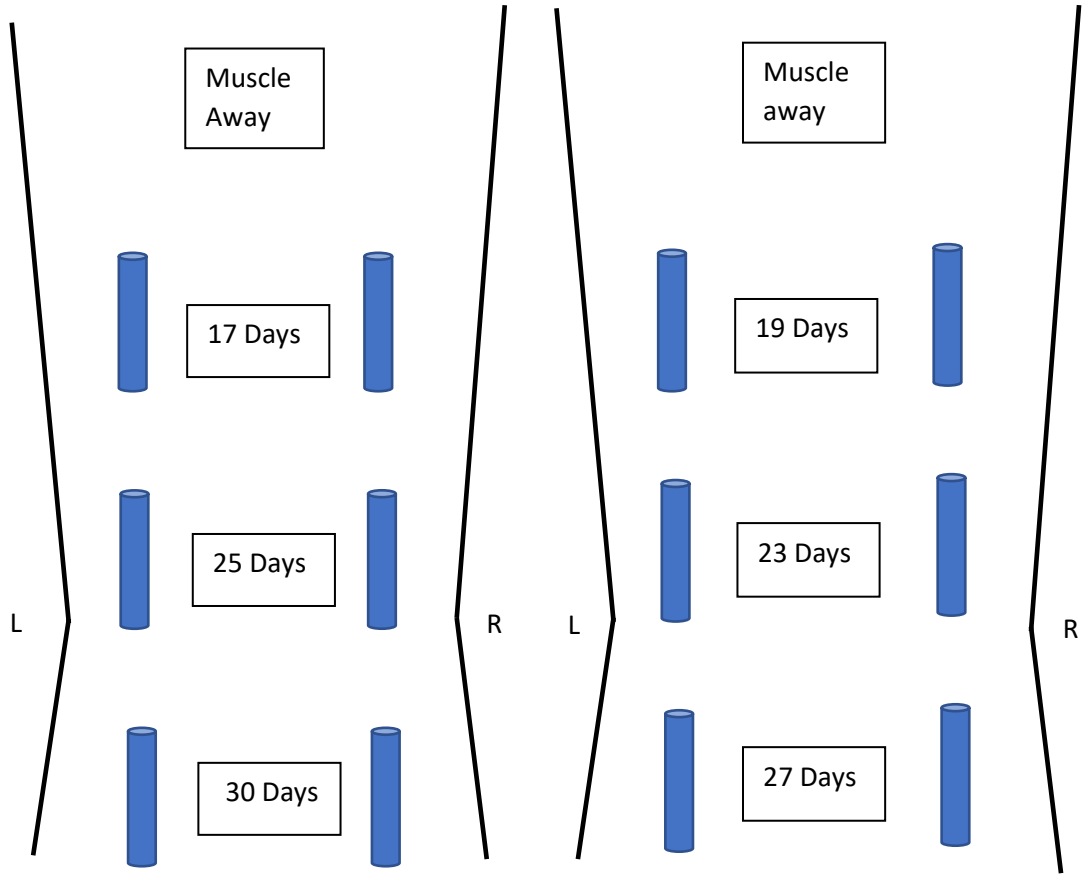


Figure 4. Heterotopic *rectus abdominis* implantation design and surgical model for 4 adult baboons, *Papio ursinus*. In each animal, four cylinders of coral-derived calcium carbonate macroporous constructs were implanted heterotopically in duplicate, within the *rectus abdominis* muscle. Coral-derived constructs pre-treated with 125 µg of recombinant human recombinant human transforming growth factor-β_3 (hTGF-β_3) were implanted for 19, 23 and 27 days in two of the baboons and 17, 25, 30 days in the other two baboons prior to harvesting.

Devices were harvested together with the surrounding muscle tissue and each sample cut into 2 sections using sterile blades and processed as follows:

i) One half was snap frozen in liquid nitrogen and stored at -80°C for gene expression analysis by qRT-PCR.

ii) One half was fixed in 10% neutral buffered formalin for histological analysis

3.2 To investigate the temporal expression pattern of TGF-β isoforms, BMP isoforms, SMADs and stem cell markers using qRT-PCR.

3.2.1 RNA extraction

Under sterile conditions, surrounding muscle tissue (termed muscle) was removed from the heterotopic specimens (termed device). The muscle and device samples, along with a control muscle sample (control muscle) from each baboon were ground to powder in liquid nitrogen using a pestle and mortar. Total RNA was extracted from the ground tissue using the Maxwell® 16 tissue LEV total RNA purification kit (Promega, Madison, Wisconsin, United States) on the Maxwell® 16 benchtop DNA extraction system. Thirty milligrams of ground tissue were homogenised using a Silentcrusher S (Heidolph Instruments) in lysis buffer and the lysed samples taken through the Maxwell® 16 LEV automated purification procedure as per manufacturer's recommendations. The Maxwell® 16 LEV automated purification procedure uses MagneSil™ Paramagnetic Particles which are silica-paramagnetic particles with an affinity for DNA or RNA under defined conditions to ensure particle structure and solution composition to selectively adsorb RNA. The automated purification method uses a three-step procedure: binding of the RNA to the silica-paramagnetic particles, a series of wash steps to remove contaminates and finally elution in nuclease free water. A low elution volume of 30 µl was used to yield more concentrated RNA. The RNA samples and any remaining ground tissue were stored at -80 °C until required.

3.2.2 Assessment of RNA concentration, quality, and integrity

RNA Concentration

RNA concentration was determined using the NanoDrop ND-1000 Spectrophotometer (Inqaba Biotech, Johannesburg, South Africa). The NanoDrop ND-1000 Spectrophotometer measured of absorbance of nucleic acids at 260 nm (1 OD_{260} = 40ng/µl RNA) and the 260/280 nm ratio; a ratio of ~2 signifies pure RNA, with minimal protein contamination. RNA quality was assessed using the Pico6000 RNA kit (Agilent Technologies, Santa Clara, CA, USA) on a Bioanalyzer 2100 (Agilent Technologies). The bioanalyzer uses an algorithm that is user-independent, automated and reliable for standardization of RNA quality and allowed for the calculation of an RNA integrity number. An electropherogram of each sample was produced to determine the quality of the extracted RNA.

3.3 cDNA synthesis by RT-PCR

Reverse transcription involves the generation of cDNA from an mRNA template and enables researchers to study RNA with the same molecular technique used for DNA investigations. cDNA generated by reverse transcription can be amplified using polymerase chain reaction (PCR). The combination of reverse transcription and PCR (RT-PCR) allows the detection of RNAs within a sample even if the RNA is expressed in low levels. The High Capacity cDNA Reverse Transcription kit (Applied Biosystems, Foster City, CA, USA) was used to reverse transcribe the RNA to cDNA. Following isolation and quantification, 2 µg total RNA was reverse transcribed in a 20 µl reaction. The mRNA strand was reverse transcribed with a reverse transcriptase enzyme producing a complementary cDNA-RNA hybrid strand. Initially, samples are incubated at 25°C to allow for annealing of the random oligonucleotide primers to their respective complementary sequence(s) of interest. Reverse transcriptase is then added to the reaction to allow for DNA synthesis and the temperature raised to the optimal activity temperature of the reverse transcriptase for synthesis. Table 1 shows the reverse transcription mix to which 10 µl (2µg) of RNA sample is added. Reverse transcription was performed in a thermal cycler according to the conditions set out in Table 2. The reverse transcription reactions (cDNA) were used for quantitative RT-PCR.

Table 1: Master mix for cDNA synthesis reactions

Component	Volume/Reaction (µL) Master mix	RNA solution (µL)
10× RT Buffer	2	-
25× dNTP Mix (100 mM)	0.8	-
10× RT Random Primers	2	-
MultiScribe™ Reverse Transcriptase (50 U/µl)	1	-
Nuclease-free H2O	4.2	-
RNA (200ng/µl)	-	10
Total	10	10

Table 2: Thermocycler conditions

Stage	Temperature (°C)	Time (minutes)
Initiating reverse transcription	25	10
Reverse transcription of mRNA	37	120
Termination of reverse transcription reaction	85	5
Storage	-20	∞

3.4 Primer design for quantitative reverse transcription polymerase chain reaction (qRT-PCR)

Primers were designed using the web-based primer design programme primer3 (http://bioinfo.ut.ee/primer3/) from sequences obtained from the NCBI nucleotide sequence databank (Appendix 2). Where available, primers were designed against *Papio* sequences; otherwise, they were designed against *Homo sapiens* sequence information. Primers were designed to be ~20 nucleotides long and contain 50-60% GC. Additionally, primers were designed with a GC clamp at the 3' end to enhance specific binding due to the stronger bonding of G and C bases. Secondary structures and self-dimers of primers were tested for using the primer3 software to ensure limitation these structures. Furthermore, total amplicon length was limited to less than 200 nucleotides for real time PCR analysis. Primers were synthesised by Integrated DNA Technologies (Whitehead Scientific) (Appendix 2).

3.5 Optimization of PCR annealing temperatures by gradient PCR

Optimisation of annealing temperatures for newly designed primers using the primer pairs designed above (section 3.4), endpoint PCR amplification with a gradient of annealing temperatures was performed to optimise the annealing temperature. Primers of the respective genes and cDNA from a control muscle sample was used. Each primer set was run in a temperature gradient of 50 to 65 °C to determine optimal spasticity of primers.

0.5 ul of undiluted cDNA was added to a PCR master mix containing 3.5 µL H_20, 5 µl Phusion Flash High-Fidelity PCR Master Mix (Thermo Scientific™), 0.5 µl forward primer (10 µM) and 0.5 µl reverse primer (10 µM) was added. This solution was briefly centrifuged and placed in a thermal cycler c1000 system (Bio-Rad Laboratories Ltd, Hercules, California) programmed with the following cycling conditions:

Table 3: PCR thermocycler conditions

Cycles	1	30			1	1
Temperature (°C)	98	98	*	72	72	4
Time (s)	10	1	5	10	60	∞

** 8 melting temperatures ranging from 50 °C and 65 °C – namely 50 °C, 51.1 °C, 53.2 °C, 55 °C, 59,3 °C, 62 °C, 64 °C, 65 °C – were used*

1 % w/v of agarose to 1x Tris-acetate-EDTA (TAE) buffer was dissolved by heating in a microwave to allow the agarose to dissolve. The mixture was left at room temperature to cool to 50 °C - 60 °C, 1x GelRed Nucleic Acid Gel Stain (Merck KGaA, Darmstadt, Germany) was added and the molten agarose poured into a mini-gel mould electrophoresis apparatus and allowed to set completely before submerging in 1× TAE buffer. Samples were prepared by adding 1×DNA Loading buffer to 10µl PCR product prior to loading on the gel. Gels were resolved for ~35 minutes with constant voltage of (100 V) and imaged using a ChemiDoc™ MP System (Bio-Rad Laboratories Ltd, Hercules, California).

Table 4: 10x Tris-acetate-EDTA Buffer components

Component	Quantity
dH_2O	900 mL
Tris base	48.4 g
Glacial acetic acid	11.4 mL
EDTA	3.72 g
Adjust volume to 1 L with dH_2O	

3.6 Quantitative reverse transcription polymerase chain reaction (qRT-PCR)

Quantitative reverse transcription polymerase chain reaction (qRT-PCR) reactions were performed in duplicate on a CFX-96 thermocycler (Bio-Rad Laboratories Ltd) using 10 ng of cDNA; 1x Eva-Green Master Mix (Bio-Rad Laboratories Ltd) and 0.3 µl of forward primer (10 M) and 0.3 µl reverse primer (10 µM) (Appendix 2). Genes assayed included: members of TGF-β, BMP, FGF and WNT signalling pathways and stem cell markers.

Thermocycling parameters included a denaturation step of 94°C for 2 min.; 40 cycles of 95°C for 10 sec., 60°C for 10 sec. and 72°C for 30 sec; and a final extension at 72°C for 5 min

(Appendix 3). Gene expression was normalized against the expression of three reference genes: ß-Actin; Succinate dehydrogenase complex subunit A (SDHA) and Ribosomal Protein Large PO (RPLPO). These reference genes were selected based on previous GeNorm analysis (http://medgen.ugent.be/~jvdesomp/genorm) that established these were the most stably expressed internal reference genes in *Papio ursinus* (Klar *et al.*, 2014). Gene expression from the harvested macroporous devices and adjacent muscle tissue was normalized to the control muscle tissue in each animal and to the geometric mean of the reference genes using the $2^{-\Delta\Delta Cq}$ method (Hellemans *et al*., 2007).

Calibrated normalized relative quantities (CNRQs), which reflect the $\log_{10}{}^{\Delta\Delta Ct}$, were determined and a Student's T-test used to determine statistical significance with $p<0.05$ considered significant.

3.7 Data analysis: Quantitative real-time PCR experiments

Minimum Information for Publication of Quantitative Real-time PCR Experiments (MIQE) guidelines were followed to ensure all experimental parameters were of high quality and that results would be reliable, reproducible and acceptable for submission to any journal.

Normalised relative quantities (NRQs) were log-transformed to give $\log_{10} 2^{-\Delta\Delta Ct}$ values resulting in statistically normal distributions. Gene expression levels was analysed with the use of Excel (Microsoft®). hTGF-β_3 treated devices and adjacent muscle samples were compared to control muscle to determine how the TGF-β_3 affected gene expression patterns over time. All statistical analysis was performed in excel, where a Student's T-test with a 95% confidence interval was used to see if these differences were statistically significant. P-values of less than 0.05 were considered significant.

4. Results

4.1 Optimisation of PCR annealing temperatures

Primers for qRT-PCR analysis were tested using a conventional PCR approach with control muscle tissue as template. Samples were run using a gradient of 3 different annealing temperatures namely 59^{0}C, 60^{0}C and 61^{0}C. *RPLO*, *β-actin*, *TGF-β$_2$*, *β-catenin*, *POU5F1*, *FGF-R1* and *SMAD-3* where found to amplify products of the expected lengths (Fig. 5). For all these primer pairs an annealing temperature of 60^{0}C was found to amplify successfully and this annealing temperature was therefore used for the real time PCR.

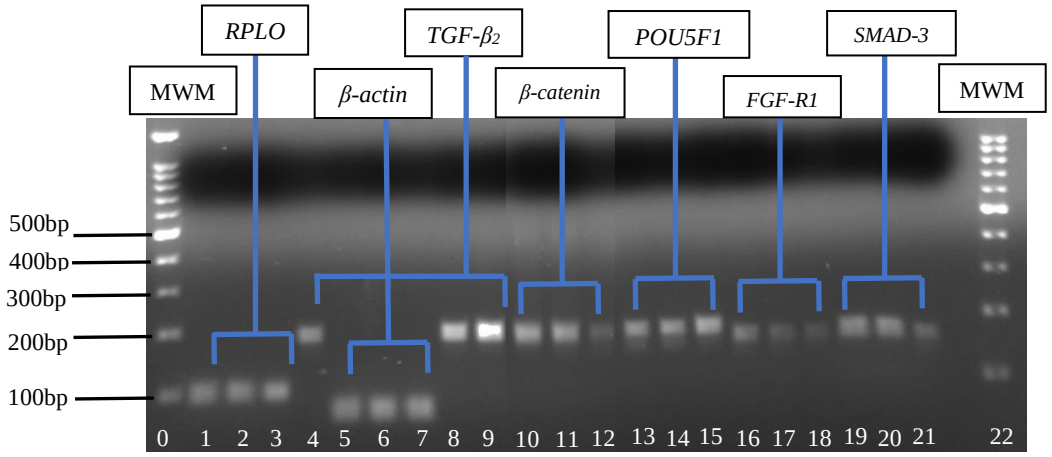


Figure 5: Composite 1% Agarose gel of optimized qRT-PCR primer amplicons

Composite 1% agarose gel of qRT-PCR primer products *RPLO*, *β-actin*, *TGF-β$_2$*, *β-catenin*, *POU5F1*, *FGF-R1*, *SMAD-3* were run using a gradient of 3 different annealing temperature namely 59^{0}C, 60^{0}C and 61^{0}C. Lanes 0 & 22: 100 bp molecular weight marker, lanes 1-3: *RPLO* at 59^{0}C, 60^{0}C and 61^{0}C annealing temperatures, lanes 5-7*: β-actin* at 59^{0}C, 60^{0}C and 61^{0}C annealing temperatures, lanes 4,8,9*: TGF-β$_2$* at 59^{0}C, 60^{0}C and 61^{0}C annealing temperatures, lanes 10-12: *β-catenin* at 59^{0}C, 60^{0}C and 61^{0}C annealing temperatures, lanes :13-15 *POU5F1* at 59^{0}C, 60^{0}C and 61^{0}C annealing temperatures, lanes: 16-18 *FGF-R1* at 59^{0}C, 60^{0}C and 61^{0}C annealing temperatures, lanes: 19-21 *SMAD-3* at 59^{0}C, 60^{0}C and 61^{0}C annealing temperatures.

Figure 6 shows the amplification products with primers for *SMAD-4*, *CD-10*, *FGF-2*, *TGF-β_3*, *SMAD-5*, *RPL13a*, *FGF-R1*, *WNT3a*, *Noggin*, *SMAD-1*, *SOX-2* and *BMP-7/OP-1*. PCR products of the expected length were amplified and the optimal annealing temperature for downstream qPCR analysis was determined to be 60^0C.

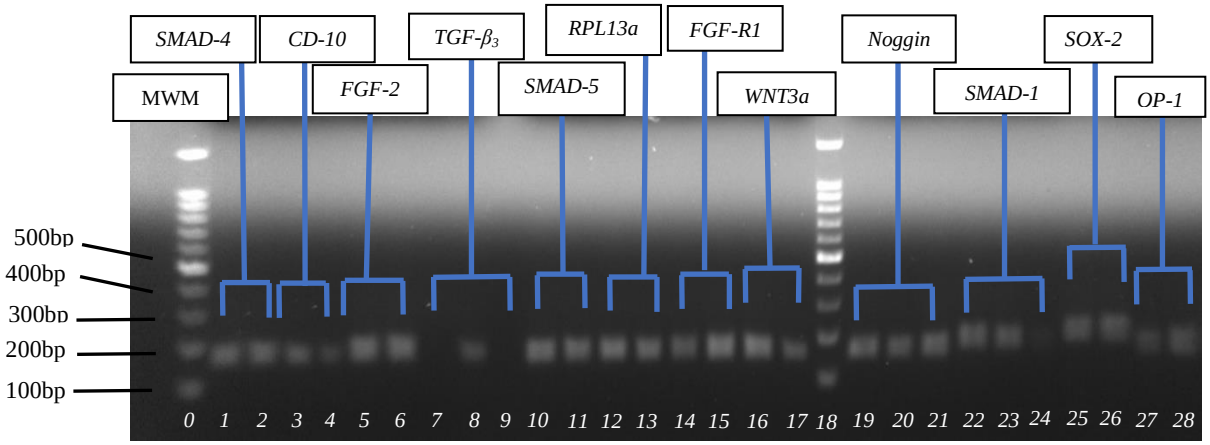


Figure 6: 1% Agarose gel of optimized qRT-PCR primer amplicons

1% agarose gel of qRT-PCR primer products *SMAD-4*, *CD-10*, *FGF-2*, *TGF-β_3*, *SMAD-5*, *RPL13a*, *FGF-R1*,*WNT3a*, *Noggin*, *SMAD-1*, *SOX-2*, *BMP-7/OP-1*were run using a gradient of 2 different annealing temperature namely 59^0C and 60^0C. Lanes 0 and 18: 100 bp molecular weight marker, lanes 1-2: *SMAD-4* at 59^0C and 60^0C annealing temperatures, lanes 3-4: *CD-10* at 59^0C and 60^0C annealing temperatures, lanes 5-6: *FGF-2* at 59^0C and 60^0C annealing temperatures, lanes7-9: *TGF-β_3* at 59^0C, 60^0C and 61^0C annealing temperatures, lanes :10-11 *SMAD-5* at 59^0C and 60^0C annealing temperatures, lanes: 12-13 *RPL13a* at 59^0C and 60^0C annealing temperatures, lanes: 14-15 *FGF-R1* at 59^0C and 60^0C annealing temperatures, lanes: 16-17 *WNT3a* at 59^0C and 60^0C annealing temperatures, lanes: 19-21 *Noggin* at 59^0C, 60^0C and 61^0C annealing temperatures, lanes: 22-24 *SMAD-1* at 59^0C, 60^0C and 61^0C annealing temperatures, lanes: 25-26 *SOX-2* at 59^0C and 60^0C annealing temperatures, lanes:27-28 *BMP-7/OP-1* at 59^0C and 60^0C annealing temperatures.

In figure 7, *BMP-6*, *TGF-β_1*, *BMP-2*, *BMP-4*, *SMAD-2*, *BMP-9*, *CRYαB*, *FGF-1*, *SDHA*, *ColI*, *CD-92* amplified with products of the expected length and gradient temperature analysis determined optimal annealing temperatures for these primer pairs to be 60^0C.

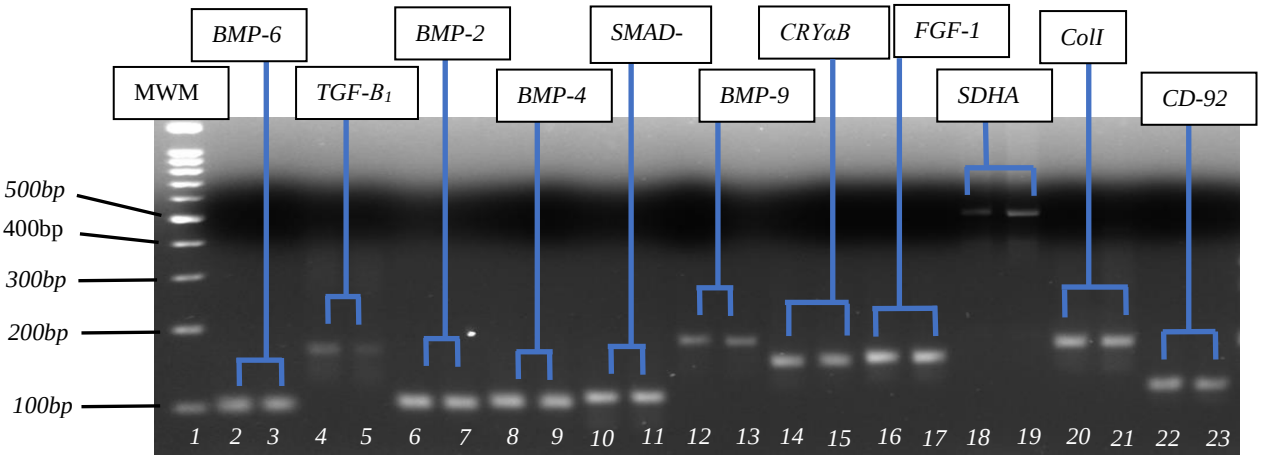


Figure 7: 1% Agarose gel of optimized qRT-PCR primer amplicons

1% agarose gel of qRT-PCR primer products *BMP-6*, *TGF-β_1*, *BMP-2*, *SMAD-2*, *BMP-9*, *CRYαB* , *FGF-1*, *SDHA*, *Col1*, *CD-92* were run using a gradient of 2 different annealing temperature namely 59^0C and 60^0C. Lanes 1: 100 bp molecular weight marker, lanes 2-3: *BMP-6* at 59^0C and 60^0C annealing temperatures, lanes 4-5: *TGF-β_1* at 59^0C and 60^0C annealing temperatures, lanes 6-7: *BMP-2* at 59^0C and 60^0C annealing temperatures, lanes 8-9: *BMP-4* at 59^0C and 60^0C annealing temperatures, lanes :10-11 *SMAD-2* at 59^0C and 60^0C annealing temperatures, lanes: 12-13 *BMP-9* at 59^0C and 60^0C annealing temperatures, lanes: 14-15 *FGF-R1* at 59^0C and 60^0C annealing temperatures, lanes: 14-15 *CRYαB* at 59^0C and 60^0C annealing temperatures, lanes: 16-17 *FGF-1* at 59^0C and 60^0C annealing temperatures, lanes: 18-19 *SDHA-1* at 59^0C and 60^0C annealing temperatures, lanes: 20-21 *ColI* at 59^0C and 60^0C annealing temperatures, lanes:22-23 *CD-92* at 59^0C and 60^0C annealing temperatures.

4.2 qRT-PCR

Gene expression analysis by qRT-PCR was performed to monitor the relative changes in the expression of the TGF isoforms, BMP isoforms, FGFs and their receptors, SMADs and stem cell markers. The results portrayed represent a snapshot of the changes in gene expression levels on days 17, 19, 23, 25, 27 and 30 after the implantation of the hTGF-β_3 treated bioreactors *in vivo.* Analyses were performed on both the devices themselves and on the surrounding muscle tissue. Results are expressed relative to the distant muscle control and normalised to three reference genes namely, *RPLPO*, *SDHA* and *ACTB*.

4.2.1 *β-Catenin*

Seventeen days after implantation with the treated 7% HA/CC constructs, *β-catenin* expression was found to be down-regulated in the device relative to the control muscle tissue (Fig. 8). At 19, 23 and 27 days *β-catenin* expression the device was up-regulated. However, a reduction in gene expression was seen at 25 days. *β-catenin* expression in the device returned to levels similar to the muscle control at day 30. The decrease in *β-catenin* expression levels in the device was significant between days 23 and 25 (p=0.035). In the surrounding muscle, *β-catenin* expression was down-regulated at 17, 25 and 27 days and was up-regulated relative to the distant muscle control at days 19, 23 and 30. Significant increases in gene expression were present between 19 days and 30 days (p=0.032) and 27 days and 30 days (p=0.029).

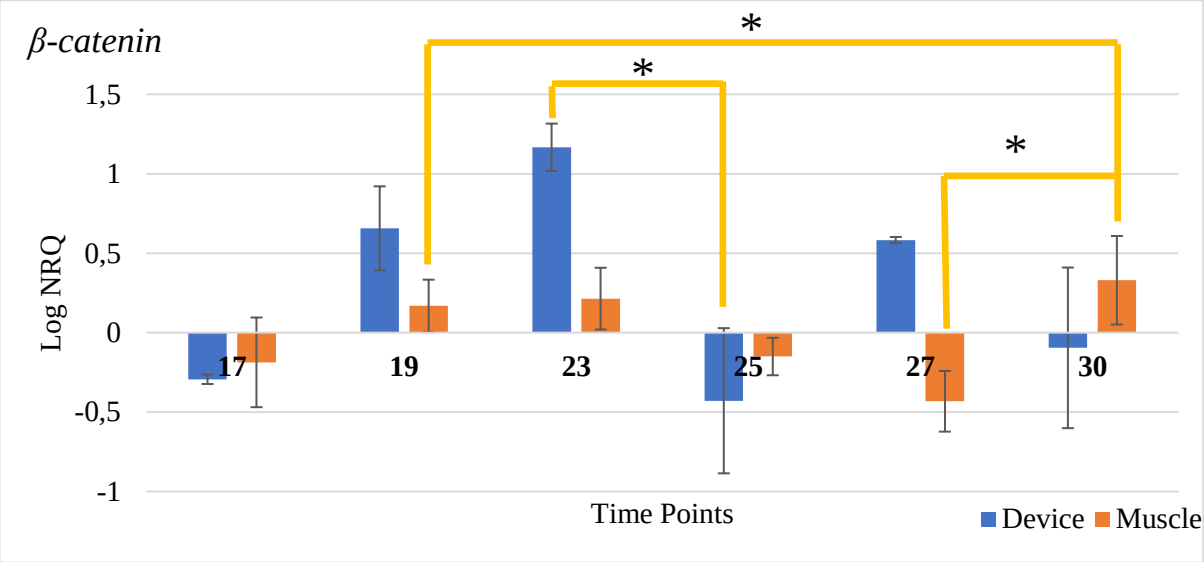


Figure 8: Relative changes in the expression of *β-catenin* at 17, 19, 23, 25, 27 and 30 days after implantation of the 125 µg hTGF-β_3 preloaded coral-derived constructs into the *rectus abdominis* muscle of four adult *Papio ursinus*, Chacma baboons. Gene expression is reported relative to the control muscle tissue harvested away from the site of implantation and was normalised to 3 reference genes. Student T-test was used to determine significance (green, yellow and red lines represent: p<0,07; *p<0.05 and **p<0.01 respectively).

4.2.2 *Bone morphogenic protein-2, -3, -4, -6 & -7*

At day 17 *BMP-2* expression in the device was found to be down-regulated relative to the control muscle tissue (Fig. 9A). From days 19 to 30, *BMP-2* expression in the device samples was up-regulated. A significant increase in *BMP-2* expression was present between days 17 and 30 ($p=0.042$). Muscle samples at 17 days were found to be up-regulated but expression was down-regulated at days 19 and 23. *BMP-2* expression in the adjacent muscle was up-regulated at days 25, 27 and 30. Significant increases in *BMP-2* expression in muscle samples was found to be present between 19 and 30 days ($p=0.01$), 23 and 25 days ($p=0.005$), 23 and 27 days ($p=0.029$) and 23 and 30 days ($p=1.5 \times 10^{-5}$). A significant decrease in expression was present between 25 and 30 days ($p=0.045$).

At days 17, 19 and 30 *BMP-4* expression in the device samples was found to be down-regulated relative to the control muscle tissue (Fig. 9B). At days 23 and 27, *BMP-4* expression in the device samples was up-regulated. At day 25 *BMP-4* expression in the device samples did not differ from the control muscle levels. A significant increase in *BMP-4* expression was present between days 25 and 27 ($p=0.047$). In the adjacent muscle samples, *BMP-4* expression was found to be down-regulated at day 19. *BMP-4* expression in the muscle samples did not differ from control muscle levels at days 17, 23, 25 and 30. A significant increase in *BMP-4* expression in muscle samples was found to be present between 19 and 30 days ($p=0.014$).

In the device samples, *BMP-6* expression was down-regulated relative to the control muscle tissue at days 17, 19, 23, 25, 27 and 30 (Fig. 9C). Significant decreases in *BMP-6* expression in the device samples was found between days 19 and 23 ($p=0.032$) and between days 19 and 25 ($p=0.044$). In the adjacent muscle samples, *BMP-6* expression was down-regulated relative to the control muscle tissue at days 17, 19, 23, 25, 27 and 30 (Fig. 9C). Significant differences in *BMP-6* expression in muscle samples was found between days 23 and 25 ($p=0.049$), days 25 and 30 ($p=0.047$) and days 23 and 30 ($p=7.05 \times 10^{-5}$).

In the device samples, *BMP-7/OP-1* expression at days 17 and 25 were found to be down-regulated, but at day 17 was not significant. At days 19 and 23 *BMP-7/OP-1* expression in the device samples were found to be up-regulated. Up-regulation at day 19 was found not to be statistically significant. *BMP-7/OP-1* expression was up-regulated at day 27 and 30 in device samples, but this was not statistically significant. (Fig. 9D). Within the muscle samples *BMP-7/OP-1* expression remained at the levels of the distant muscle control at days 17, 25 and 30.

Down-regulation of *BMP-7/OP-1* in the muscle samples was found at days 19, 23 and 27 (Fig. 9D).

Up-regulation of *BMP-9* expression in the device samples was found at 17, 19, 23, and 25 days. *BMP-9* expression in the device was found to be up-regulated, but not statistically significant at days 27 and 30. Significant decreases in *BMP-9* expression in the device was found between days 19 and 25 ($p=0.033$) and a decreasing trend between days 23 and 25 ($p=0.059$) (Fig. 9E). In the muscle samples *BMP-9* expression was up-regulated at days 17, 23 and 25. Down-regulation of *BMP-9* in the muscle sample was found at days 19, 27 and 30. Significant decreases in *BMP-9* expression in the muscle samples were found between days 17 and 19 ($p=0.0001$), days 17 and 27 ($p=0.009$), days 17 and 30 ($p=0.0006$), days 23 and 30 ($p=0.004$), days 25 and 27 ($p=0.016$) and days 25 and 30 ($p=0.006$). Significant increases in *BMP-9* expression in muscle samples were found between days 19 and 23 ($p=0.04$) and days 19 and 25 ($p=0.008$) (Fig. 9E).

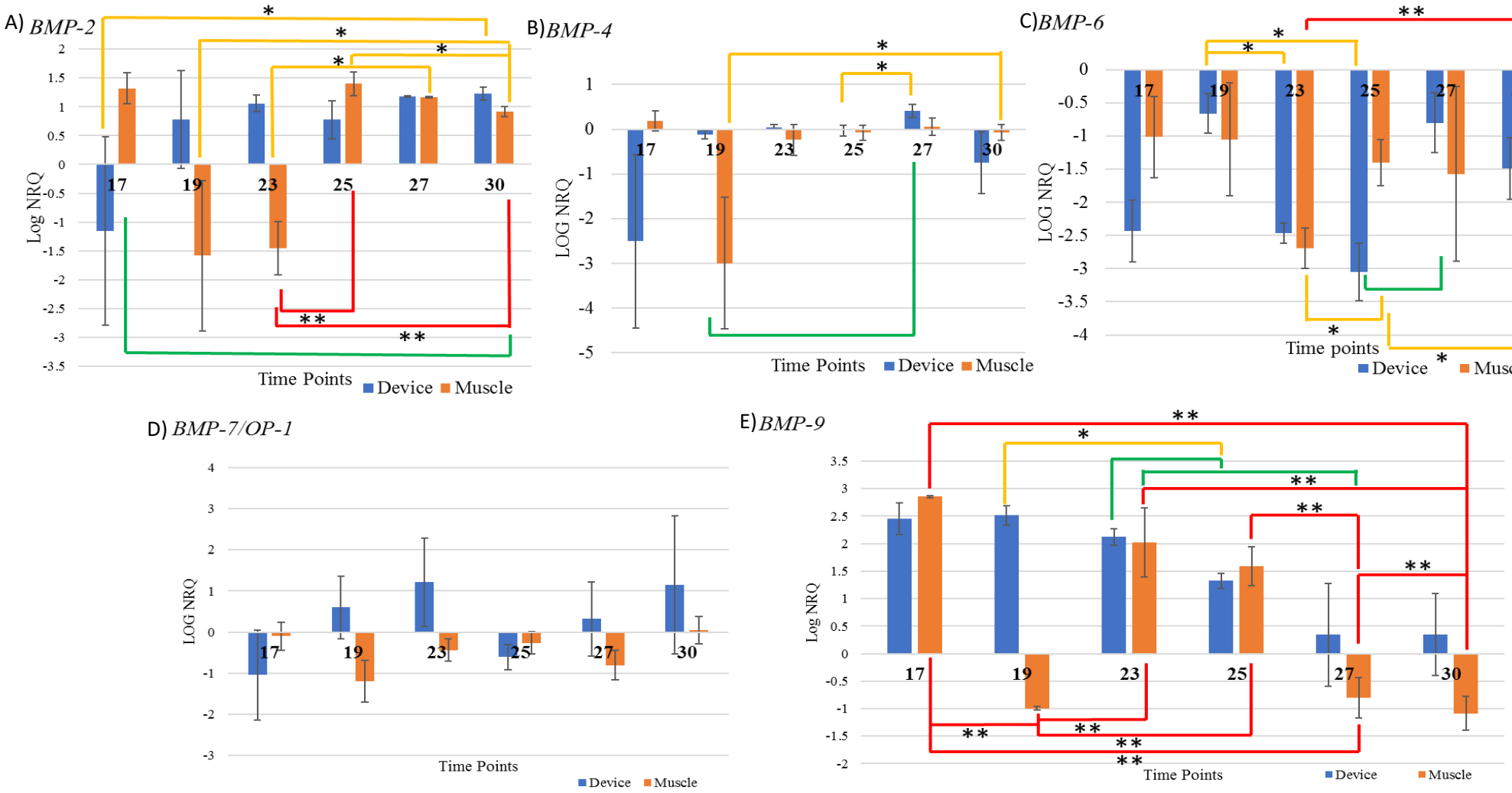


Figure 9: Relative changes in the expression of *BMP-2* (A), *BMP-4* (B), *BMP-6* (C), *BMP-7* (D) *and BMP-9* (E) at 17, 19, 23, 25, 27 and 30 days after implantation of the 125 µg hTGF-β_3 preloaded coral-derived constructs into the *rectus abdominis* muscle of four adult *Papio ursinus*, Chacma baboons. Gene expression is reported relative to the control muscle tissue harvested away from the site of implantation and was normalised to 3 reference genes. Student T-test was used to determine significance (green, yellow and red lines represent: $p<0,07$; *$p<0.05$ and **$p<0.01$ respectively).

4.2.3 *CD-10*

In the device samples *CD-10* expression was down-regulated at days 17, 19, 23, 25, 27 and 30 relative to the expression observed in normal control muscle tissue (Fig. 10). Significant decreases in *CD-10* expression were found in the device samples between days 17 and 25 (p= 0.014), days 19 and 25 (p=0.027) and days 23 and 25 (p=0.04). Similarly, in muscle samples at days 17, 19, 23, 25, 27 and 30, *CD-10* expression was down-regulated in muscle samples (Fig. 10). Down-regulation of *CD-10* at day 17 was found to be non-statistically significant in muscle samples.

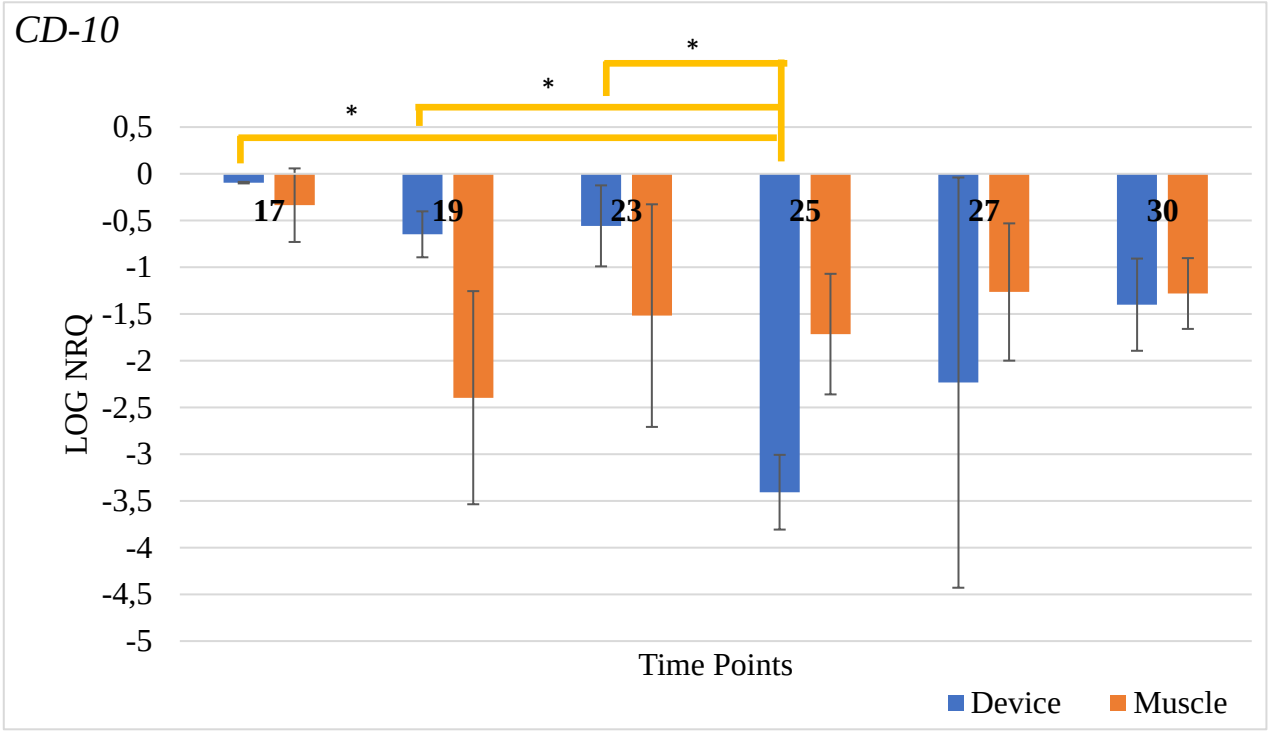


Figure 10: Relative changes in the expression of *CD-10* at 17, 19, 23, 25, 27 and 30 days after implantation of the 125 µg hTGF-β_3 preloaded coral-derived constructs into the *rectus abdominis* muscle of four adult *Papio ursinus*, Chacma baboons. Gene expression is reported relative to the control muscle tissue harvested away from the site of implantation and was normalised to 3 reference genes. Student T-test was used to determine significance (green, yellow and red lines represent: p<0,07; *p<0.05 and **p<0.01 respectively).

4.2.4 *CD-92*

At day seventeen and day 30 after implantation of treated 7% HA/CC constructs, *CD-92* expression was found to be down-regulated in the device samples. *CD-92* expression at days 19, 23, 25 and 27 were at levels similar to that seen in the control muscle tissue (Fig. 11). In muscle samples *CD-92* expression was similar to control muscle tissue expression levels at day 17. Muscle samples were down-regulated at days 19, 23, 27 and 30. However, *CD-92* expression in muscle samples was up-regulated at day 25. A significant increase in expression in muscle samples was found between days 17 and 25 (p=0.002), with an increasing expression trend between days 23 and 25. Significant decreases in expression were found between days 25 and 27 (p=0.02) and days 25 and 30 (p=0.018) (Fig. 11).

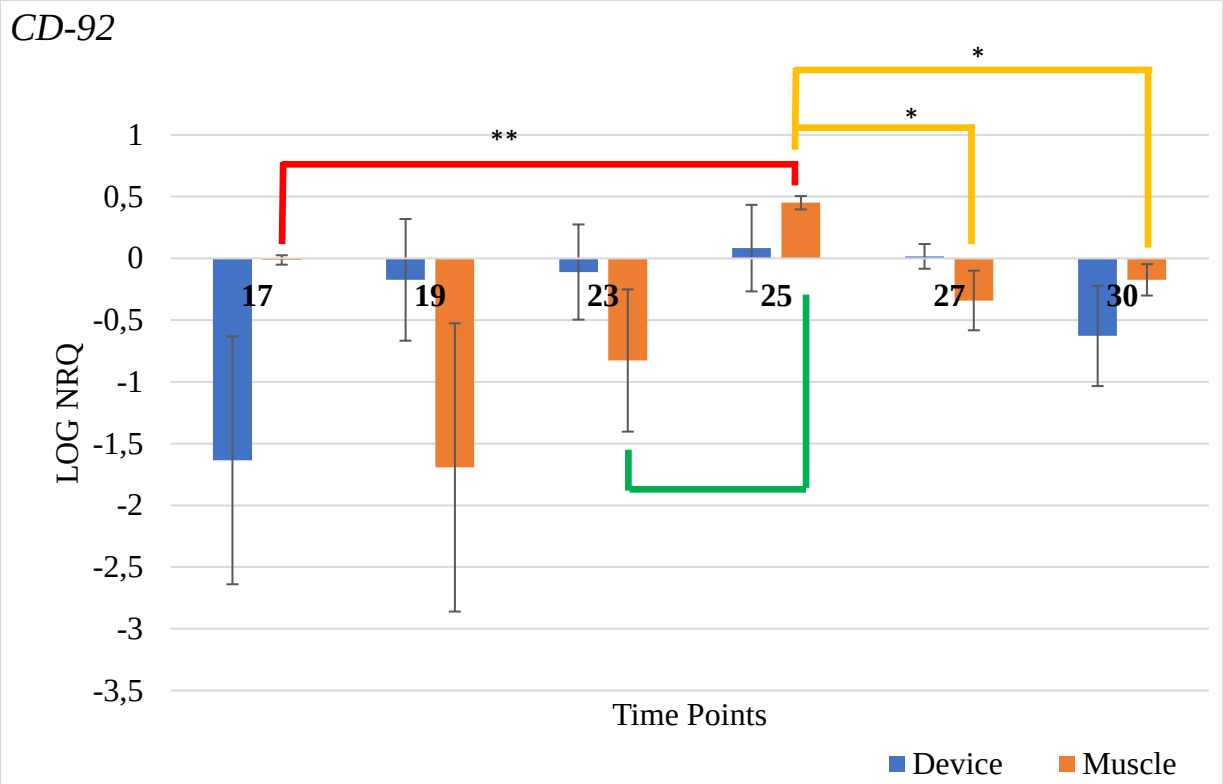


Figure 11: Relative changes in the expression of *CD-92* at 17, 19, 23, 25, 27 and 30 days after implantation of the 125 µg hTGF-β_3 preloaded coral-derived constructs into the *rectus abdominis* muscle of four adult *Papio ursinus*, Chacma baboons. Gene expression is reported relative to the control muscle tissue harvested away from the site of implantation and was normalised to 3 reference genes. Student T-test was used to determine significance (green, yellow and red lines represent: p<0,07; *p<0.05 and **p<0.01 respectively).

4.2.5 *Collagen type I*

Collagen type I expression in device samples was up-regulated at days 17, 19, 23, 25, 27 and 30. Significant increases in *ColI* expression in the devices was found between days 17 and 19 (p=0.008), days 17 and 23 (p=0.003), days 19 and 23 (p=0.019) and days 17 and 25 (p=0.043) (Fig. 12). A significant decrease in gene expression was found in device samples between days 23 and 25 (p=0.018) (Fig. 12). In muscle samples *ColI* expression was up-regulated at days 17, 19, 23, 25, 27 and 30 (Fig. 12).

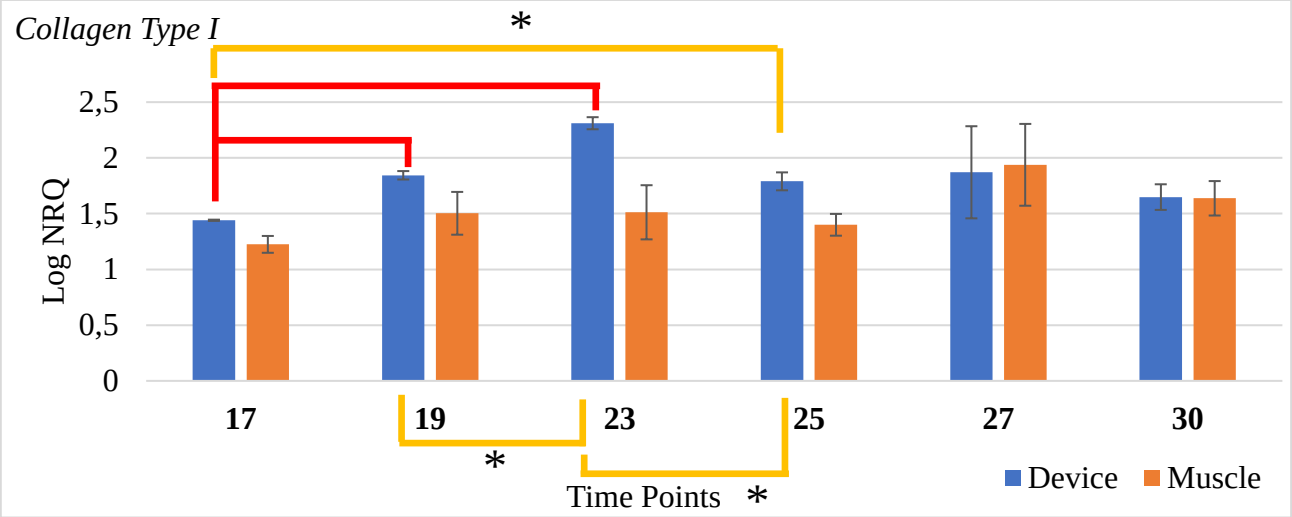


Figure 12: Relative changes in the expression of *Collagen type I* at 17, 19, 23, 25, 27 and 30 days after implantation of the 125 µg hTGF-β_3 preloaded coral-derived constructs into the *rectus abdominis* muscle of four adult *Papio ursinus*, Chacma baboons. Gene expression is reported relative to the control muscle tissue harvested away from the site of implantation and was normalised to 3 reference genes. Student T-test was used to determine significance (green, yellow and red lines represent: p<0,07; *p<0.05 and **p<0.01 respectively).

4.2.6 *CRYαB-14*

CRYαB-14 expression was down-regulated in the device samples on days 17, 19, 23, 25, 27 and 30 after implantation of the treated 7% HA/CC constructs (Fig. 13). Down-regulation of *CRYαB-14* at day 19 was found to be non-statistically significant in device samples. In muscle samples *CRYαB-14* expression was found to be down-regulated at days 17, 23, 25 and 30. *CRYαB-14* expression was at levels similar to the control muscle tissue at day 19 and 27 in muscle samples. An increasing trend in *CRYαB-14* expression was present between days 23 and 30 within muscle samples (Fig. 13).

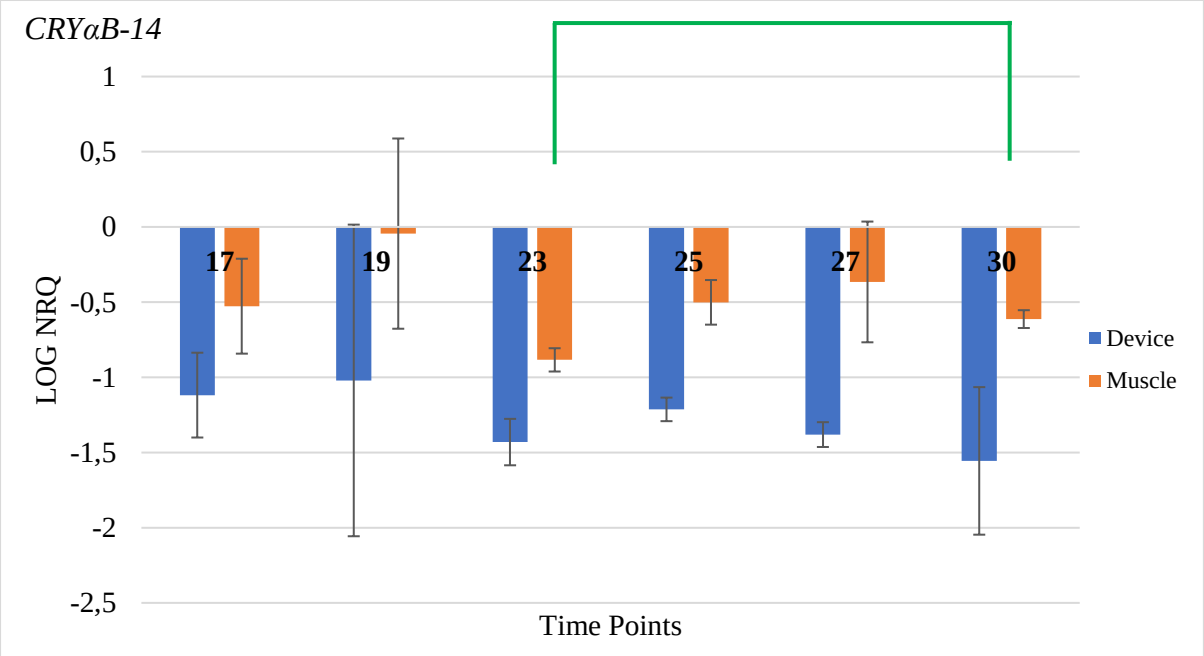


Figure 13: Relative changes in the expression of *CRYαB-14* at 17, 19, 23, 25, 27 and 30 days after implantation of the 125 µg hTGF-β_3 preloaded coral-derived constructs into the *rectus abdominis* muscle of four adult *Papio ursinus*, Chacma baboons. Gene expression is reported relative to the control muscle tissue harvested away from the site of implantation and was normalised to 3 reference genes. Student T-test was used to determine significance (green, yellow and red lines represent: $p<0,07$; *$p<0.05$ and **$p<0.01$ respectively).

4.2.7 *Fibroblast growth factors*

At days 17, 19, 25, 27 and 30 after implantation with the treated 7% HA/CC constructs, *FGF-1* expression was down-regulated in the device samples relative to the control muscle tissue. *Fibroblast Growth Factor-1* was at levels similar to the control muscle tissue at day 23. Significant decreases in *FGF-1* expression were found between days 23 and 25 ($p=0.008$), and days 23 and 30 ($p=0.035$) (Fig. 14A). In the adjacent muscle samples, *FGF-1* expression was found to be down-regulated at days 17, 19, 23, 25, 27 and 30 (Fig. 14A).

At days 17, 19, 23, 27 and 30 after implantation with the treated 7% HA/CC constructs, *FGF-2* expression was found to be down-regulated in the device samples relative to the control muscle tissue (Fig. 14B). At day 25, *FGF-2* expression in the device samples was found to be at levels similar to the control muscle tissue. Significant differences were found between days 17 and 23 ($p=0.027$) and days 17 and 27 ($p=0.035$) in the device samples. In muscle samples *FGF-2* expression was found to be down-regulated at days 17, 19, 23, 25, 27 and 30 (Fig. 14B).

FGF-R1 expression was found to be down-regulated at day 17 in the device samples. At days 19 and 27, *FGF-R1* expression in device samples was up-regulated. *FGF-R1* expression remained at levels similar to that of the control at days 23, 25 and 30 (Fig. 14C). In muscle samples, *FGF-R1* expression levels were similar to the control levels at days 17, 25 and 30. At days 19, 23 and 27, *FGF-R1* expression was found to be down-regulated. Significant increases in *FGF-R1* expression was found between days 19 and 30 ($p=0.045$) in the adjacent muscle samples (Fig. 14C).

FGF-R2 expression in the device samples was found to be down-regulated at days 19 and 23. *FGF-R2* expression was non-significantly downregulated on days 17, 27 and 30 in device samples relative to control muscle tissue expression levels (Fig. 14D). In muscle samples *FGF-R2* expression was down-regulated at days 17, 19, 23, 25 and 30. Muscle sample expression was similar to control muscle tissue levels at day 27. Significant differences in *FGF-R2* expression was found between day 19 and 30 ($p=0.048$) in the adjacent muscle samples (Fig. 14D).

.

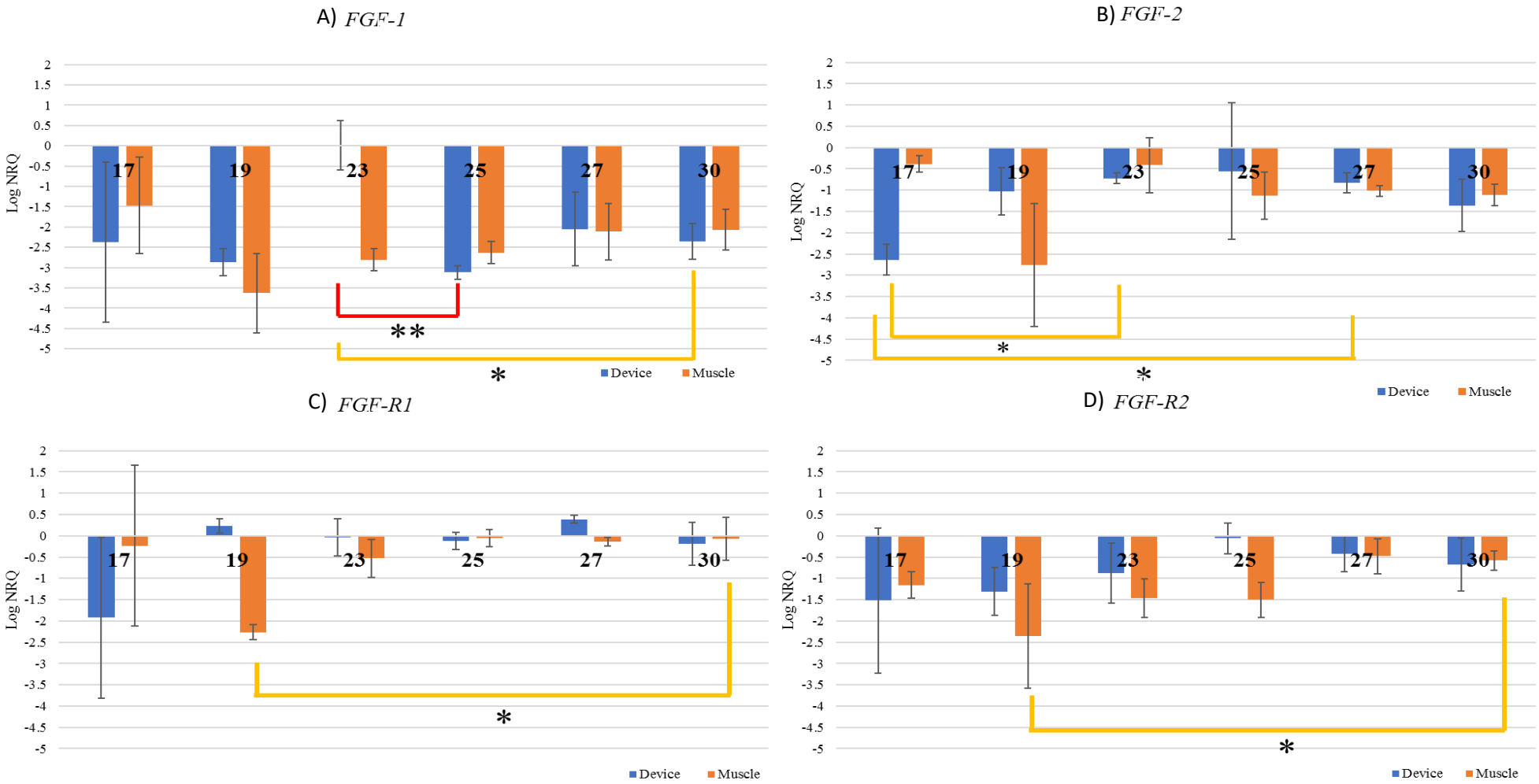


Figure 14: Relative changes in the expression of *FGF-1* (A), *FGF-2* (B), *FGF-R1* (C), *FGF-R2* (D) at 17, 19, 23, 25, 27 and 30 days after implantation of the 125 µg hTGF-β_3 preloaded coral-derived constructs into the *rectus abdominis* muscle of four adult *Papio ursinus*, Chacma baboons. Gene expression is reported relative to the control muscle tissue harvested away from the site of implantation and was normalised to 3 reference genes. Student T-test was used to determine significance (green, yellow and red lines represent: $p<0,07$; *$p<0.05$ and **$p<0.01$ respectively).

4.2.8 *Noggin*

Noggin expression in the device samples was found to be down-regulated at days 17, 19, 23, 25, 27 and 30 although the downregulation was not significant at day 23. A significant decrease in *Noggin* expression was found between days 25 and 27 (p=0.018) in the device samples (Fig. 15). In the muscle samples, *Noggin* expression was down-regulated at days 19, 23, 27 and 30. Significant decreases in *Noggin* expression were found between days 17 and 19 (p=0.04), days 17 and 27 (p=0.0008), days 17 and 30 (p=0.04), days 25 and 27 (p=0.0006) and days 25 and 30 (p=0.024). In muscle samples *Noggin* expression was found to be up-regulated at days 17 and 25. Significant increases in *Noggin* expression were found between days 19 and 25 (p=0.025), days 19 and 27 (p=0.014) and days 19 and 30 (p=0.0003) (Fig. 15).

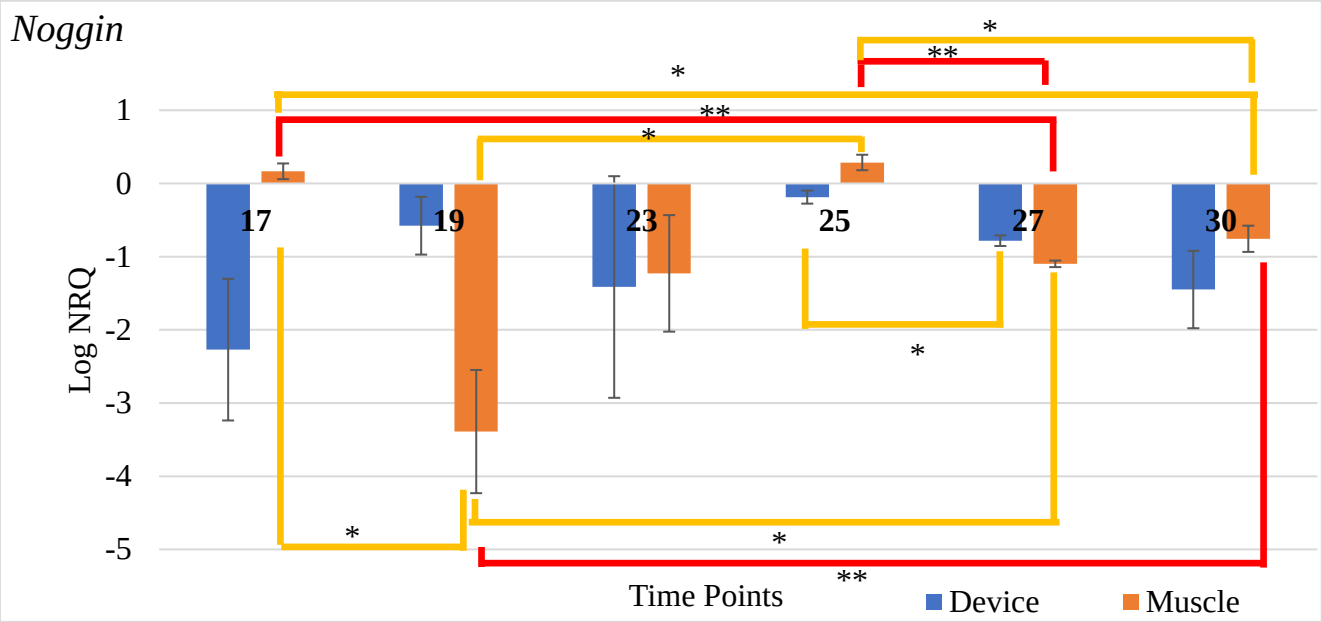


Figure 15: Relative changes in the expression of *Noggin* at 17, 19, 23, 25, 27 and 30 days after implantation of the 125 µg hTGF-β_3 preloaded coral-derived constructs into the rectus abdominis muscle of four adult *Papio ursinus*, Chacma baboons. Gene expression is reported relative to the control muscle tissue harvested away from the site of implantation and was normalised to 3 reference genes. Student T-test was used to determine significance (green, yellow and red lines represent: p<0,07; *p<0.05 and **p<0.01 respectively).

4.2.9 *POU5F1*

POU5F1 expression in device samples was found to be at control expression levels on days 17, 19 and 30. *POU5F1* expression was found to be down-regulated at day 23 and up-regulated at days 25 and 27 in the device samples (Fig. 16). In muscle samples *POU5F1* expression was found to be down-regulated at days 17, 23 and 30 and was at the level of the control muscle at days 19, 25 and 27. Trends of increasing *POU5F1* expression were found in muscle samples between days 23 and 25 and days 23 and 27 (Fig. 16).

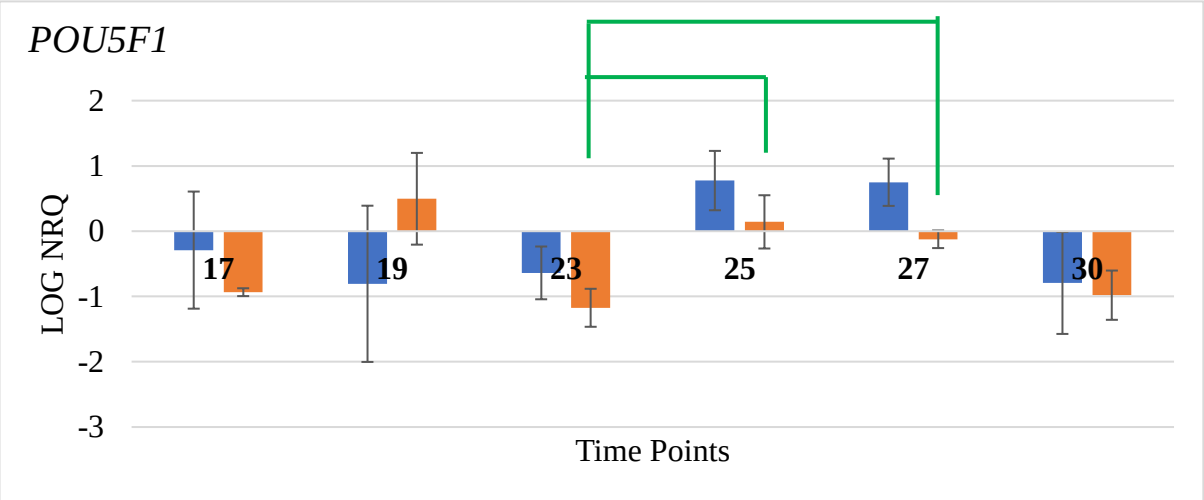


Figure 16: Relative changes in the expression of *POU5F1* at 17, 19, 23, 25, 27 and 30 days after implantation of the 125 µg hTGF-β_3 preloaded coral-derived constructs into the rectus abdominis muscle of four adult *Papio ursinus*, Chacma baboons. Gene expression is reported relative to the control muscle tissue harvested away from the site of implantation and was normalised to 3 reference genes. Student T-test was used to determine significance (green, yellow and red lines represent: $p<0,07$; *$p<0.05$ and **$p<0.01$ respectively).

4.2.10 *SMADs*

At days 17, 23 and 27 *SMAD-1* expression were found to be up-regulated in the device samples and it was found to be down-regulated at day 19. At days 25 and 30 *SMAD-1* expression were found to be similar to control muscle tissue expression levels in the device samples. Significant increases in gene expression were found between days 19 and 23 ($p=0.04$) and days 19 and 27 ($p=0.006$) in device (Fig. 17A). In muscle samples *SMAD-1* expression was found to be down-regulated at 17, 19, 23 and 25 days. Expression of *SMAD-1* in the adjacent muscle was at levels similar to the control muscle tissue at days 27 and 30 (Fig. 17A).

Seventeen days after implantation with the treated 7% HA/CC constructs, *SMAD-2* was found to be down-regulated in device samples relative to the control muscle tissue (Fig. 17B). At days 19, 23, 25 and 27 *SMAD-2* expression were up-regulated in the device samples. At day 30 *SMAD-2* expression in the device samples was at levels similar to that of the control muscle tissue. Significant differences in *SMAD-2* expression in the device samples were found between days 17 and 19 ($p=0.012$), days 17 and 23 ($p=0.005$), days 17 and 25 ($p=0.003$), days 17 and 27 ($p=0.007$) and days 23 and 27 ($p=0.029$). In muscle samples *SMAD-2* expression up-regulated but not statistically significant relative to control muscle tissue at days 17. At days 23, 25, 27 and 30 *SMAD-2* expression were up-regulated. Down-regulation at day 19 of *SMAD-2* was found not to be statistically significant. Significant increases in *SMAD-2* expression in muscle samples was present between days 19 to 23 ($p=0.024$), 19 to 25 ($p=0.027$) and 19 to 30 ($p= 0.0003$).

At 17, 19, 23 and 30 days *SMAD-3* expression in the device samples was at expression levels similar to the control muscle tissue. At 25 and 27 days, *SMAD-3* expression was found to be up-regulated in device samples (Fig. 17C). In muscle samples *SMAD-3* expression was found to be down-regulated at 17, 19, 23 and 25 days. At days 27 and 30 *SMAD-3* expression was found to be up-regulated. Significant increases in *SMAD-3* expression in the adjacent muscle tissue was found between days 17 and 25 ($p=0.048$), days 17 and 30 ($p=0.0005$), days 19 and 25 ($p=0.036$), days 19 and 30 ($p=0.0001$), days 23 and 25 ($p=0.007$), days 23 and 27 ($p=0.022$) and days 23 and 30 ($p=1.07 \times 10^{-5}$) (Fig. 17C).

At days 17, 19, 23, 25 27 and 30 *SMAD-4* expression was found to be up-regulated in the device samples relative to control muscle tissue. A trend towards a significant difference between days 17 and 30 was found in device samples (Fig. 17D). In adjacent muscle samples *SMAD-4*

expression at days 17, 25, 27 and 30 was up-regulated. *SMAD-4* expression levels were at the levels of the control tissue at days 19 and 23. A trend towards differences in expression levels was found between days 25 and 27 in the muscle samples (Fig. 17D).

At days 17, 25 and 30 *SMAD-5* expression were down-regulated in device samples. At days 19 *SMAD-5* expression in the device samples was similar to control muscle expression levels. *SMAD-5* expression was up-regulated in the device samples at day 27. A significant increase in *SMAD-5* expression was found between days 25 and 27 ($p=0.03$) and a trend towards a significant decrease in expression between days 23 and 25 (Fig. 17E). In muscle samples *SMAD-5* expression was down-regulated at days 17, 19, 25, 27 and 30. At day 23 *SMAD-5* expression was similar to control muscle expression levels (Fig. 17D).

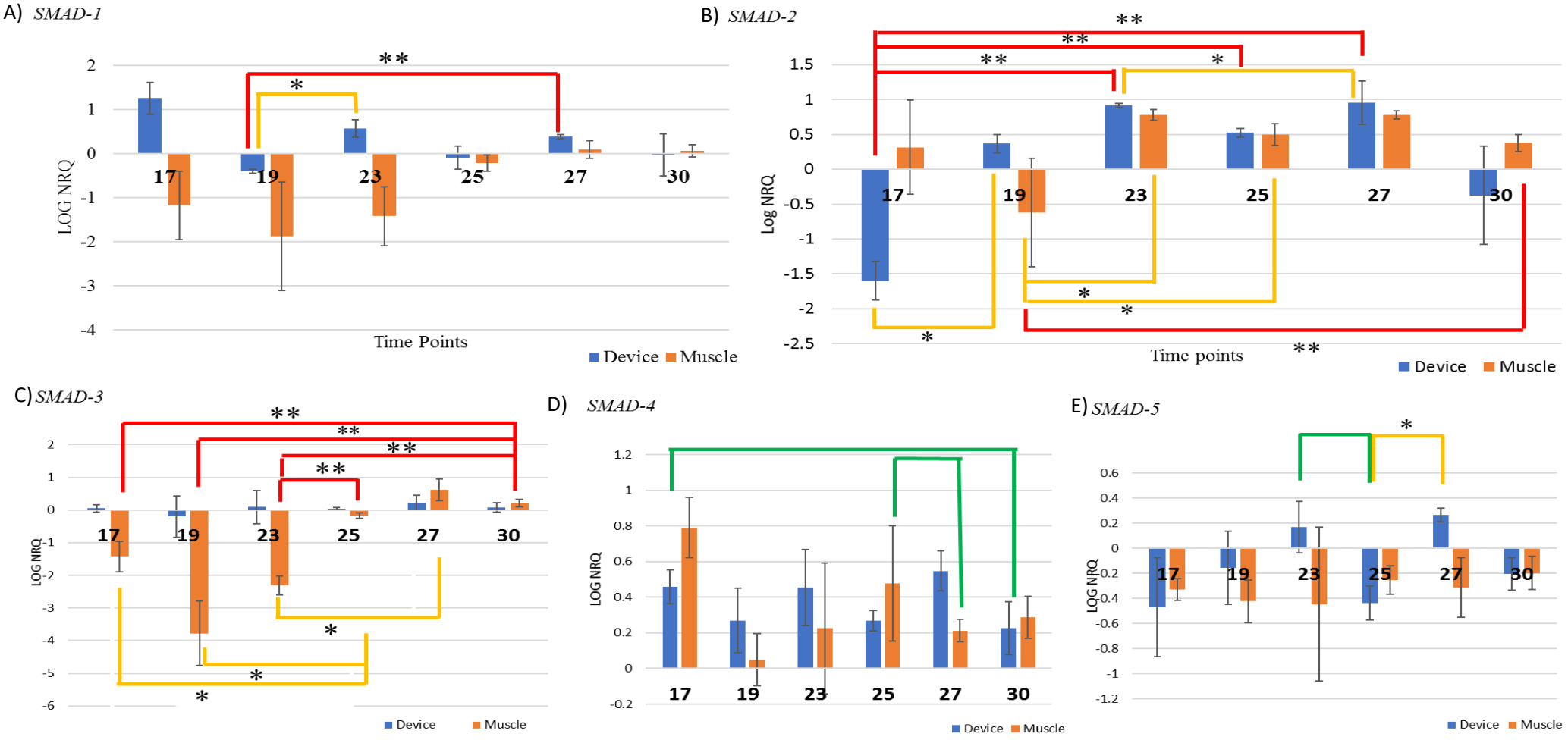


Figure 17: Relative changes in the expression of *SMAD-1* (A), *SMAD-2* (B), *SMAD-3* (C), *SMAD-4* (D) *and SMAD-5* (E) at 17, 19, 23, 25, 27 and 30 days after implantation of the 125 µg hTGF-β_3 preloaded coral-derived constructs into the *rectus abdominis* muscle of four adult *Papio ursinus*, Chacma baboons. Gene expression is reported relative to the control muscle tissue harvested away from the site of implantation and was normalised to 3 reference genes. Student T-test was used to determine significance (green, yellow and red lines represent: $p<0,07$; *$p<0.05$ and **$p<0.01$ respectively).

4.2.11 *TGF-β*

At days 17, 19, 23, 25, 27 and 30 *TGF-* β_1 expression in the device samples was up-regulated. Significant increases in *TGF-* β_1 expression device samples were found between days 17 and 23 ($p=0.029$) and days 17 and 27 ($p=0.038$) with a trend towards a difference in gene expression present between days 23 to 25 and days 25 to 27 (Fig. 18A). In muscle samples *TGF-* β_1 expression was up-regulated at days 17, 23, 25, 27 and 30. *TGF-* β_1 expression was down-regulated at day 19. Significant increases in *TGF-* β_1 expression in muscle samples was found between days 17 and 27 ($p=0.038$) days 17 and 30 ($p=0.041$), days 19 and 23 ($p=0.042$), days 19 and 25 ($p=0.026$), days 19 and 30 ($p=8.84 \times 10^{-5}$), days 23 and 25 ($p=0.035$) and days 23 and 30 ($p=0.004$). Significant decreases in *TGF-* β_1 expression was found in muscle samples between days 17 and 19 ($p=0.031$) (Fig. 18A)

At days 17, 19, 23, 25, 27 and 30 *TGF-* β_2 expression was down-regulated relative to control muscle tissue expression levels (Fig. 18B). In muscle samples *TGF-* β_2 expression also was downregulated at days 17, 19, 23, 25, 27 and 30. A significant decrease in *TGF-* β_2 expression was found between days 17 and 23 ($p=0.025$) and significant increases in *TGF-* β_2 expression found between days 17 and 25 ($p=0.035$), days 19 and 25 ($p=0.018$) and days 23 and 25 ($p=0.03$) in muscle samples (Fig. 18B)

Seventeen days after implantation with the treated 7% HA/CC constructs, *TGF-*β_3 expression was found to be down-regulated in the device samples relative to the control muscle tissue (Fig. 18C). At days 19, 23, 25 and 27 *TGF-*β_3 expression was found to be up-regulated in the device samples. At day 30 *TGF-*β_3 expression was found to be at levels similar to the control tissue. In the muscle samples *TGF-*β_3 expression at 17, 23, 25, 27 and 30 days was found to be up-regulated. At days 23 and 27 the up-regulation was found to be non-statistically significant. At day 19 *TGF-*β_3 expression was found to be down-regulated relative to the muscle control tissue. Significant increases in *TGF-*β_3 expression was found in muscle samples between days 17 and 25 ($p=0.016$) and days 19 and 30 ($p=0.029$) (Fig. 18C).

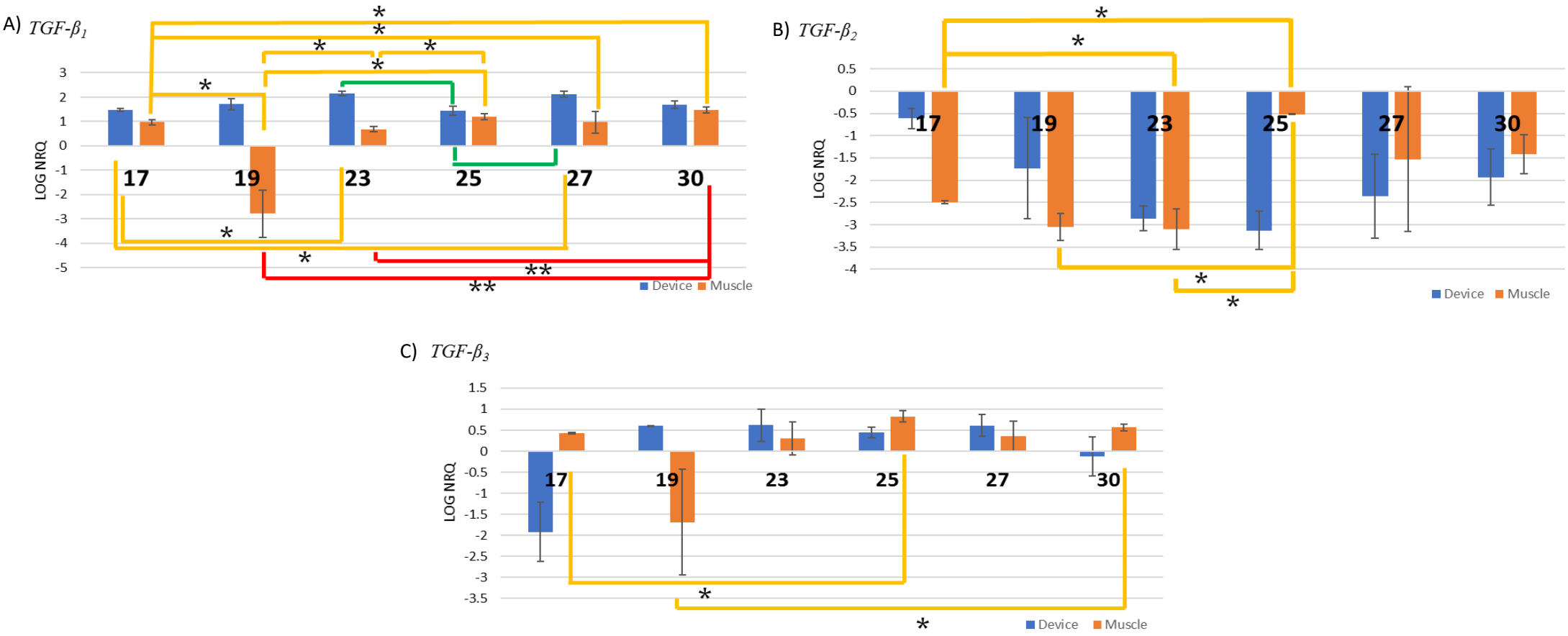


Figure 18: Relative changes in the expression of *TGF-β_1* (A), *TGF-β_2* (B) and *TGF-β_3* (C) at 17, 19, 23, 25, 27 and 30 days after implantation of the 125 µg hTGF-β_3 preloaded coral-derived constructs into the *rectus abdominis* muscle of four adult *Papio ursinus*, Chacma baboons. Gene expression is reported relative to the control muscle tissue harvested away from the site of implantation and was normalised to 3 reference genes. Student T-test was used to determine significance (green, yellow and red lines represent: $p<0,07$; *$p<0.05$ and **$p<0.01$ respectively).

4.2.12 *SOX-2*

Seventeen, twenty-seven and thirty days post implantation with the treated 7% HA/CC constructs, *SOX-2* expression was found to be up-regulated in device samples relative to the control muscle tissue. At days 19, 23 and 25 *SOX-2* expression was found to non-significantly up-regulated relative to control muscle tissue (Fig. 19). In muscle samples, *SOX-2* expression was found to be up-regulated at days 17, 19, 25 and day 30. *SOX-2* expression was at levels similar to the control muscle tissue at day 23. At day 27 *SOX-2* expression was found to be down-regulated in the muscle samples. Significant decreases in *SOX-2* expression were found between days 19 and 27 (p=0.036) and days 25 and 27 (p=0.005).

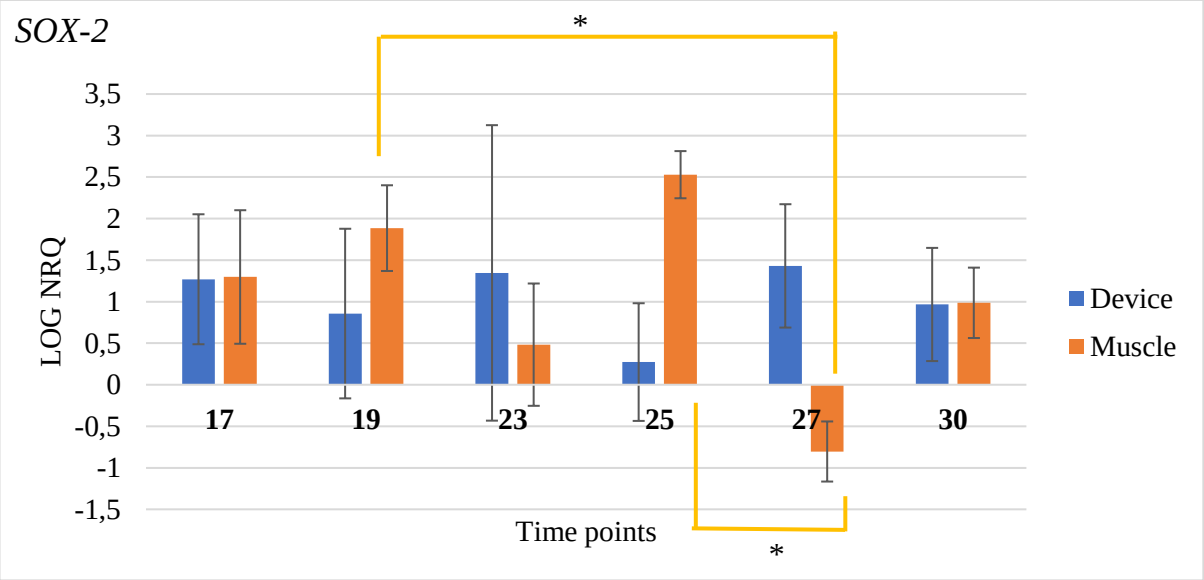


Figure 19: Relative changes in the expression of *SOX-2* at 17, 19, 23, 25, 27 and 30 days after implantation of the 125 µg hTGF-β_3 preloaded coral-derived constructs into the *rectus abdominis* muscle of four adult *Papio ursinus*, Chacma baboons. Gene expression is reported relative to the control muscle tissue harvested away from the site of implantation and was normalised to 3 reference genes. Student T-test was used to determine significance (green, yellow and red lines represent: p<0,07; *p<0.05 and **p<0.01 respectively).

5. Discussion

To comprehend the changes in patterns of gene expression during regenerative processes, it is imperative to understand the underlying molecular mechanisms that control and induce the regenerative potential of morphogenetic matrices. This study was focused on understanding the complexities involved in gene expression events that occur during the induction of bone formation during a defined period of time when macroporous bioreactors treated with hTGF-β_3 are implanted in heterotopic intramuscular sites in *Papio ursinus*. Treated bioreactors were harvested 17, 19, 23, 25, 27 and 30 days post implantation and RNA extracted from both the implanted device and surrounding adjacent muscle tissue. Relative quantitative real-time PCR analysis was used to analyse gene expression changes at the various time points in members of the *TGF-β, BMP*, *FGF*s, *SMAD* families as well as *ColI, POU5F1* and *SOX-2*.

In hTGF-β_3 treated devices, *β-catenin* expression was up-regulated especially at early time periods. Other studies have shown TGF-β induced up-regulation and subsequent activation of β-catenin transcription leading to the activation of WNT/ β-catenin signalling (Wang *et al.*, 2014). Transforming growth factor-β and WNT interactions play a critical role controlling multiple biological processes such as differentiation, the blockage of epithelial proliferation, organogenesis and the specification of tissue in vertebrate embryos (Sato, 2006, Duan and Bonewald, 2016). While evidence of crosstalk between the two pathways is present, the underlying mechanisms and interactions between TGF-β and WNT are still largely unknown (Sato, 2006). Studies have shown TGF-β and WNT relationships and interactions to have multiple effects and the outcomes of these interactions are frequently context-specific (Duan and Bonewald, 2016). The activation of WNT signals has been shown to be related to the activation of the differentiation of osteoblasts (Duan and Bonewald, 2016). When examining the cross-talk between TGF-β and WNT signalling, it has been demonstrated that TGF-β_1 stimulates myofibroblast differentiation by the activation of the WNT pathway and by the down-regulation of $PPAR_{\gamma}$ expression (Sato, 2006). The activation of the WNT pathway leads to the increase of collagen deposition (Wang *et al.*, 2014). Thus, the influence of TGF-β_3 on the activation of the WNT signalling pathway assists in the up-regulation of *collagen* expression by up-regulation of β-catenin in *Papio ursinus.*

The lower levels of β-catenin within the muscle samples could possibly be explained by the relationship of β-catenin to SMAD-3. Studies have demonstrated that the inhibition and or down-regulation of SMAD-3 leads to a reduced expression of *β-catenin* (Guo *et al.*, 2008). This was found to be a result of the over-expression of *ICAT* and *Axin* which lead to the

ubiquitination and degradation of SMAD-3 (Guo *et al.,* 2008). In our study, a significant decrease of *SMAD-3* expression was seen within muscle samples which is in line with the above studies. This demonstrates that a delayed activation of signalling is present in the adjacent muscle and follows histological analysis of bone formation. This may highlight and provide evidence of TGF-β induction and activation of β-catenin, mediating the transcription of WNT (Guo *et al.*, 2008).

Previous studies using 7% HA/CC bioreactors treated with 125 µg hTGF-β_3 and implanted in *Papio ursinus* demonstrated a significant down-regulation of *BMP-2* expression on day 15 followed by an up-regulation of *BMP-2* on days 60 and 90 (Klar *et al.*, 2014). Further analysis reinforced this finding by the simultaneous down-regulation of *Noggin*, an antagonist of the BMP pathway, expression in later periods days 60 and 90 of bone induction (Klar *et al.*, 2014). These data provided evidence that the induction of heterotopic bone formation is initiated and regulated via the BMPs pathway and more specifically implicates the expression of *BMP-2*, which can be regulated by *Noggin* expression in this process. From studies in *Papio ursinus* it was noted acute *BMP-2* expression is adequate for the commitment of MSC to undergo osteogenesis and to irreversibly induce bone formation (Noel *et al*., 2004). This finding corroborates not only the results observed in previous studies in the Chacma baboon but also the results obtained in this study. Histological analysis of hTGF-β_3 treated macroporous bioreactors showed pronounced induction of bone, observed as early as 17 days post implantation (Ripamonti *et al.,*2015) (Appendix 4).

Current results suggest a molecular switch in *BMP-2* expression over a 4 day period; where there is a down-regulation of *BMP-2* expression at day 15 as found by Klar *et al.,* (2014) and at day 17 (shown in this study) within the microporous device samples mimicked within muscle samples at 19 and 23 days) after which both device and muscle samples experience an up-regulation of *BMP-2* expression. This *BMP-2* expression is in line with the induction of bone formation observed histologically which demonstrated that bone formed tightly attached to the substratum and expanded into the macroporous spaces together with prominent angiogenesis and capillary sprouting at 19 days (Appendix 4 A and B). At 23 days, there was still induction of bone formation taking place outside the implanted super-activated bioreactor (Appendix 4 C and D). Taken together, these gene expression and histological findings highlight a possible temporal window of activation of gene expression for about four days in adult non-human primates *Papio ursinus* that may initiate a series of signal pathways committing MSC to osteogenesis and bone induction.

A previous study in osteoblast cells has found that an initial increase in *BMP-4* expression is short-lived due to its short mRNA half-life and in response to increased signalling of BMP-2. (Pereira *et al.*, 2000). *Bone morphogenic protein-2* expression has been found to lead to the down-regulation of *BMP-4*, and *BMP-6* and retains an autocrine regulation loop in osteoblasts (Pereira *et al.*, 2000). Within the present study, treatment of hTGF-β_3 resulted in the return of BMP-4 expression to levels similar to that of the control muscle tissue after an initial down-regulation of expression at day 17 and 19 in the device and adjacent muscle respectively. The down-regulation of *BMP-4* in muscle samples occurring after the down-regulation in the device within *Papio ursinus* supports the BMP-4 negative feedback loop described by Pereira *et al.*, (2000) establishing a link in BMP-4 expression between the two microenvironments.

Studies on BMP-2/-6 and -9 have demonstrated that these three BMPs are key proteins involved in the induction of bone formation and the differentiation of osteogenic stem cells into osteoblasts. (Chen *et al*., 2010, Jain *et al*., 2013). In this study, after implantation of hTGF-β_3 treated macroporous bioreactors *BMP-6* expression was down-regulated in device and muscle samples at all time points a decrease in *BMP-6* expression was found to link with differentiation of chondrocytes (Kugimiya *et al*., 2005). *In vivo* experiments have demonstrated that BMP-6 stimulates heterotopic bone formation due to its ability to significantly increase and induce osteogenesis as well as the differentiation of chondroblasts (Jain *et al.*, 2013, Ebisawa *et al.*, 1999). Bone morphogenic protein-6 can induce alkaline phosphatase (ALP) in several osteoblastic cell line such as C2C12 cells and MC3T3 E cells (Ebisawa *et al.*, 1999). In addition the treatment of both cell lines with TGF-β_3 was found to down-regulate *BMP-6* and *BMP-7* expression (Miyamoto *et al.*, 2007). The use of TGF-β_3 was found to enhance differentiation of chondrocytes as the expression of cartilage oligomeric matrix genes and bone proteoglycan genes were up-regulated (Miyamoto *et al.*, 2007). Additionally, studies on MSCs have found that *BMP-6* is able to induce osteogenesis at a more effective rate than *BMP-2* (Ebisawa *et al.*, 1999). This was further corroborated in mouse studies where, in the formation of long bone, *BMP-2* and *-6* were the main BMPs expressed in hypertrophic chondrocytes and in the induction of endochondral bone formation (Kugimiya *et al.*, 2005).

Studies in primary human osteoblasts cultures treated with hTGF-β was able to completely block BMP-2 and -7 signalling by the inhibition of either *SMAD-1/-5* or *-8* expression (Ehnert *et al.*, 2010, Ehnert *et al.*, 2012). In this study, *BMP-7* expression within muscle samples of *Papio ursinus* showed a down-regulation from 17 to 30 days. This may demonstrate how the

combination of the coral-derived constructs and the TGF-β microenvironment assist in the regulation and expression of *BMP-7.*

One essential signalling molecule in the induction of bone is expression of *BMP-9,* as BMP-9 plays a vital role in BMP/TGF-β transcription factor regulation and has been shown to have a direct effect on vascular function, bone induction and formation (Li *et al.*, 2015). TGF-β contributes to BMP-9 up-regulation through the SMAD-JNK pathway (Li *et al.*, 2015). *Bone morphogenic protein-9* induces MSC differentiation and osteogenesis through the signalling of the Ras-Raf-MEK-ERK pathway (MAK/ERK) pathway and, BMP-9 has been shown to induce calcification in vascular smooth muscle cells (VSMC) (Zhu *et al.*, 2015). Furthermore, *in vitro* studies have demonstrated that BMP-9 treatment leads to a significant increase in ALP activity, VSMC calcium content and mRNA expression of osteogenic markers (Chen *et al*., 2006, Zhu *et al*., 2015). Signal transduction studies revealed that *BMP-9* expression induced the phosphorylation of SMAD-1/-2/-3/-5 and -8. This results in these SMAD proteins directly binding to SMAD-4 leading to the activation of target genes (Zhu *et al.*, 2015). This demonstrates the ability of BMP-9 to induce osteogenic differentiation and calcification via ALK1, SMAD and ALP dependent mechanisms (Zhu *et al.*, 2015). In this study, BMP-9 was up-regulated at days 17 to 25 in the device on similar days in muscle samples. This up-regulation of *BMP-9* may result in rapid osteoblast differentiation when hTGF-β_3 treated macroporous bioreactors are implanted heterotopically in *Papio ursinus.*

Collagen type I expression within *Papio ursinus* was up-regulated at all timepoints post implantation of hTGF-β_3 treated constructs. Previous studies showed *ColIV* expression to be up-regulated in both untreated and treated hTGF-β_3 treated 7% HA/CC constructs at all time points examined viz. 15, 60 and 90 days after heterotopic implantation, in *Papio ursinus* (Klar *et al.*, 2014). This was suggested to be due to the macroporous coral-derived constructs *per se* being intrinsically angiogenic (Klar *et al.*, 2014). *In vivo* studies have further shown that the treatment of TGF-β isoforms results in increased expression of various types of collagen: types *I, III, IV,* and *V* (Creely *et al.*, 1992). In cell culture experiments the expression of *type I, III* and *V* was found to be increased by eight, two and three fold respectively with *ColIV* showing only slight over-expression (Creely *et al.*, 1992). Additionally, the total collagen production was found to be increased fivefold (Creely *et al.*, 1992). However, at high doses, TGF-β_3 has been found to suppress the expression of *ColI* via the CCAAT displacement protein (CUX-1) (Fragiadaki *et al.*, 2011). CUX-1 suppresses *ColI* by its ability to rapidly bind DNA and transiently act as a repressor (Fragiadaki *et al.*, 2011). The suppression of *ColI* has been found

to be transient and cannot be permanently switched off as it is required during tissue remodelling and normal development (Fragiadaki *et al.*, 2011). Within normal collagen-producing cells, TGF-β is able to activate collagen synthesis at high doses only in the absence of CUX-1 (Fragiadaki *et al.*, 2011). Moreover, Fragiadaki *et al.*, (2011) performed further experimentation on SMAD-3, due to its important role in inducing CUX-1 expression. It was found that *ColI* expression levels increased, following down-regulation of *CUX-1*. These observations corroborate the observed down-regulation of *SMAD-3* in the current experimental scenario, and link with the expression of *ColI* in *Papio ursinus.*

These studies demonstrate that the up-regulation of *ColI* expression is linked to TGF-β. Transforming growth factor-β is a master regulator of collagen, *ColI* and *IV* seen to be up-regulated within the early periods, 15 to 30 days, of bone induction. This could give insight into previous experimentation that has highlighted a profound and rapid recruitment of stem cells from 15 to 30 days to the site of bone induction. Rapid bone differentiation was seen by Klar *et al.*, (2014) between 15 and 30 days with increased invasion of vascular capillaries sprouting within the construct and surrounding tissue with increased multicellular osteoblasts by day 30, predated by up-regulation of *ColIV* and *ColI.*

Previous techniques have used morphological assessment of alkaline phosphatase activity and bone nodule formation to identify osteoblasts (Shipp *et al.*, 1991). However, cluster of differentiation (CD) expression patterns have also been utilised to identify osteoblasts (Benayahu *et al.*, 1994). Common acute lymphoblastic leukaemia antigen, also referred to as CD-10, a glycoprotein, which plays an essential role as a neutral endopeptidase, is predominantly expressed on the surface of various neoplastic and non-neoplastic cells (Shipp *et al.*, 1991). In our study, *CD-10* expression in both the device and the adjacent muscle tissue was down-regulated at all time points. The expression of *CD-10* is used as an indicator of the osteoblast phenotypes as CD-10 has been identified in adult bone marrow and within lymphoid tissue, specifically germinal center B cells (Reyes-Botella *et al*., 1999). *In vitro* studies using MBA-15.4, a proteogenic cell line, demonstrated reduction of *CD-10* expression and activation at early culture periods with expression returning to baseline levels with time (Benayahu *et al.*, 1994). In mature osteoblast cell line, MBA-15.6, the expression and activation of CD-10 significantly increased above baseline levels (Benayahu *et al.*, 1994). Further studies investigating the synergistic effect of BMP-2 and TGF-β as antagonists to CD-10. It found that the expression of *BMP-2* and *TGF-β* either singularly or together inhibited *CD-10* expression (Benayahu *et al.*, 1994).

These afore mentioned studies corroborate the findings of this study. Down-regulation of *CD-10* may indicate the induction of bone formation due to rapid recruitment of pre-osteoblasts at the site of bone differentiation. It may indicate that hTGF-β_3 treatment prolongs the up-regulation of *BMP*s and concomitant down-regulation of *CD-10* to allow for a continuous induction of bone formation and recruitment of pre-osteoblasts to increasing the extent of bone formation.

A study utilising human bone marrow stromal cells (hBMSC) aimed to identify membrane proteins during osteogenic differentiation *in vitro* (Graneli *et al.*, 2014). The study demonstrated that when undifferentiated and osteogenically differentiated cells where compared in hBMSCs, 11 membrane proteins were differentially expressed (Graneli *et al.*, 2014). One membrane protein, CD-92, had the highest relative expression change between undifferentiated and differentiated states (Graneli *et al.*, 2014). Relative *CD-92* expression was increased in osteogenically differentiated BMSCs when compared to undifferentiated cells (Graneli *et al.*, 2014). The study demonstrated that the surface markers, CD10 and CD92, displayed a significantly higher expression in both osteogenically and adipogenic differentiated hBMSCs (Graneli *et al.*, 2014).

Crystallin Alpha B (CRY-αB) also known as αB-crystallin, is a molecular chaperone able to assist in signal transduction, stabilization of the cytoskeleton, unfolding of proteins and the prevention of protein aggregation (Boelens, 2014). It has been noted to be highly expressed in lens, heart and skeletal muscle tissues and has been shown to be highly expressed in the early stages of chondrogenic differentiation (Chen *et al.*, 2005). Although CRY-αB has been identified in as a possible osteogenic marker very little is known about its role in osteogenic differentiation (Foster *et al.*, 2005, Boelens, 2014). In hBMSCs, an increase in *CRY-αB* expression occurs during osteogenic differentiation while a reduction in expression was present in dedifferentiating chondrocytes (Lambrecht *et al.*, 2009). Lambrecht *et al.*, (2009) also showed that CRY-αB, in combination with CD-10 and CD-92, act as osteogenic markers within specific cell lineages with CRY-αB not present during early chondrogenic or adipogenic differentiation. Crystallin Alpha B has also been associated with bone metabolism during differentiation of osteoblasts in hBMSCs (Kulterer *et al.*, 2007). These studies demonstrate the variable differences in the expression of CRY-αB in osteogenically differentiated hBMSCs and undifferentiated hBMSCs. Boelens (2014) noted that CRY-αB can be used as an intracellular marker of osteogenic differentiation (Boelens, 2014).

Whilst the afore mentioned studies indicate that osteogenic differentiation is accompanied by an increase in *CRY-αB* expression, results from this time study suggest that hTGF-β_3 treatment has resulted in the down-regulation of *CRY-αB* gene expression over the 30 day period. Furthermore, histological analysis demonstrated rapid induction of bone formation with recruitment of osteoblasts to the site of bone induction. This demonstrates possible adverse expression effects of TGF-β_3 on expression patterns of genes such as *CRY-αB*.

In this study in *Papio ursinus*, there was a constant down-regulation of *FGF-1*, *FGF-2, FGF-R1* and *FGF-R2* at the sites of the implanted hTGF-β_3 treated coral-derived constructs compared to the control tissue. *FGF-2* and its receptor *FGF-R1,* share a similar trend with respect to their levels of temporal down-regulation. In both *FGF-2* and *FGF-R1*, expression was down-regulated on day 17 in the device and on day 19 in surrounding muscle. By day 23 however, *FGF-2* expression in both the device and adjacent muscle had a returned to baseline levels. This indicates a close link between *FGF-2* and *FGF-R1*. *FGF-1* and its receptor *FGF-R2* both showed a down-regulation in gene expression at all time points. This demonstrates a molecular pathway of FGF regulation during the induction of bone formation orchestrated by hTGF-β_3 preloaded onto macroporous bioreactors. The down-regulation of *FGF* expression by hTGF-β_3 is in line with the induction of bone differentiation seen histologically (Appendix 4). Morphological analyses of hTGF-β_3 treated coral-derived macroporous bioreactors showed multicellular osteoblastic cell differentiation together with pronounced angiogenesis and capillary sprouting from 17 to 19 days (Appendix 4).

Several studies have used rodent models to examine the role of *FGF*s and their receptors in bone induction and regeneration (Jacob *et al*., 2006, Lu *et al*., 2009). A knockout of *FGF-R1* in adult mice resulted in a significant increase in bone mass and was proposed to lead to increased cellular proliferation and delayed differentiation of osteoblasts in osteochondro-progenitor cells (Jacob *et. al.,* 2006). It was thus proposed that the decreased expression of *FGF-R1* promotes the differentiation of mesenchymal progenitors into pre-osteoblasts (Jacob *et. al.*, 2006). The decrease in *FGF-R1* was shown to inhibit the proliferation of mesenchymal progenitor cells as well as the maturation and mineralization of osteoblasts (Jacob *et. al.*, 2006). In a mouse model with a targeted deletion of *FGF-R1* in bone marrow monocytes and osteoclasts, mice exhibited increased bone mass and impaired osteoclastic activity and formation (Lu *et. al.*, 2009). Low-doses of FGF-2 in the presence of BMP-2 markedly increased angiogenesis and calcium deposition in a rat ectopic bone formation model compared to the

addition of BMP-2 alone (Song *et al*., 2017). Notably, increasing the dose of FGF-2 resulted in a decrease in bone formation (Song *et. al.*, 2017).

Fibroblast growth factor receptor-2 is expressed mainly in osteoprogenitor cells that differentiate into osteoblasts (Su *et. al.*, 2014). The activation of *FGF-R2* was shown to increase osteoblast apoptosis in murine and human osteoblasts (Lemonnier *et al*., 2001). In the mouse model, *FGF-1* was found to play a vital role in bone induction and the bone remodelling cycle (Dunstan *et al*., 1999). When FGF-1 was injected locally into mice 4 times per day for 3 days, new bone formation continued for at least the next 18 days (Dunstan *et. al.*, 1999). *Fibroblast growth factor-1* was found to enhance bone formation, consistent with a signalling cascade in which initiation triggers mitogenesis in osteoblasts (Dunstan *et. al.*, 1999).

Studies in murine chondrosarcoma cell lines found that by activating *FGF* signalling, chondrocyte proliferation was inhibited via the phosphorylation of STAT-1 (Sahni *et al*., 1999, Dailey *et al*., 2003). Additional studies in rodent chondrosarcoma chondrocytes treated with FGF showed an inhibition of *Indian hedgehog* (IHH) and chondrocyte proliferation (Kim et al., 2013). Fibroblast growth factor activated signalling pathways inhibited E2 Transcription Factor which in turn repressed *IHH* expression (Kim *et. al.*, 2013). Indian hedgehog is one of the essential hedgehog signalling molecules, known to control and regulate bone replacement and hypertrophy of chondrocytes (Kim *et. al.*, 2013). It is also a known enhancer of the proliferation and differentiation of mesenchymal cells where decreased *IHH* expression leads to decreased *RUNX-2* expression (Yoshida *et al*., 2004). An *IHH* conditional knock out mouse model exhibited decreased *RUNX-2* expression (Yoshida *et. al.*, 2004). After exogenous recombinant IHH protein treatments, increased *RUNX-2* expression was observed, and it was thus proposed that IHH regulates *RUNX-2* which in turn regulates chondro-osteogenesis (Yoshida *et. al.*, 2004).

The results of the above studies support the current experiments whereby down-regulation of *FGFs* and their receptors are in line with an increase in bone formation (Jacob *et. al.*, 2006; Lu *et. al.*, 2009). hTGF-β_3 treated bioreactors initiated the robust and rapid induction of bone formation on days 19 and 23. Previous studies in *Papio ursinus* have shown over-expression of *OP-1, BMP-2, Osteocalcin* and *RUNX-2* (Klar *et. al.*, 2014; Ripamonti *et. al.*, 2015; Ripamonti *et. al.*, 2016a). Under normal physiological conditions, *FGF* inhibits *IHH*, reducing the synthesis of *RUNX-2* as well as bone induction. It suggests that hTGF-β_3 down-regulates

FGF and its receptors resulting in an increase in *IHH* expression which regulates the master gene *RUNX-2* (Fig. 20). This would result in the rapid and substantial induction of bone by hTGF-β_3 combined with coral-derived macroporous bioreactors.

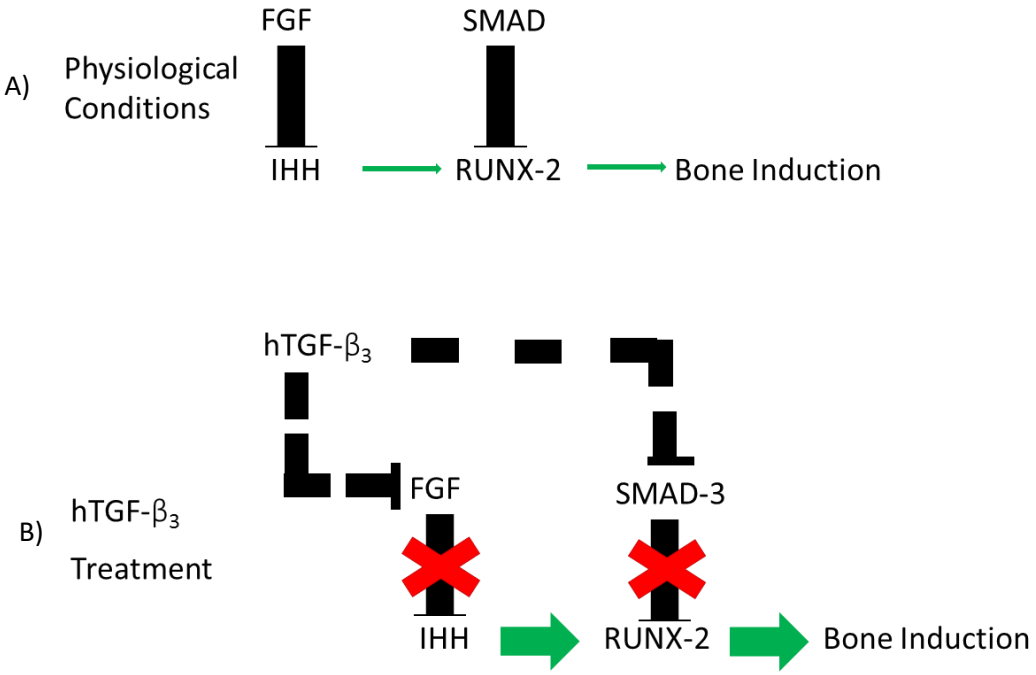


Figure 20: Overview of proposed heterotrophic transforming growth factor- β (hTGF- β_3) mechanism with fibroblast growth factor (FGF) Indian hedgehog (IHH) and RUNX-2 pathways in bone induction. (A) Under normal physiological conditions FGF inhibits IHH reducing the presence of RUNX-2 and bone induction. (B) hTGF- β_3 treatment inhibits FGF, to reducing FGF inhibition on IHH. Increased IHH promotes the increased expression of RUNX-2, increased RUNX-2 leads to increased bone induction. Therefore, down-regulation of FGF, increases IHH and RUNX-2 allowing for increased bone induction.

The current study also showed temporal expression of *SMAD-1* to *-5* in *Papio ursinus* after the implantation of the 7% HA/CC bioreactors treated with hTGF-β_3. At days 17, 23 and 27 *SMAD-1* expression were found to be up-regulated in the device samples and down-regulated at day 19. *SMAD-1* expression at days 25 and 30 were found to be similar to control muscle tissue expression levels in the device samples. *SMAD-2* was found to be initially down-regulated in device samples and up-regulated on from day 19 to 27. In device sample *SMAD-3* expression levels where similar to the control muscle tissue at 17, 19, 23 and 30 days. Up-regulation of

SMAD-3 at days 25 and 27 in device samples. In muscle samples *SMAD-3* expression was found to be down-regulated at 17, 19, 23 and 25 days and up-regulated at days 27 and 30. *SMAD-4* expression was found to be up-regulated at all time points in the device and muscle samples. *SMAD-5* expression was down-regulated at days 17, 25 and 30 in device samples with an up-regulation 27. *SMAD-5* expression was down-regulated at all time points.

The current study showed temporal expression of *SMAD-1* to *-5* in *Papio ursinus* after implantation of 7% HA/CC bioreactors treated with hTGF-β. Understanding the role of SMADs and their interaction with BMP and TGF-β signalling during bone induction is still not completely understood (Yu *et al.*, 2002). However, some information on BMPs/ TGF-β signalling pathways, and their downstream signal transducers, SMADs, has been obtained. BMPs promote osteo-induction through mesenchymal cell proliferation and differentiation, osteogenesis and chondrogenesis (Yu *et al.*, 2002). TGF-β signalling promotes extracellular matrix formation, cell migration, and angiogenesis (Yu *et al.*, 2002).

SMADs regulate and transduce BMP and TGF-β signals. In this study using 3-month old female CD-COB rats in which the right femur was fractured and the rats euthanised at days 3, 10, or 28 harvested specimens and underwent immunohistochemical analysis for protein marker expression evaluation (Yu *et al.*, 2002). By day 3, immunostaining of SMAD-1 to SMAD-6 demonstrated elevated levels of all SMADs within the osteoprogenitor cells and mesenchymal cells in the thickened periosteum and in bone marrow osteoblast-like cells and mesenchymal cells near the fracture site when compared to the non-fracture controls (Yu *et al.*, 2002). However, by day 10 the pattern of expression altered; *SMAD-1* and *SMAD-5* demonstrated significantly decreased expression; *SMAD-2* and *SMAD-3* had slightly increased expression, while *SMAD-4* expression was reduced but remained high. By day 28 expression levels of all SMADs had returned to levels of the non-fracture control (Yu *et al.*, 2002).

In this study in *Papio ursinus*, similar trends in expression were seen. *SMAD-1* expression was initially elevated in device samples but returned to control levels by day 25. Expression of *SMAD-2* & *-4* was generally remained elevated over the whole time period while *SMAD-5* expression mainly down-regulated as in the mouse model by day 10.

Yu *et al.*, (2002) demonstrated that BMP and SMAD expression levels were highest within the first 2 weeks of fracture healing. *Bone morphological protein-2* and *BMP-7* expression levels peaked at 3 days post fracture, as did *SMAD-1* and *SMAD-5* expression levels. Yu *et. al.*, (2002) additionally found that at day 3 *BMP-4* was elevated fivefold together with TGF-β, and peaked

at day 10. Both *SMAD-2* and *SMAD-3* showed a similar pattern of expression. Expression of *SMAD-4* peaked at 3 days and remained elevated at day 10. These results demonstrated that SMAD-1, SMAD-4, and SMAD-5 may transduce signals of BMP-7 and BMP-2 while SMAD-2, SMAD-3, and SMAD-4 transduce TGF-β_1 signalling (Yu *et al.*, 2002). Yu *et. al.*, further showed that *SMAD-5* expression was down-regulated from 15 to 30 days and *SMAD-2* and *SMAD-3* were down-regulated from 15 to 25 days. Thus, in mouse models, SMAD signalling and expression occurs at earlier time points (from day 3) in the bone induction pathway. Thus, there is a need to investigate expression levels of genes like SMADs involved in the bone induction before 15 days in order to allow for a deeper understanding in the temporal expression and signalling involved of baboon bone induction model.

Studies using transgenic knock out mice have been used to understand SMAD signalling. These studies have demonstrated that SMAD-1 is a vital mediator in BMP's osteogenic function. Wang *et. al.*, (2011) used Col2a1-Cre, a chondrocyte-specific deletion transgenic mouse line that expresses *Cre* recombinase under the control of the mouse *collagen type II* gene (Col2a1) (Sakai *et al.*, 2001), crossed with a SMAD-1 fx/fx mice to produce a chondrocyte-specific SMAD-1 conditional knockout (cKO) mouse (Wang *et al.*, 2011). Wang *et. al.*, (2011) demonstrated that in the SMAD-*1* cKO mice BMP signalling was partially inhibited and osteoblast proliferation and differentiation were impaired. Deletion of chondrocyte-specific SMAD-1 additionally lead to delayed and impaired calvaria bone development and shortening of the growth plate (Wang *et. al.*, 2011). Wang *et. al.*, (2011) concluded that both SMAD-1 and SMAD-5 function together to mediate the essential role BMPs play in endochondral bone development.

BMP-2 knockout mice models demonstrate both cartilage and bone suffer from increased levels of spontaneous fractures and impaired healing. This was found to be due to a reduction of chondrogenic or osteogenic process and reduction in recruitment of cells to the site of injury (Yu *et al.*, 2002). Within the BMP-2 knock out mice model, *SMAD-1* and *SMAD-5* expression patterns were found to be similar to those of *BMP-7*; whereas *SMAD-2* and *-3* expression patterns are similar to those of *TGF-β* (Yu *et al.*, 2002, Song *et al.*, 2009). This suggested that, at least partially, BMP/TGF-β signalling in fracture healing is mediated by canonical SMAD pathways (Yu *et al.*, 2002, Song *et al.*, 2009). However, even though SMADs mediate the BMP/TGF-β signalling pathways, it is possible that SMAD proteins have multiple other interactions with signalling molecules to promote chondrogenesis and osteogenesis.

To understand TGF-β_1 to -β_3 signalling it is essential to understand its functions and roles. Transforming growth factor-β_1 is a potent regulatory cytokines with various effects on stem cells (Kasagi and Chen, 2013). *Transforming growth factor-β_1* maintains and induces various immune tolerance mechanisms by the regulating lymphocyte differentiation, proliferation and survival (Kasagi and Chen, 2013). Studies have demonstrated that TGF-β_1 interacts with various hormones, such as parathyroid hormone (PTH), estrogen, vitamin D and gluco-corticoids. Estrogen assists in the production of osteoblasts by the stimulation of TGF-β_1, further promoting osteoblast differentiation and proliferation (Kasagi and Chen, 2013). Additionally, estrogen prevents bone loss by preventing the activation of osteoclast apoptosis through a TGF-β dependent mechanism (Hughes *et al.*, 1996). This is due to estrogen receptor α being a co-repressor for SMAD signal transduction, with SMAD-3 was identified as an enhancer of estrogen receptor α. SMAD-3 mediates the transcriptional activity, and may indicate that estrogen and TGF-β_1 are coordinated during the induction of bone formation (Centrella *et al.*, 1991).

Studies have demonstrated that gluco-corticoids promote osteoblasts apoptosis, but also inhibit their differentiation and proliferation while promoting osteoclasts differentiation (Ash *et al.*, 1980). Gluco-corticoids have been found to up-regulate *TGF-β_1* expression in osteoblasts, however, unlike estrogen, gluco-corticoids synergise with TGF-β_1 to heighten osteoclast formation by the stimulation of osteoclast progenitors cells to differentiate into osteoclasts (Centrella *et al.*, 1991).

Transforming growth factor-β_1 blocks apoptosis of osteoblasts, enhances osteoblast proliferation and also recruits matrix-producing osteoblasts or osteoblastic precursors to the site through chemotactic attraction (Lucas, 1989, Jilka *et al.*, 1998, Kassem *et al*., 2000). Transforming growth factor-β_1 in the early stages of osteoblast differentiation enhance extracellular bone matrix protein production (Alliston *et al.*, 2001). However, *TGF-β_1* has also been found to inhibit osteoblast mineralization and proliferation (Maeda *et al.*, 2004). Studies have shown that within murine, rat, and human osteoblasts there was decreased TGF-β receptor I and receptor II expression during osteoblast differentiation, and possibly implying that osteoblasts in the late phase of their differentiation are less sensitive to TGF-β_1 (Centrella *et al.*, 1995). In contrast, regulation of late stages osteoblasts are positively regulated by BMPs (Canalis *et al.*, 2003). Therefore, the co-operation of TGF-β_1 with BMPs regulate the differentiation of osteoblasts could explain the increased gene expression levels of *TGF-β* and *BMP-2* seen in this baboon study and the high levels of bone formation in *Papio ursinus.*

Transforming growth factor-β_1 activates SMAD-3 by allowing for the formation of SMAD-3-RUNX-2 complex which suppresses the expression of RUNX-2 (Spinella-Jaegle *et al.*, 2001). Runt-related transcription factor 2 maintains a resting state of osteoblast by preventing the differentiation of mature osteoblasts into osteocytes (Spinella-Jaegle *et al.*, 2001). Therefore, TGF-β_1 the down-regulation of *RUNX-2* in mature osteoblasts may promote osteocyte development (Jilka *et al*., 1998, Komori, 2010) highlighting how TGF-β_1 finely tunes osteoblast differentiation. In previous studies and in this study in *Papio ursinus*,

Human transforming growth factor-β_3 treated bioreactors increased the induction of bone formation and was accompanied by a significant increases in *BMP-7*, *BMP-2*, *Osteocalcin* and *RUNX-2* expression as well as a decrease in *FGF-1* and *FGF-2* expression (Klar *et al.*, 2014, Ripamonti *et al.*, 2015, Ripamonti *et al.*, 2016b). Under normal physiological conditions FGF inhibits IHH reducing the presence of *RUNX-2*, additionally the association of SMAD-3 with TGF-β_1 reduces *RUNX-2* and thus bone induction (Fig. 20A). In this study, hTGF-β_3 downregulates *FGF-1* and *-2* and their receptors. Since FGF inhibits IHH it is proposed that hTGF-β_3 down regulates *FGF*; results in an increase *IHH*, and thus increasing the master gene *RUNX-2* (Fig. 20B). Increased expression of *IHH* and *RUNX-2* results in the rapid and substantial induction of bone formation. hTGF-β_3 and also down-regulates *SMAD-3* expression in adjacent muscle tissue, possibly preventing the association of SMAD-RUNX-2, a negative regulator of bone formation thus increasing *RUNX-2* expression levels leading to rapid and substantial bone induction.

This study showed a decrease in *TGF-* β_2 expression levels in both device and adjacent muscle tissue at all time points. Most mouse models studies involving the investigation of TGF-β_2 knock-out demonstrate severe skeletal abnormalities in both endochondral and intramembranous bone (Wu *et al.*, 2016). Transforming growth factor-β_2 is known to be a vital regulator of osteocyte differentiation and assist in the regulation of bone growth (Wu *et al.*, 2016). This has further been confirmed by knockout *TGF-*β_2 mice models that presented generalized chondrodysplasia and the late onset of gestation stages in the development of transgenic mice (Sanford *et al.*, 1997). Furthermore, the loss of TGF-β_2 in mice prevented mice from the ability of exogenous sonic hedgehog expression which inhibited hypertrophic differentiation (Alvarez and Serra, 2004). However, in mice lacking *TGF-*β_2 expression, growth plate reduction and chondrocytes production were recovered by the treatment with TGF-β_3 (Wu *et al.*, 2016). Thus, in *Papio ursinus* the increased bone formation seen with the presence of highly down-regulated TGF-β_2 may be because of the treatment with hTGF- β_3.

Ripamonti *et al*., (1991; 1992; 1993; 1996; 1997; 2000; 2004; 2006; 2009; 2010; 2012; 2016a; 2016b) have published numerous studies in *Papio ursinus* investigating the role of TGF-β_3 in bone induction. At 15, 60 and 90 days post implantation of 7% HA/CC treated bioreactors, *TGF-β_3* expression did not appear to differ significantly between devices treated with hTGF-β_3 and untreated devices (Klar *et al.*, 2014). Similar results were seen for adjacent muscle tissue at 60 and 90 days (Ripamonti, 2015). In murine and avian osteoclast, Yang *et al.,* (1996) demonstrated that raloxifene, an estrogen agonist, activates the TGF-β_3 promoter, leading to significantly inhibited differentiation of osteoblasts and bone-resorptive activities osteoclasts allowing for increased bone mass (Yang *et al*., 1996).

Two key factors essential in determining cellular pluripotency and cell fate are SOX-2 and POU5F1 (Wang *et. al.*, 2006, *Hackett et. al.,* 2012). Sex Determining Region Y-Box 2 and POU5F1 play an essential role in the maintenance and regulation of pluripotency, however no factor on its own can regulate pluripotency (Wang *et. al.,* 2006). Pluripotency is reliant on a multitude of non-linear interactions, whereby a combination of signals are essential to exert their effects (Zandstra *et. al.,* 2000). Increased expression of SOX-2 and POU5F1 in mesenchymal progenitor cells (MPCs), induced pluripotent stem (iPS) and embryonic stem (ES) cells and were linked to increased levels of pluripotency (Hackett *et. al.,* 2012). It was noted that within iPS cells expression of SOX-2 and POU5F1 were significantly higher than in MPCs (Hackett *et. al.*, 2012).

Under normal physiological conditions, SOX-2 and POU5F1 expression has been linked to increased cellular pluripotency; treatment of bioreactors with hTFG-β_3 in this study demonstrated a significant increase in SOX-2 expression. This may be an indication of the presence of a mechanism within *Papio ursinus* for the rapid induction of bone by up-regulating SOX-2 allowing for an increased level of pluripotency in osteoblast progenitor cells over the 30 day period. Additionally, studies have demonstrated that a lack of or inhibition of POU5F1 expression leads to the up-regulation of FGF-8 (Belting *et. al.*, 2011). Fibroblast growth factor-8 expression is essential for the activation of BMP-2 within embryos and leads to the increase of angiogenesis (Belting et. al., 2011). Multiple studies from our research group have reported rapid capillary sprouting and angiogenesis in Papio ursinus after treatment with TGF-β_3 (Klar *et. al.*, 2013, Klar *et. al.*, 2014) (Appendix 4).

Sex Determining Region Y-Box 2 maintains the self-renewal and stemness of pluripotent cells by transcriptional mechanisms and promotes gene expression changes for the self-renewal of

osteoprogenitor cells (Seo *et. al.,* 2011). It has also been linked to the regulation of osteoblast lineage via additional mechanisms that impact WNT signalling. SOX2 regulates the transcription of WNT pathway genes such as *glycogen synthase kinase 3 beta* (*GSK3β*) and *adenomatous polyposis coli* (*APC*). Down-regulation of these genes leads to the inhibition of WNT signalling (Seo *et. al.,* 2011). The ability of SOX2 to disrupt WNT signalling has also been attributed to the binding of the SOX2 C-terminal R1 domain to β-catenin directly (Seo *et. al.*, 2011). Significantly for this purposes of this research, the mechanism of *SOX2* binding sequences in *GSK3* and *APC* genes are conserved across different species (Seo *et. al*., 2011). In our study, an increase in *β-catenin* and *SOX2* expression was seen within the implanted device and adjacent muscle samples. This demonstrates that a within *Papio ursinus* the upregulation of *SOX2* and the concomitant up-regulation of *β-catenin*, are induced by TGF-β by targeting WNT pathway genes (Guo *et. al*., 2008).

A further role for *SOX2* in the bone induction paradigm has been its observed effects on FGFs. FGFs play a critical role as antagonists of osteoblast differentiation and target the WNT pro-differentiation programme. The two domains located closest to the 5′ end (R2-3) have been shown to function in conjunction with Oct-3/4 to activate *FGF-4* transcription (Ambrosetti *et. al.*, 2000; Dailey and Basilico, 2001). Findings by Seo *et. al*., (2011) show that the modulation and extent of the activity was dependant on the synergistic action of SOX2 and Oct-3 on the *FGF-4* gene promoter. Furthermore, SOX2 induction by FGFs plays an essential a role due to SOX2's ability to bind β-catenin and inhibit WNT-induced transcription (Mansukhani *et. al.,* 2005; Ambrosetti *et. al.,* 2008). Additionally, these studies show that the induction of WNT target genes are inhibited by FGF. These studies also found that the down regulation of FGF inhibited the WNT pathway due to multiple FGF mechanisms that were previously thought to be unrelated to the inhibition WNT canonical signalling (Mansukhani *et. al.,* 2005; Ambrosetti *et. al.,* 2008).

6. Limitations and Future Work

One limitation of the current work is the availability and recruitment of *Papio ursinus* baboons for the use in research. There are a limited number of *Papio ursinus* available and cleared for research, which limits the number of samples and time points that are able to be investigated. Thus, future work would require the use of additional baboons to allow for a more extensive range of time points to be examined and greater statistical robustness. Furthermore, untreated control constructs were left in vivo for 90 days, meaning that untreated control samples were not available for comparison at each of the individual time points. Analysis of day 90 samples, both treated and untreated, will form part of the subsequent larger study.

Future work will include investigation of the spatial expression of genes related to osteogenic programming in *Papio ursinus.* This will allow us to understand how hTGF-β_3 effects the expression of key genes and the resulting alterations in signal transduction pathways. Techniques would include: western blotting and *in situ* hybridisation on samples harvested at 17, 19, 23, 25, 27 and 30 days. This will allow for insight between the qRT-PCR gene expression results presented in this study and the temporal and spatial expression of the genes in their respective microenvironments.

To mechanistically understand the complex signalling networks initiated by hTGF-β_3 will require the analysis of essential pathways such as IHH during bone induction. Techniques such as i*n situ* hybridisation allow for the direct visualization of RNA targets in the context of the tissue architecture and measures the RNA distribution within the tissues. This will allow further fine mapping and elucidation of the molecular pathways that underlie the rapid induction of bone in a heterotopic model and possibly identify proteins that could be targeted in a clinical setting.

7. Conclusions

The study shows that implantation of 125µg hTGF-β_3 preloaded coral-derived calcium phosphate macroporous bioreactors induces bone formation in heterotopic sites of the *rectus abdominus* muscle by day 19. The induction of bone formation rapidly colonises the macroporous spaces of the implanted bioreactor. This rapid induction of bone formation is sustained by a prominent capillary invasion that develops a tight relationship with the newly formed bone.

Molecularly, the rapid induction of bone formation is sustained and highlighted by *β-catenin* and *collagen type I* overexpression at days 19 and 23, with down-regulation of *CD-10*, *CryαB*,

Noggin, *POU5F1* and *FGF-1*, *-2* and their receptors. The SMAD signalling cascade is prominent with the up-regulation of *SMAD-2* and *-4* and the down-regulation of *SMAD-5*. Stemness genes such as *SOX-2*, where over-expressed while *CD-10* and *CD-92* were down-regulated. There is a fine tuning and modulation of *BMP* genes in *Papio ursinus* in particular down-regulation of *BMP-6* and up-regulation of *BMP-2* and *-9* as seen in summary table in appendix 6

8. References

Ambrosetti, D. C., Schöler, H.R., Dailey, L. & Basilico, C. 2000. Modulation of the activity of multiple transcriptional activation domains by the DNA binding domains mediates the synergistic action of SOX-2 and Oct-3 on the fibroblast growth factor-4 enhancer. *J Biol Chem*. 275(**30**)**,**23387-97.

Ambrosetti, D., Holmes, G., Mansukhani, A. & Basilico, C. 2008. Fibroblast growth factor signaling uses multiple mechanisms to inhibit WNT-induced transcription in osteoblasts. Mol Cell Biol. 28(**15**)**,**4759-71

Alliston, T., Choy, L., Ducy, P., Karsenty, G. & Derynck, R. 2001. TGF-β-induced repression of CBFA1 by Smad3 decreases cbfa1 and osteocalcin expression and inhibits osteoblast differentiation. *EMBO J,* 20**,** 2254-72.

Alvarez, J. & Serra, R. 2004. Unique and redundant roles of Smad3 in TGF-β -mediated regulation of long bone development in organ culture. *Dev Dyn,* 230**,** 685-99.

Ash, P., Loutit, J. F. & Townsend, K. M. 1980. Osteoclasts derived from haematopoietic stem cells. *Nature,* 283**,** 669-70.

Baroli, B. 2009. From natural bone grafts to tissue engineering therapeutics: Brainstorming on pharmaceutical formulative requirements and challenges. *J Pharm Sci,* 98**,** 1317-75.

Beederman, M., Lamplot, J. D., Nan, G., Wang, J., Liu, X., Yin, L., Li, R., Shui, W., Zhang, H., Kim, S. H., Zhang, W., Zhang, J., Kong, Y., Denduluri, S., Rogers, M. R., Pratt, A., Haydon, R. C., Luu, H. H., Angeles, J., Shi, L. L. & He, T. C. 2013. BMP signaling in mesenchymal stem cell differentiation and bone formation. *J Biomed Sci Eng,* 6**,** 32-52.

Belting, H. G., Wendik, B., Lunde, K., Leichsenring, M., Mossner, R., Driever, W. & Onichtchouk, D. 2011. Pou5f1 contributes to dorsoventral patterning by positive regulation of vox and modulation of fgf8a expression. *Dev Biol,* 356**,** 323-36.

Beltrami, A. P., Barlucchi, L., Torella, D., Baker, M., Limana, F., Chimenti, S., Kasahara, H., Rota, M., Musso, E., Urbanek, K., Leri, A., Kajstura, J., Nadal-Ginard, B. and Anversa, P. 2003. Adult cardiac stem cells are multipotent and support myocardial regeneration. *Cell,* 114, 763-776.

Benayahu, D., Fried, A., Shamay, A., Cunningham, N., Blumberg, S. & Wientroub, S. 1994. Differential effects of retinoic acid and growth factors on osteoblastic markers and CD10/NEP activity in stromal-derived osteoblasts. *J Cell Biochem,* 56**,** 62-73.

Boelens, W. C. 2014. Cell biological roles of αB-crystallin. *Prog Biophys Mol Biol,* 115**,** 3-10.

Boilly, B., Vercoutter-Edouart, A. S., Hondermarck, H., Nurcombe, V. & Le Bourhis, X. 2000. FGF signals for cell proliferation and migration through different pathways. *Cytokine Growth Factor Rev,* 11**,** 295-302.

Borton, A. J., Frederick, J. P., Datto, M. B., Wang, X. F. & Weinstein, R. S. 2001. The loss of Smad3 results in a lower rate of bone formation and osteopenia through dysregulation of osteoblast differentiation and apoptosis. *J Bone Miner Res,* 16**,** 1754-64.

Cao, C. & Dong, Y. 2005. Study on culture and in vitro osteogenesis of blood-derived human mesenchymal stem cells. *Zhongguo Xiu Fu Chong Jian Wai Ke Za Zhi*. 19**,** 642-647.

Canalis, E., Economides, A. N. & Gazzerro, E. 2003. Bone morphogenetic proteins, their antagonists, and the skeleton. *Endocr Rev,* 24**,** 218-35.

Centrella, M., Casinghino, S., Kim, J., Pham, T., Rosen, V., Wozney, J. & Mccarthy, T. L. 1995. Independent changes in type I and type II receptors for transforming growth factor beta induced by bone morphogenetic protein 2 parallel expression of the osteoblast phenotype. *Mol Cell Biol,* 15**,** 3273-81.

Centrella, M., Mccarthy, T. L. & Canalis, E. 1991. Glucocorticoid regulation of transforming growth factor β 1 activity and binding in osteoblast-enriched cultures from fetal rat bone. *Mol Cell Biol,* 11**,** 4490-6.

Charoenlarp, P., Rajendran, A. K. & Iseki, S. 2017. Role of fibroblast growth factors in bone regeneration. *Inflamm Regen,* 37**,** 10.

Chen, D., Zhao, M. & Mundy, G. R. 2004. Bone morphogenetic proteins. *Growth Factors,* 22**,** 233-41.

Chen, G., Deng, C. & Li, Y. P. 2012. TGF-β and BMP signaling in osteoblast differentiation and bone formation. *Int J Biol Sci,* 8**,** 272-88.

Chen, L., Fink, T., Zhang, X. Y., Ebbesen, P. & Zachar, V. 2005. Quantitative transcriptional profiling of ATDC5 mouse progenitor cells during chondrogenesis. *Differentiation,* 73**,** 350-63.

Chen, L., Jiang, W., Huang, J., He, B. C., Zuo, G. W., Zhang, W., Luo, Q., Shi, Q., Zhang, B. Q., Wagner, E. R., Luo, J., Tang, M., Wietholt, C., Luo, X., Bi, Y., Su, Y., Liu, B., Kim, S. H., He, C. J., Hu, Y., Shen, J., Rastegar, F., Huang, E., Gao, Y., Gao, J. L., Zhou, J. Z., Reid, R. R., Luu, H. H., Haydon, R. C., He, T. C. & Deng, Z. L. 2010.

Insulin-like growth factor 2 (IGF-2) potentiates BMP-9-induced osteogenic differentiation and bone formation. *J Bone Miner Res,* 25**,** 2447-59.

Chen, N. X., Duan, D., O'neill, K. D., Wolisi, G. O., Koczman, J. J., Laclair, R. & Moe, S. M. 2006. The mechanisms of uremic serum-induced expression of bone matrix proteins in bovine vascular smooth muscle cells. *Kidney Int,* 70**,** 1046-53.

Creely, J. J., Dimari, S. J., Howe, A. M. & Haralson, M. A. 1992. Effects of transforming growth factor-β on collagen synthesis by normal rat kidney epithelial cells. *Am J Pathol,* 140**,** 45-55.

Dailey, L. & Basilico, C. 2001. Coevolution of HMG domains and homeodomains and the generation of transcriptional regulation by Sox/POU complexes. *J Cell Physiol*. 186(**3**)**,**315-28.

Dailey, L., Laplantine, E., Priore, R. & Basilico, C. 2003. A network of transcriptional and signaling events is activated by FGF to induce chondrocyte growth arrest and differentiation. *J Cell Biol,* 161**,** 1053-66.

Delaissé, J. M., Andersen, T. L., Engsig, M. T., Henriksen, K., Troen, T. & Blavier, L. 2003. Matrix metalloproteinases (MMP) and cathepsin K contribute differently to osteoclastic activities. *Microsc Res Tech.* 61**,** 504–513.

Devlin, R. D., Du, Z., Pereira, R. C., Kimble, R. B., Economides, A. N., Jorgetti, V. & Canalis, E. 2003. Skeletal overexpression of noggin results in osteopenia and reduced bone formation. *Endocrinology,* 144**,** 1972-8.

Duan, P. & Bonewald, L. F. 2016. The role of the wnt/beta-catenin signaling pathway in formation and maintenance of bone and teeth. *Int J Biochem Cell Biol,* 77**,** 23-29.

Dunstan, C. R., Boyce, R., Boyce, B. F., Garrett, I. R., Izbicka, E., Burgess, W. H. & Mundy, G. R. 1999. Systemic administration of acidic fibroblast growth factor (FGF-1) prevents bone loss and increases new bone formation in ovariectomized rats. *J Bone Miner Res,* 14**,** 953-9.

Ebisawa, T., Tada, K., Kitajima, I., Tojo, K., Sampath, T. K., Kawabata, M., Miyazono, K. & Imamura, T. 1999. Characterization of bone morphogenetic protein-6 signaling pathways in osteoblast differentiation. *J Cell Sci,* 112 (Pt 20)**,** 3519-27.

Ehnert, S., Baur, J., Schmitt, A., Neumaier, M., Lucke, M., Dooley, S., Vester, H., Wildemann, B., Stockle, U. & Nussler, A. K. 2010. TGF-beta1 as possible link between loss of bone mineral density and chronic inflammation. *PLoS One,* 5**,** e14073.

Ehnert, S., Zhao, J., Pscherer, S., Freude, T., Dooley, S., Kolk, A., Stockle, U., Nussler, A. K. & Hube, R. 2012. Transforming growth factor β1 inhibits bone morphogenic protein (BMP)-2 and BMP-7 signaling via upregulation of Ski-related novel protein N (SnoN): possible mechanism for the failure of BMP therapy? *BMC Med,* 10**,** 101.

Foster, L. J., Zeemann, P. A., Li, C., Mann, M., Jensen, O. N. & Kassem, M. 2005. Differential expression profiling of membrane proteins by quantitative proteomics in a human mesenchymal stem cell line undergoing osteoblast differentiation. *Stem Cells,* 23**,** 1367-77.

Fragiadaki, M., Ikeda, T., Witherden, A., Mason, R. M., Abraham, D. & Bou-Gharios, G. 2011. High doses of TGF-β potently suppress type I collagen via the transcription factor CUX1. *Mol Biol Cell,* 22**,** 1836-44.

Frost, H. M. 1990. Skeletal structural adaptations to mechanical usage (SATMU): 4. Mechanical influences on intact fibrous tissues. *Anat Rec,* 226**,** 433-9.

Gamblin, A. L., Brennan, M. A., Renaud, A., Yagita, H., Lezot, F., Heymann, D., Trichet, V. & Layrolle, P. 2014. Bone tissue formation with human mesenchymal stem cells and biphasic calcium phosphate ceramics: the local implication of osteoclasts and macrophages. *Biomaterials,* 35**,** 9660-7.

Gordon, M. D. & Nusse, R. 2006. Wnt signaling: multiple pathways, multiple receptors, and multiple transcription factors. *J Biol Chem,* 281**,** 22429-33.

Graneli, C., Thorfve, A., Ruetschi, U., Brisby, H., Thomsen, P., Lindahl, A. & Karlsson, C. 2014. Novel markers of osteogenic and adipogenic differentiation of human bone marrow stromal cells identified using a quantitative proteomics approach. *Stem Cell Res,* 12**,** 153-65.

Groenen, L. C., Nice, E. C. & Burgess, A. W. 1994. Structure-function relationships for the EGF/TGF-α family of mitogens. *Growth Factors,* 11**,** 235-57.

Guan, M., Yao, W., Liu, R., Lam, K. S., Nolta, J., Jia, J., Panganiban, B., Meng, L., Zhou, P., Shahnazari, M., Ritchie, R. O. & Lane, N. E. 2012. Directing mesenchymal stem cells to bone to augment bone formation and increase bone mass. *Nat Med,* 18**,** 456-62.

Guo, X., Ramirez, A., Waddell, D. S., Li, Z., Liu, X. & Wang, X. F. 2008. Axin and GSK3-control Smad3 protein stability and modulate TGF- signaling. *Genes Dev,* 22**,** 106-20.

Hackett, C. H., Greve, L., Novakofski, K. D. & Fortier, L. A. 2012. Comparison of gene-specific DNA methylation patterns in equine induced pluripotent stem cell lines with cells derived from equine adult and fetal tissues. *Stem Cells Dev,* 21**,** 1803-11.

Hadjidakis, D. J. & Androulakis, Ii 2006. Bone remodeling. *Ann N Y Acad Sci,* 1092**,** 385-96.

Hellemans, J., Mortier, G., De Paepe, A., Speleman, F. & Vandesompele, J. 2007. qBase relative quantification framework and software for management and automated analysis of real-time quantitative PCR data. *Genome Biol,* 8**,** R19.

Hass, R., Kasper, C., Böhm, S. & Jacobs, R. 2011. Different populations and sources of human mesenchymal stem cells (MSC): A comparison of adult and neonatal tissue-derived MSC. *Cell Commun Signal*. 9**,** 12.

Hogan, B. L. 1996. Bone morphogenetic proteins: multifunctional regulators of vertebrate development. *Genes Dev,* 10**,** 1580-94.

Huang, W., Yang, S., Shao, J. & Li, Y. P. 2007. Signaling and transcriptional regulation in osteoblast commitment and differentiation. *Front Biosci,* 12**,** 3068-92.

Hughes, D. E., Dai, A., Tiffee, J. C., Li, H. H., Mundy, G. R. & Boyce, B. F. 1996. Estrogen promotes apoptosis of murine osteoclasts mediated by TGF-β. *Nat Med,* 2**,** 1132-6.

Imamura, T., Takase, M., Nishihara, A., Oeda, E., Hanai, J., Kawabata, M. & Miyazono, K. 1997. Smad6 inhibits signalling by the TGF-β superfamily. *Nature,* 389**,** 622-6.

Issack, P. S., Helfet, D. L. & Lane, J. M. 2008. Role of Wnt signaling in bone remodeling and repair. *HSS J,* 4**,** 66-70.

Jacob, A. L., Smith, C., Partanen, J. & Ornitz, D. M. 2006. Fibroblast growth factor receptor 1 signaling in the osteo-chondrogenic cell lineage regulates sequential steps of osteoblast maturation. *Dev Biol,* 296**,** 315-28.

Jain, A. P., Pundir, S. & Sharma, A. 2013. Bone morphogenetic proteins: The anomalous molecules. *J Indian Soc Periodontol,* 17**,** 583-6.

Jilka, R. L., Weinstein, R. S., Bellido, T., Parfitt, A. M. & Manolagas, S. C. 1998. Osteoblast programmed cell death (apoptosis): modulation by growth factors and cytokines. *J Bone Miner Res,* 13**,** 793-802.

Kang, Q., Sun, M. H., Cheng, H., Peng, Y., Montag, A. G., Deyrup, A. T., Jiang, W., Luu, H. H., Luo, J., Szatkowski, J. P., Vanichakarn, P., Park, J. Y., Li, Y., Haydon, R. C. & He, T. C. 2004. Characterization of the distinct orthotopic bone-forming activity of 14 BMPs using recombinant adenovirus-mediated gene delivery. *Gene Ther,* 11**,** 1312-20.

Kapinas, K. & Delany, A. M. 2011. MicroRNA biogenesis and regulation of bone remodeling. *Arthritis Res Ther,* 13**,** 220.

Kasagi, S. & Chen, W. 2013. TGF-β 1 on osteoimmunology and the bone component cells. *Cell Biosci,* 3**,** 4.

Kassem, M., Kveiborg, M. & Eriksen, E. F. 2000. Production and action of transforming growth factor-β in human osteoblast cultures: dependence on cell differentiation and modulation by calcitriol. *Eur J Clin Invest,* 30**,** 429-37.

Kelpke, S. S., Reiff, D., Prince, C. W. & Thompson, J. A. 2001. Acidic fibroblast growth factor signaling inhibits peroxynitrite-induced death of osteoblasts and osteoblast precursors. *J Bone Miner Res,* 16**,** 1917-25.

Khouri, R. K., Koudsi, B. & Reddi, H. 1991. Tissue transformation into bone in vivo. A potential practical application. *JAMA,* 266**,** 1953-5.

Kim, E. J., Cho, S. W., Shin, J. O., Lee, M. J., Kim, K. S. & Jung, H. S. 2013. Ihh and Runx2/Runx3 signaling interact to coordinate early chondrogenesis: a mouse model. *PLoS One,* 8**,** e55296.

Klar, R. M., Duarte, R., Dix-Peek, T., Dickens, C., Ferretti, C. & Ripamonti, U. 2013. Calcium ions and osteoclastogenesis initiate the induction of bone formation by coral-derived macroporous constructs. *J Cell Mol Med,* 17**,** 1444-57.

Klar, R. M., Duarte, R., Dix-Peek, T. & Ripamonti, U. 2014. The induction of bone formation by the recombinant human transforming growth factor- β_3. *Biomaterials,* 35**,** 2773-88.

Kobayashi, Y. 2012. [Roles of Wnt signaling in bone metabolism]. *Clin Calcium,* 22**,** 1701-6.

Komori, T. 2010. Regulation of osteoblast differentiation by Runx2. *Adv Exp Med Biol,* 658**,** 43-9.

Kugimiya, F., Kawaguchi, H., Kamekura, S., Chikuda, H., Ohba, S., Yano, F., Ogata, N., Katagiri, T., Harada, Y., Azuma, Y., Nakamura, K. & Chung, U. I. 2005. Involvement of endogenous bone morphogenetic protein (BMP) 2 and BMP6 in bone formation. *J Biol Chem,* 280**,** 35704-12.

Kular, J., Tickner, J., Chim, S. M. & Xu, J. 2012. An overview of the regulation of bone remodelling at the cellular level. *Clin Biochem,* 45**,** 863-73.

Kulterer, B., Friedl, G., Jandrositz, A., Sanchez-Cabo, F., Prokesch, A., Paar, C., Scheideler, M., Windhager, R., Preisegger, K. H. & Trajanoski, Z. 2007. Gene expression profiling of human mesenchymal stem cells derived from bone marrow during expansion and osteoblast differentiation. *BMC Genomics,* 8**,** 70.

Kuro-O, M. 2008. Endocrine FGFs and Klothos: emerging concepts. *Trends Endocrinol Metab,* 19**,** 239-45.

Lai, C. F. & Cheng, S. L. 2002. Signal transductions induced by bone morphogenetic protein-2 and transforming growth factor-β in normal human osteoblastic cells. *J Biol Chem,* 277**,** 15514-22.

Lambrecht, S., Verbruggen, G., Elewaut, D. & Deforce, D. 2009. Differential expression of αB-crystallin and evidence of its role as a mediator of matrix gene expression in osteoarthritis. *Arthritis Rheum,* 60**,** 179-88.

Lee, K. S., Hong, S. H. & Bae, S. C. 2002. Both the Smad and p38 MAPK pathways play a crucial role in Runx2 expression following induction by transforming growth factor-β and bone morphogenetic protein. *Oncogene,* 21**,** 7156-63.

Lemonnier, J., Hay, E., Delannoy, P., Fromigue, O., Lomri, A., Modrowski, D. & Marie, P. J. 2001. Increased osteoblast apoptosis in apert craniosynostosis: role of protein kinase C and interleukin-1. *Am J Pathol,* 158**,** 1833-42.

Li, X. L., Liu, Y. B., Ma, E. G., Shen, W. X., Li, H. & Zhang, Y. N. 2015. Synergistic effect of BMP9 and TGF-β in the proliferation and differentiation of osteoblasts. *Genet Mol Res,* 14**,** 7605-15.

Livingston, D. H., Anjaria, D., Wu, J., Hauser, C. J., Chang, V., Deitch, E. A. & Rameshwar, P. 2003. Bone marrow failure following severe injury in humans. *Ann Surg,* 238**,** 748-53.

Lotz, S., Goderie, S., Tokas, N., Hirsch, S. E., Ahmad, F., Corneo, B., Le, S., Banerjee, A., Kane, R. S., Stern, J. H., Temple, S. & Fasano, C. A. 2013. Sustained levels of FGF2 maintain undifferentiated stem cell cultures with biweekly feeding. *PLoS One,* 8**,** e56289.

Lu, X., Su, N., Yang, J., Huang, W., Li, C., Zhao, L., He, Q., Du, X., Shen, Y., Chen, B. & Chen, L. 2009. Fibroblast growth factor receptor 1 regulates the differentiation and activation of osteoclasts through Erk1/2 pathway. *Biochem Biophys Res Commun,* 390**,** 494-9.

Lucas, P. A. 1989. Chemotactic response of osteoblast-like cells to transforming growth factor β. *Bone,* 10**,** 459-63.

Maeda, S., Hayashi, M., Komiya, S., Imamura, T. & Miyazono, K. 2004. Endogenous TGF-β signaling suppresses maturation of osteoblastic mesenchymal cells. *EMBO J,* 23**,** 552-63.

Mansukhani, A., Ambrosetti, D., Holmes, G., Cornivelli, L. & Basilico, C. 2005. SOX-2 induction by FGF and FGFR2 activating mutations inhibits WNT signaling and osteoblast differentiation. J Cell Biol. 168(**7**)**,**1065-76.

Massague, J. 1990. The transforming growth factor-β family. *Annu Rev Cell Biol,* 6**,** 597-641.

Matsunobu, T., Torigoe, K., Ishikawa, M., De Vega, S., Kulkarni, A. B., Iwamoto, Y. & Yamada, Y. 2009. Critical roles of the TGF-β type I receptor ALK5 in perichondrial formation and function, cartilage integrity, and osteoblast differentiation during growth plate development. *Dev Biol,* 332**,** 325-38.

Miyamoto, C., Matsumoto, T., Sakimura, K. & Shindo, H. 2007. Osteogenic protein-1 with transforming growth factor-β1: potent inducer of chondrogenesis of synovial mesenchymal stem cells in vitro. *J Orthop Sci,* 12**,** 555-61.

Nishimura, R., Kato, Y., Chen, D., Harris, S. E., Mundy, G. R. & Yoneda, T. 1998. Smad5 and DPC4 are key molecules in mediating BMP-2-induced osteoblastic differentiation of the pluripotent mesenchymal precursor cell line C2C12. *J Biol Chem,* 273**,** 1872-9.

Noel, D., Gazit, D., Bouquet, C., Apparailly, F., Bony, C., Plence, P., Millet, V., Turgeman, G., Perricaudet, M., Sany, J. & Jorgensen, C. 2004. Short-term BMP-2 expression is sufficient for in vivo osteochondral differentiation of mesenchymal stem cells. *Stem Cells,* 22**,** 74-85.

Nusse, R. 2005. Wnt signaling in disease and in development. *Cell Res,* 15**,** 28-32.

Orr-Urtreger, A., Bedford, M. T., Burakova, T., Arman, E., Zimmer, Y., Yayon, A., Givol, D. & Lonai, P. 1993. Developmental localization of the splicing alternatives of fibroblast growth factor receptor-2 (FGFR2). *Dev Biol,* 158**,** 475-86.

Papachroni, K. K., Karatzas, D. N., Papavassiliou, K. A., Basdra, E. K. & Papavassiliou, A. G. 2009. Mechanotransduction in osteoblast regulation and bone disease. *Trends Mol Med,* 15**,** 208-16.

Parfitt, A. M. 1994. Osteonal and hemi-osteonal remodeling: the spatial and temporal framework for signal traffic in adult human bone. *J Cell Biochem,* 55**,** 273-86.

Pereira, R. C., Rydziel, S. & Canalis, E. 2000. Bone morphogenetic protein-4 regulates its own expression in cultured osteoblasts. *J Cell Physiol,* 182**,** 239-46.

Public Service Department. National code for animal use in research, education, diagnosis and testing of drugs and related substances in South Africa.Pretoria, South Africa: Public Service Department; 1990.

Rahman, M. S., Akhtar, N., Jamil, H. M., Banik, R. S. & Asaduzzaman, S. M. 2015. TGF-β /BMP signaling and other molecular events: regulation of osteoblastogenesis and bone formation. *Bone Res,* 3**,** 15005.

Raisz, L. G. 1999. Physiology and pathophysiology of bone remodeling. *Clin Chem,* 45**,** 1353-8.

Reddi, A. H. 1994. Symbiosis of biotechnology and biomaterials: applications in tissue engineering of bone and cartilage. *J Cell Biochem,* 56**,** 192-5.

Reddi, A. H. 1998. Role of morphogenetic proteins in skeletal tissue engineering and regeneration. *Nat Biotechnol,* 16**,** 247-52.

Reddi, A. H. 2000. Morphogenetic messages are in the extracellular matrix: biotechnology from bench to bedside. *Biochem Soc Trans,* 28**,** 345-9.

Reyes-Botella, C., Montes, M. J., Abadia-Molina, A. C., Vallecillo-Capilla, M. F. & Ruiz, C. 1999. CD10 expression in cultured human osteoblast-like cells. *Folia Biol (Praha),* 45**,** 257-60.

Ripamonti, U. 1991. The morphogenesis of bone in replicas of porous hydroxyapatite obtained from conversion of calcium carbonate exoskeletons of coral. *J Bone Joint Surg Am,* 73**,** 692-703.

Ripamonti, U. 1992. Calvarial regeneration in primates with autolyzed antigen-extracted allogeneic bone. *Clin Orthop Relat Res***,** 293-303.

Ripamonti, U. 2004. Soluble, insoluble and geometric signals sculpt the architecture of mineralized tissues. *J Cell Mol Med,* 8**,** 169-80.

Ripamonti, U. 2006. Soluble osteogenic molecular signals and the induction of bone formation. *Biomaterials,* 27**,** 807-22.

Ripamonti, U. 2009. Biomimetism, biomimetic matrices and the induction of bone formation. *J Cell Mol Med,* 13**,** 2953-72.

Ripamonti, U., Crooks, J., Matsaba, T. & Tasker, J. 2000. Induction of endochondral bone formation by recombinant human transforming growth factor- β_2 in the baboon (*Papio ursinus*). *Growth Factors,* 17**,** 269-85.

Ripamonti, U., Dix-Peek, T., Parak, R., Milner, B. & Duarte, R. 2015. Profiling bone morphogenetic proteins and transforming growth factor- βs by hTGF- β_3 pre-treated coral-derived macroporous bioreactors: the power of one. *Biomaterials,* 49**,** 90-102.

Ripamonti, U., Duarte, R., Parak, R., Dickens, C., Dix-Peek, T. & Klar, R. M. 2016a. Redundancy and Molecular Evolution: The Rapid Induction of Bone Formation by the Mammalian Transforming Growth Factor- β3 Isoform. *Front Physiol,* 7**,** 396.

Ripamonti, U., Duneas, N., Van Den Heever, B., Bosch, C. & Crooks, J. 1997. Recombinant transforming growth factor- β_1 induces endochondral bone in the baboon and synergizes with recombinant osteogenic protein-1 (bone morphogenetic protein-7) to initiate rapid bone formation. *J Bone Miner Res,* 12**,** 1584-95.

Ripamonti, U. & Klar, R. M. 2010. Regenerative frontiers in craniofacial reconstruction: grand challenges and opportunities for the mammalian transforming growth factor-β proteins. *Front Physiol,* 1**,** 143.

Ripamonti, U., Parak, R., Klar, R. M., Dickens, C., Dix-Peek, T. & Duarte, R. 2016b. The synergistic induction of bone formation by the osteogenic proteins of the TGF-β supergene family. *Biomaterials,* 104**,** 279-96.

Ripamonti, U., Richter, P. W., Nilen, R. W. & Renton, L. 2008. The induction of bone formation by smart biphasic hydroxyapatite tricalcium phosphate biomimetic matrices in the non-human primate *Papio ursinus*. *J Cell Mol Med,* 12**,** 2609-21.

Ripamonti, U., Richter, P. W. & Thomas, M. E. 2007. Self-inducing shape memory geometric cues embedded within smart hydroxyapatite-based biomimetic matrices. *Plast Reconstr Surg,* 120**,** 1796-807.

Ripamonti, U., Teare, J. & Ferretti, C. 2012. A Macroporous Bioreactor Super Activated by the Recombinant Human Transforming Growth Factor-β (3). *Front Physiol,* 3**,** 172.

Ripamonti, U., Van Den Heever, B., Sampath, T. K., Tucker, M. M., Rueger, D. C. & Reddi, A. H. 1996. Complete regeneration of bone in the baboon by recombinant human osteogenic protein-1 (hOP-1, bone morphogenetic protein-7). *Growth Factors,* 13**,** 273-89,color plates III-VIII,pre bk.

Ripamonti, U., Van Den Heever, B. & Van Wyk, J. 1993. Expression of the osteogenic phenotype in porous hydroxyapatite implanted extraskeletally in baboons. *Matrix,* 13**,** 491-502.

Roberts, A. B., Anzano, M. A., Lamb, L. C., Smith, J. M. & Sporn, M. B. 1981. New class of transforming growth factors potentiated by epidermal growth factor: isolation from non-neoplastic tissues. *Proc Natl Acad Sci U S A,* 78**,** 5339-43.

Rodan, G. A. 1998. Bone homeostasis. *Proc Natl Acad Sci U S A,* 95**,** 13361-2.

Sahni, M., Ambrosetti, D. C., Mansukhani, A., Gertner, R., Levy, D. & Basilico, C. 1999. FGF signaling inhibits chondrocyte proliferation and regulates bone development through the STAT-1 pathway. *Genes Dev,* 13**,** 1361-6.

Sakai, K., Hiripi, L., Glumoff, V., Brandau, O., Eerola, R., Vuorio, E., Bosze, Z., Fassler, R. & Aszodi, A. 2001. Stage-and tissue-specific expression of a Col2a1-Cre fusion gene in transgenic mice. *Matrix Biol,* 19**,** 761-7.

Salomon, D. S., Brandt, R., Ciardiello, F. & Normanno, N. 1995. Epidermal growth factor-related peptides and their receptors in human malignancies. *Crit Rev Oncol Hematol,* 19**,** 183-232.

Sampath, T. K. & Reddi, A. H. 1981. Dissociative extraction and reconstitution of extracellular matrix components involved in local bone differentiation. *Proc Natl Acad Sci U S A,* 78**,** 7599-603.

Sanford, L. P., Ormsby, I., Gittenberger-De Groot, A. C., Sariola, H., Friedman, R., Boivin, G. P., Cardell, E. L. & Doetschman, T. 1997. TGF-β2 knockout mice have multiple developmental defects that are non-overlapping with other TGF-β knockout phenotypes. *Development,* 124**,** 2659-70.

Sato, M. 2006. Upregulation of the Wnt/ β-catenin pathway induced by transforming growth factor-β in hypertrophic scars and keloids. *Acta Derm Venereol,* 86**,** 300-7.

Schnitzler, C. M., Ripamonti, U. & Mesquita, J. M. 1993. Histomorphometry of iliac crest trabecular bone in adult male baboons in captivity. *Calcif Tissue Int,* 52**,** 447-54.

Seo, E., Basu-Roy, U., Zavadil, J., Basilico, C. & Mansukhani, A. 2011. Distinct functions of SOX-2 control self-renewal and differentiation in the osteoblast lineage. *Mol Cell Biol*. 31(**22**)**,**4593-608.

Shipp, M. A., Stefano, G. B., Switzer, S. N., Griffin, J. D. & Reinherz, E. L. 1991. CD10 (CALLA)/neutral endopeptidase 24.11 modulates inflammatory peptide-induced changes in neutrophil morphology, migration, and adhesion proteins and is itself regulated by neutrophil activation. *Blood,* 78**,** 1834-41.

Siegel, P. M. & Massague, J. 2003. Cytostatic and apoptotic actions of TGF-β in homeostasis and cancer. *Nat Rev Cancer,* 3**,** 807-21.

Silver, I. A., Murrills, R. J. & Etherington, D. J. 1988. Microelectrode studies on the acid microenvronment beneath adherent macrophages and osteoclasts. *Exp Cell Res*. 175**,** 266–276.

Singhatanadgit, W., Salih, V. & Olsen, I. 2006. Up-regulation of bone morphogenetic protein receptor IB by growth factors enhances BMP-2-induced human bone cell functions. *J Cell Physiol,* 209**,** 912-22.

Song, B., Estrada, K. D. & Lyons, K. M. 2009. Smad signaling in skeletal development and regeneration. *Cytokine Growth Factor Rev,* 20**,** 379-88.

Song, R., Wang, D., Zeng, R. & Wang, J. 2017. Synergistic effects of fibroblast growth factor-2 and bone morphogenetic protein-2 on bone induction. *Mol Med Rep,* 16**,** 4483-4492.

Spinella-Jaegle, S., Roman-Roman, S., Faucheu, C., Dunn, F. W., Kawai, S., Gallea, S., Stiot, V., Blanchet, A. M., Courtois, B., Baron, R. & Rawadi, G. 2001. Opposite effects of

bone morphogenetic protein-2 and transforming growth factor-β1 on osteoblast differentiation. *Bone,* 29**,** 323-30.

Stauber, D. J., Digabriele, A. D. & Hendrickson, W. A. 2000. Structural interactions of fibroblast growth factor receptor with its ligands. *Proc Natl Acad Sci U S A,* 97**,** 49-54.

Su, N., Jin, M. & Chen, L. 2014. Role of FGF/FGFR signalling in skeletal development and homeostasis: learning from mouse models. *Bone Res,* 2**,** 14003.

Tachi, K., Takami, M., Sato, H., Mochizuki, A., Zhao, B., Miyamoto, Y., Tsukasaki, H., Inoue, T., Shintani, S., Koike, T., Honda, Y., Suzuki, O., Baba, K. & Kamijo, R. 2011. Enhancement of bone morphogenetic protein-2-induced ectopic bone formation by transforming growth factor- β1. *Tissue Eng Part A,* 17**,** 597-606.

Thouverey, C. & Caverzasio, J. 2015. Focus on the p38 MAPK signaling pathway in bone development and maintenance. *Bonekey Rep,* 4**,** 711.

Tolar, J., Teitelbaum, S. L. & Orchard, P. J. 2004. Osteopetrosis. *N Engl J Med*. 351**,** 2839–2849.

Urist, M. R., Silverman, B. F., Buring, K., Dubuc, F. L. & Rosenberg, J. M. 1967. The bone induction principle. *Clin Orthop Relat Res,* 53**,** 243-83.

Van De Laar, I. M., Oldenburg, R. A., Pals, G., Roos-Hesselink, J. W., De Graaf, B. M., Verhagen, J. M., Hoedemaekers, Y. M., Willemsen, R., Severijnen, L. A., Venselaar, H., Vriend, G., Pattynama, P. M., Collee, M., Majoor-Krakauer, D., Poldermans, D., Frohn-Mulder, I. M., Micha, D., Timmermans, J., Hilhorst-Hofstee, Y., Bierma-Zeinstra, S. M., Willems, P. J., Kros, J. M., Oei, E. H., Oostra, B. A., Wessels, M. W. & Bertoli-Avella, A. M. 2011. Mutations in SMAD3 cause a syndromic form of aortic aneurysms and dissections with early-onset osteoarthritis. *Nat Genet,* 43**,** 121-6.

Wang, J., Rao, S., Chu, J., Shen, X., Levasseur, D. N., Theunissen, T. W. & Orkin, S. H. 2006. A protein interaction network for pluripotency of embryonic stem cells. *Nature,* 444**,** 364-8.

Wang, M., Jin, H., Tang, D., Huang, S., Zuscik, M. J. & Chen, D. 2011. Smad1 plays an essential role in bone development and postnatal bone formation. *Osteoarthritis Cartilage,* 19**,** 751-62.

Wang, Y., Li, Y. P., Paulson, C., Shao, J. Z., Zhang, X., Wu, M. & Chen, W. 2014. Wnt and the Wnt signaling pathway in bone development and disease. *Front Biosci (Landmark Ed),* 19**,** 379-407.

Wu, M., Chen, G. & Li, Y. P. 2016. TGF-β and BMP signaling in osteoblast, skeletal development, and bone formation, homeostasis and disease. *Bone Res,* 4**,** 16009.

Wu, X. B., Li, Y., Schneider, A., Yu, W., Rajendren, G., Iqbal, J., Yamamoto, M., Alam, M., Brunet, L. J., Blair, H. C., Zaidi, M. & Abe, E. 2003. Impaired osteoblastic differentiation, reduced bone formation, and severe osteoporosis in noggin-overexpressing mice. *J Clin Invest,* 112**,** 924-34.

Xu, J. & Testa, J. R. 2009. DLX5 (distal-less homeobox 5) promotes tumor cell proliferation by transcriptionally regulating MYC. *J Biol Chem,* 284**,** 20593-601.

Yang, N. N., Bryant, H. U., Hardikar, S., Sato, M., Galvin, R. J., Glasebrook, A. L. & Termine, J. D. 1996. Estrogen and raloxifene stimulate transforming growth factor-β3 gene expression in rat bone: a potential mechanism for estrogen- or raloxifene-mediated bone maintenance. *Endocrinology,* 137**,** 2075-84.

Yoshida, C. A., Yamamoto, H., Fujita, T., Furuichi, T., Ito, K., Inoue, K., Yamana, K., Zanma, A., Takada, K., Ito, Y. & Komori, T. 2004. Runx2 and Runx3 are essential for chondrocyte maturation, and Runx2 regulates limb growth through induction of Indian hedgehog. *Genes Dev,* 18**,** 952-63.

Yu, Y., Yang, J. L., Chapman-Sheath, P. J. & Walsh, W. R. 2002. TGF-β, BMPS, and their signal transducing mediators, Smads, in rat fracture healing. *J Biomed Mater Res,* 60**,** 392-7.

Zandstra, P. W., Le, H. V., Daley, G. Q., Griffith, L. G. & Lauffenburger, D. A. 2000. Leukemia inhibitory factor (LIF) concentration modulates embryonic stem cell self-renewal and differentiation independently of proliferation. *Biotechnol Bioeng,* 69**,** 607-17.

Zarubin, T. & Han, J. 2005. Activation and signaling of the p38 MAP kinase pathway. *Cell Res,* 15**,** 11-8.

Zhu, D., Mackenzie, N. C., Shanahan, C. M., Shroff, R. C., Farquharson, C. & Macrae, V. E. 2015. BMP-9 regulates the osteoblastic differentiation and calcification of vascular smooth muscle cells through an ALK1 mediated pathway. *J Cell Mol Med,* 19**,** 165-74.

Zou, H., Choe, K. M., Lu, Y., Massague, J. & Niswander, L. 1997. BMP signaling and vertebrate limb development. *Cold Spring Harb Symp Quant Biol,* 62**,** 269-72.

9. Appendices

Appendix 1: Real-time PCR reaction volumes

Component	Volume (µL)
Biorad Itaq Mastermix	5
Forward Primer	0.3
Reverse Primer	0.3
cDNA	2.5
Nuclease free H_2O	1.9
Total volume	10

Appendix 2: Primer sequence of FGF-1, FGF-2, FGF-R1, FGF-R2, TGF-β_1, TGF-β_2, TGF-β_3 and Reference genes

Gene	Gene Primer Sequence (5'–3')	Amplicon length (bp)
β-actin	F GGAAATCGTGCGTGACATCA	63
	R ATCTCCTGCTCGAAGTCCAG	
β-catenin	F GACTCGAGCTCAGAGGGTAC	110
	R AACGCTGGACATTAGTGGGA	
BMP-2	F: CAAGCCAAACACAAACAGC	103
	R: AGCCACAATCCAGTCATTCC	
BMP-4	F: GGGAGAAGCAGCCAAACT	105
	R: CTTGAGGTAACGATCGGCTAAT	
BMP-6	F: TGTTGGTCTGTAGCAAGC	110
	R: TACTGAACCAGCTGATCC	
BMP-7/OP-1	F: TCCCTCTCCATTCCCTACAG	131
	R: TCAACACACAACCCTCCTC	
BMP-9	F: GCTGAGCTCCGACTCTATGT	182

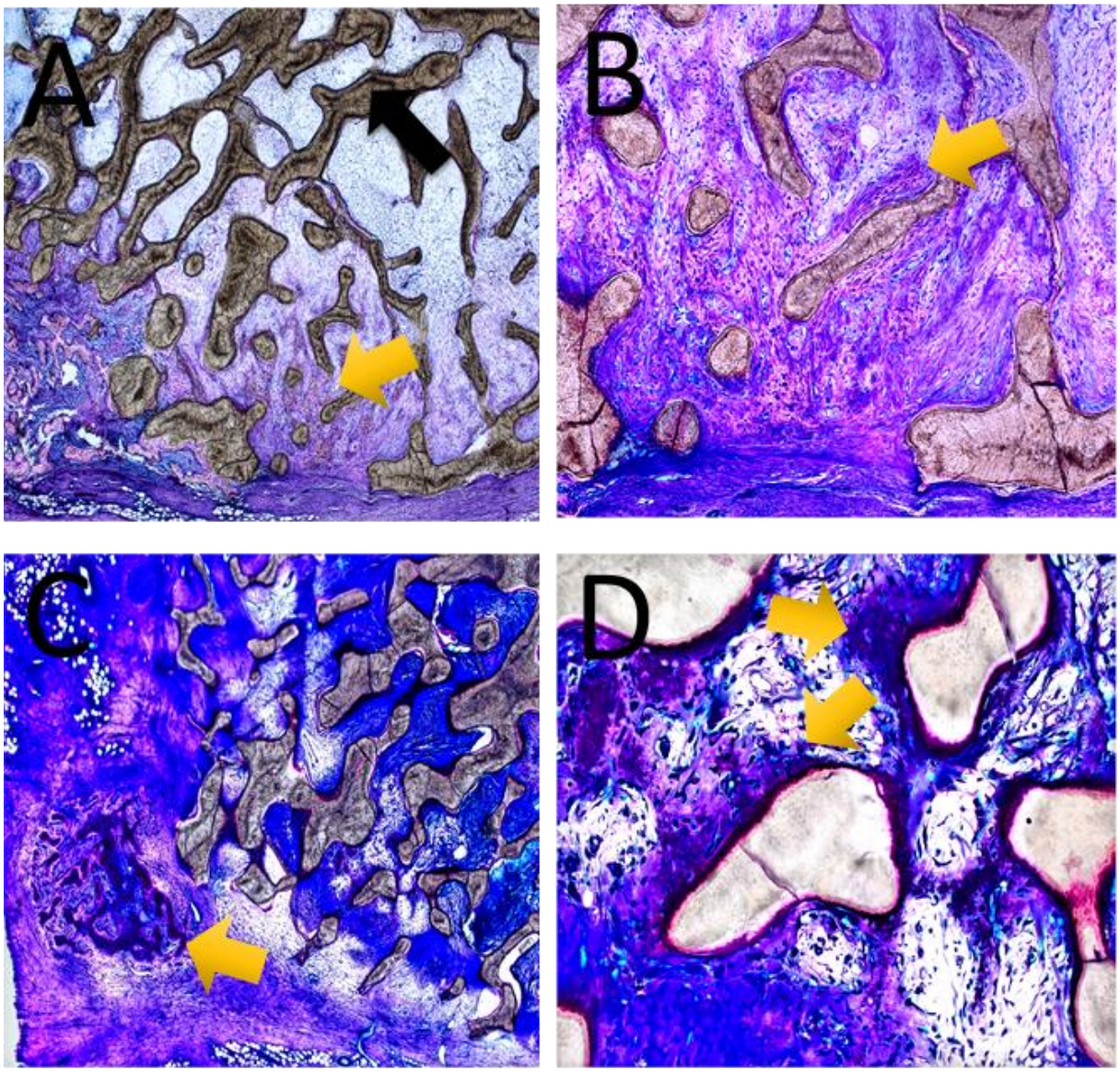
	R: CCGGACCTTCAAGAGCCTTA	
Collagen I	F: ATGTGCCACTCTGACTGGAA	174
	R: CTTGTCCTTGGGGTTCTTGC	
CD-10/MME	F: GCTGCCTTCCCATGAATCTG	155
	R: CAGTAACAGCAGCACAGACC	
CD-92/SLC	F: TCTATCGCCAGGCTACAGTG	75
	R: AGAATCGCTTGAACCTGGGA	
CRYαB	F: CAGCTGGTTTGACACTGGAC	152
	R: CCTGGCGCTCTTCATGTTTT	
FGF-1	F: GAAGTCCATTCGGCTCACAC	159
	R: AAGCAACCCCTACTCTGGAC	
FGF-2	F: AGTCTTCGCCAGGTCATTGA	157
	R: CCTGAGTATTCGGCAACAGC	
FGF-R1	F: GAGGACGCAGGGGAGTATAC	155
	R: AAGGCCCCTGTGCAATAGAT	
FGF-R2	F: TTCGGGGTGTTAATGTGGGA	158
	R: TGCCAACAGTCCCTCATCAT	
Noggin	F: GAGGAAGTTACAGATGTGGCT	162
	R: CACTCGGAAATGATGGGGTAC	
POU5F1	F: CAGAAGGGCAAGCGATCAAG	120
	R: GAAAGGGACCGAGGAGTAC	
RPLPO	F: AGGCCAAGGGAAAGAAGGT	92
	R: GGCCTTTTCTCAAACAGGGG	
RPL13A	F: TGCGTCTGAAGCCTACAAGA	173
	R: GTTCTTCTCGGCCTGTTTCC	
SDHA	F: ACATGGAGGAGGACAACTGG	187
	R: CCACCAAATGCACGCTGATA	
SMAD-1	F: AGGTTGGGAGGTGTTTGGAA	151
	R: GGAGACCCACAGAGAACACA	
SMAD-2	F: GCAGGAATTGAGCCACAGAG	176
	R: ACTGGCTGTAAGTCCAAGCT	
SMAD-3	F: CTCCTGGCCCAGTCTGTTAA	154

	R: CATTCAGGTGCAGCTCGATC	
SMAD-4	F: CTGCTGCTGGAATTGGTGTT	159
	R: CTTCGTCTAGGAGCTGGAGG	
SMAD-5	F: AGGAACCTGAGCCACAATGA	159
	R: CTTGCTGGGGAGTTGGGATA	
	R: CGAGTTCTCTGCTTTCACCG	
SOX-2	F: GAAGCTGGTGTAAGGCGATG	180
	R: TTCCCTGAGCCTCTTGTCAG	
TGF-β_1	F: AAGATGGAGAGAGGACTGC	151
	R: AGAGAGAGACAGAGATGGGG	
TGF-β_2	F: TACCACCTTTCCGATTGCCC	153
	R: ACGGCACAGGGATTTCTTCT	
TGF-β_3	F: GGTTTTCCGCTTCAATGTGT	155
	R: GCTCGATCCTCTGCTCATTC	

Appendix 3: Thermocycling parameters for Real-time PCR

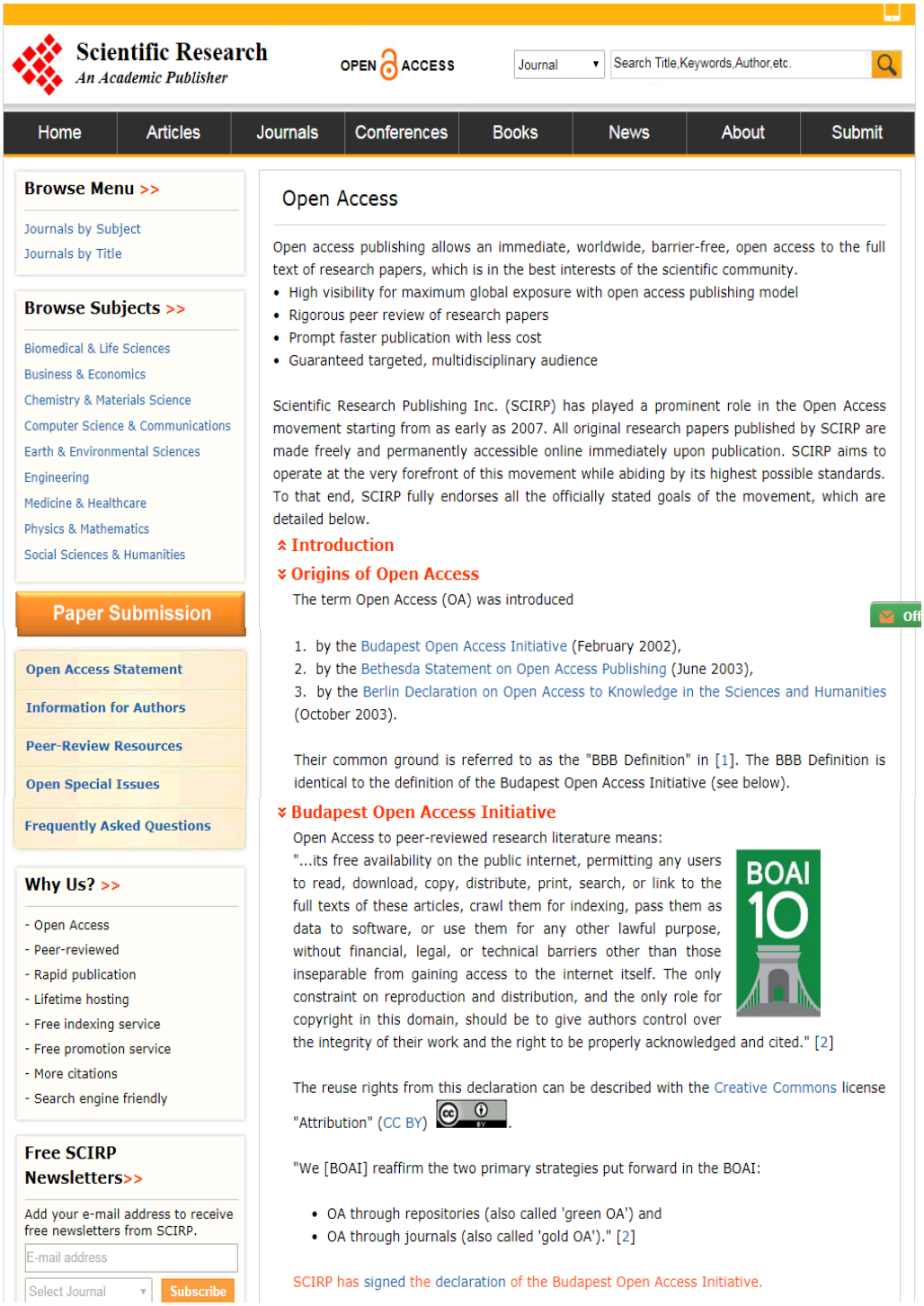
Thermocycling parameters	Time (seconds)	Temperature (°C)	Cycling
Initial Denaturation	120	94	1
Denaturation	10	95	40
Annealing	10	60	40
Extension	30	72	40
Final extension	300	72	1

Appendix 4: Tissue morphogenesis by 125 µg hTGF-β3 treated coral-derived macroporous bioreactors



Appendix 4: Tissue morphogenesis by 125 µg hTGF-β_3 treated coral-derived macroporous bioreactors. (A) A low-power view on day 19 shows the induction of cellular transformation and osteogenesis (light yellow arrow) at the periphery of the coral derived construct (black arrow). (B) A high-power image on day 19 highlighting the induction of bone formation (light yellow arrow), tightly attached to the substratum but also expanding within the macroporous spaces together with prominent angiogenesis and capillary sprouting. (C) Low-power view of day 23 showing the induction of bone formation outside the profile (light blue arrow) of the implanted super-activated bioreactor (light yellow arrow). (D) High-power image at 23 days showing the induction of bone formation (light yellow arrows) tightly attached to the substratum within macroporous spaces at the very periphery of the implanted super-activated bioreactor. Scale bar for (A), (B), (C), and (D) are 670 µm, 40 µm, 110 µm and 75 µm, respectively.

Appendix 5: Open Access of figure 2



Scientific Research
An Academic Publisher

OPEN ACCESS

Journal | Search Title,Keywords,Author,etc.

Home | Articles | Journals | Conferences | Books | News | About | Submit

Browse Menu >>

Journals by Subject
Journals by Title

Browse Subjects >>

Biomedical & Life Sciences
Business & Economics
Chemistry & Materials Science
Computer Science & Communications
Earth & Environmental Sciences
Engineering
Medicine & Healthcare
Physics & Mathematics
Social Sciences & Humanities

Paper Submission

Open Access Statement
Information for Authors
Peer-Review Resources
Open Special Issues
Frequently Asked Questions

Why Us? >>

- Open Access
- Peer-reviewed
- Rapid publication
- Lifetime hosting
- Free indexing service
- Free promotion service
- More citations
- Search engine friendly

Free SCIRP Newsletters>>

Add your e-mail address to receive free newsletters from SCIRP.

E-mail address

Select Journal | Subscribe

Open Access

Open access publishing allows an immediate, worldwide, barrier-free, open access to the full text of research papers, which is in the best interests of the scientific community.

- High visibility for maximum global exposure with open access publishing model
- Rigorous peer review of research papers
- Prompt faster publication with less cost
- Guaranteed targeted, multidisciplinary audience

Scientific Research Publishing Inc. (SCIRP) has played a prominent role in the Open Access movement starting from as early as 2007. All original research papers published by SCIRP are made freely and permanently accessible online immediately upon publication. SCIRP aims to operate at the very forefront of this movement while abiding by its highest possible standards. To that end, SCIRP fully endorses all the officially stated goals of the movement, which are detailed below.

Introduction

Origins of Open Access

The term Open Access (OA) was introduced

1. by the Budapest Open Access Initiative (February 2002),
2. by the Bethesda Statement on Open Access Publishing (June 2003),
3. by the Berlin Declaration on Open Access to Knowledge in the Sciences and Humanities (October 2003).

Their common ground is referred to as the "BBB Definition" in [1]. The BBB Definition is identical to the definition of the Budapest Open Access Initiative (see below).

Budapest Open Access Initiative

Open Access to peer-reviewed research literature means:

"...its free availability on the public internet, permitting any users to read, download, copy, distribute, print, search, or link to the full texts of these articles, crawl them for indexing, pass them as data to software, or use them for any other lawful purpose, without financial, legal, or technical barriers other than those inseparable from gaining access to the internet itself. The only constraint on reproduction and distribution, and the only role for copyright in this domain, should be to give authors control over the integrity of their work and the right to be properly acknowledged and cited." [2]

The reuse rights from this declaration can be described with the Creative Commons license "Attribution" (CC BY).

"We [BOAI] reaffirm the two primary strategies put forward in the BOAI:

- OA through repositories (also called 'green OA') and
- OA through journals (also called 'gold OA')." [2]

SCIRP has signed the declaration of the Budapest Open Access Initiative.

Appendix6: Gene expression summary of genes of interest at 17 to 30 days after implantation of the 125 µg hTGF-β_3

	Days											
	17		19		23		25		27		30	
Genes	Device	Muscle	Device	Muscle	Device	Muscle	Device	Muscle	Device	Muscle	Device	Muscle
β-catenin	-	+	+	+	+	+	-	-	+	-	=	+
BMP-2	-	+	+	-	+	-	+	+	+	+	+	+
BMP-4	-	=	-	-	+	=	=	=	+	+	-	=
BMP-6	-	-	-	-	-	-	-	-	-	-	-	-
BMP-7/OP-1	-	=	+	-	+	-	-	=	+	-	+	=
BMP-9	+	+	+	-	+	+	+	+	+	-	+	-
Collagen I	+	+	+	+	+	+	+	+	+	+	+	+
CD-10	-	-	-	-	-	-	-	-	-	-	-	-
CD-92	-	=	=	-	=	-	=	+	=	-	-	-
CRYαB	-	-	-	=	-	-	-	-	-	=	-	-
FGF-1	-	-	-	-	-	-	-	-	-	-	-	-
FGF-2	-	-	-	-	-	-	=	-	-	-	-	-
FGF-R1	-	=	+	-	=	-	=	=	+	-	=	=
FGF-R2	=	-	-	-	-	-	=	-	=	-	=	-
Noggin	-	+	-	-	-	-	-	+	-	-	-	-
POU5F1	=	-	=	=	-	-	+	=	+	=	=	-
SMAD-1	+	-	-	-	+	-	=	-	+	=	=	=
SMAD-2	-	=	+	-	+	+	+	+	+	+	=	+
SMAD-3	=	-	=	-	=	-	+	-	+	+	=	+
SMAD-4	+	+	+	=	+	=	+	+	+	+	+	+
SMAD-5	-	-	=	-	=	=	-	-	+	-	-	-
SOX-2	+	+	+	+	+	=	+	+	+	-	+	+
TGF-β_1	+	+	+	-	+	+	+	+	+	+	+	+
TGF-β_2	-	-	-	-	-	-	-	-	-	-	-	-
TGF-β_3	-	+	+	-	+	+	+	+	+	+	=	+

Green (+), red (-) and clear (=) colouring demonstrate up, down-regulation and no change respectively